THE UNIVERSITY OF ALBERTA

ANALYSIS OF DATA FROM A BROAD-BAND THREE-COMPONENT DIGITAL SEISMIC SYSTEM

BY

© JAMES FRANCIS MONTALBETTI

A THESIS

SUBMITTED TO THE FACULTY OF GRADUATE STUDIES

IN PARTIAL FULFILLMENT OF THE REQUIREMENTS

FOR THE DEGREE OF MASTER OF SCIENCE

DEPARTMENT OF PHYSICS

EDMONTON, ALBERTA

FALL 1969

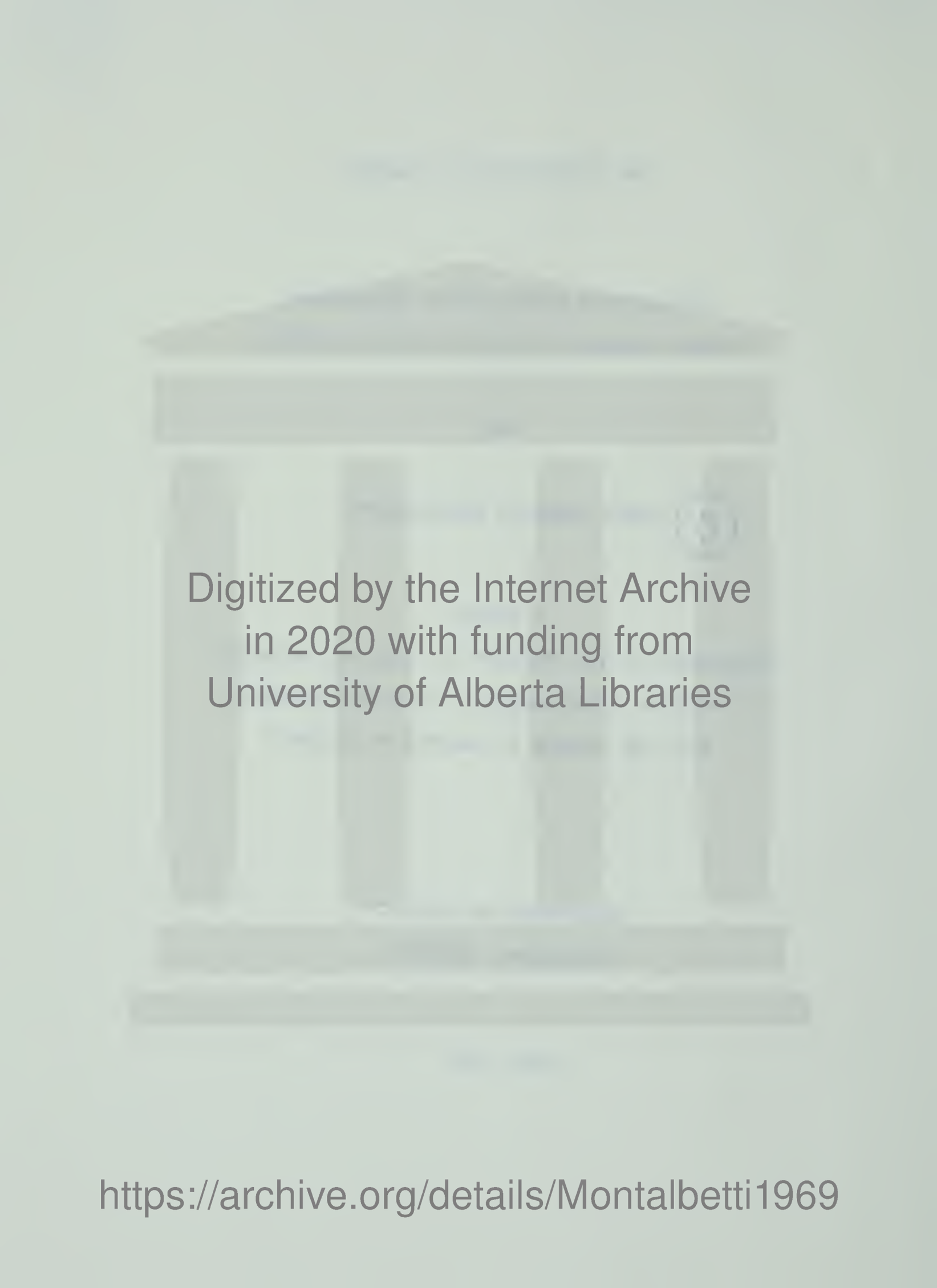

UNIVERSITY OF ALBERTA

FACULTY OF GRADUATE STUDIES

The undersigned certify that they have read, and recommend to the Faculty of Graduate Studies for acceptance, a thesis entitled ANALYSIS OF DATA FROM A BROAD-BAND THREE-COMPONENT DIGITAL SEISMIC SYSTEM, submitted by James Francis Montalbetti, in partial fulfilment of the requirements for the degree of Master of Science.

ABSTRACT

A three-component, broad-band seismic system which records directly onto seven track digital tape has been developed in the Geophysics electronic laboratories at the University of Alberta. A differential filtering technique using low noise operational amplifiers extends the usable velocity sensitivity of a Willmore Mk II seismometer having a natural period of 1.5 seconds out to about 40 seconds under normal operating conditions. A wide spectrum of seismic energy may thus be recorded.

With the availability of three component records, digital processing techniques which utilize the polarization properties of elastic body and surface waves may be applied to the data for enhancement of the signal to noise ratio. The application of two such processors is considered. The first, particularly suited for enhancement of shorter period body waves, is applied in the time domain; while the second filter is used to separate the longer period surface Rayleigh and Love waves by modification of the discrete Fourier coefficients of the data traces in the frequency domain. Results obtained from the seismograms processed by these methods show that a very good separation of phases, on the basis of the polarization of the seismic energy, can be accomplished. Better interpretation of both source

characteristics and localized recording conditions is thus possible.

ACKNOWLEDGEMENTS

I wish to sincerely thank Dr. E. A. Kanasewich for his help and encouragement throughout the course of this work.

Mr. M. D. Burke designed the instrumentation and offered many constructive suggestions during the preparation of the second chapter. His invaluable help is greatly appreciated.

Messrs. D. Malinsky and B. McGavin are to be thanked for their technical assistance throughout this project.

I would also like to thank Mrs. Mary Thorn for her fine job in typing the manuscript.

During the course of this research, the author was supported by the National Research Council of Canada.

TABLE OF CONTENTS

LIST OF ILLUSTRATIONS

CHAPTER 1

POLARIZATION FILTERS - A REVIEW

1.1 Introduction

As any seismograph record is always noise contaminated, the detection and interpretation of seismic events requires knowledge of the characteristics of both signal and noise. Elastic body waves, which may be generally separated into P (compressional) and S (shear) phases, can be considered as non-dispersive group arrivals with maximum power in the 0.3 to 10 second period range. Surface Rayleigh and Love waves may be described as dispersive group arrivals with maximum power in the 2 to 100 second period range for earthquakes of moderate magnitude, the observable periods extending up to 57 minutes for larger teleseismic events.

Superimposed on these signals is microseismic background noise as well as signal generated noise. Signal generated noise is the result of multiple reflections and refractions of P and S body waves at crustal interfaces and inhomogeneities, and originates primarily under the recording station. Microseismic noise, which is considered to consist mainly of fundamental and higher mode Rayleigh waves, has been shown to exhibit a sharp peak in the 5 to 8 second period range (Brune and Oliver 1959).

As a result of this sharp peak in the microseismic noise spectrum, frequency bandpass filtering is often employed to improve the signal to noise ratio. Initial processing of seismograph records for body wave studies often involves a bandpass filter with the low frequency cutoff at 3 to 5 seconds period, while a similar cutoff is applied as a high frequency corner to records used for the investigation of longer period surface waves. If the seismograph data is available in digital form, zero phase shift recursive digital filters are most often used for this bandpass filter processing.

However, although filtering of this type is very effective in removing microseismic background from both long and short period data, it often cannot distinguish between signal and signal generated noise. This is especially true when the higher frequency body waves are considered. The reason for this is apparent when we consider that signal generated noise, arising from reflected and refracted P and S body waves, can be expected to exhibit a frequency spectrum similar to the original phases.

Although bandpass filtering serves to improve the quality of seismic records by enhancing the signal to noise ratio, difficulty may still arise in the attempted identification of phases whose frequency characteristics are similar.

1.2 Polarization of Seismic Energy

A further property of seismic events which may be used for the enhancement of recorded data is that of signal polarization. Both compressional and shear waves exhibit a high degree of linear polarization. Particle motion coincides with the direction of propagation of energy for compressional (P) phases and is perpendicular to the direction of propagation for the transverse (S) phases. Surface waves of the Rayleigh type are generally elliptically polarized in the vertical - radial plane, the fundamental modes displaying retrograde particle motion and the higher modes prograde or retrograde ellipticity. Surface Love waves are also found to be rectilinearly polarized, but in a horizontal plane orthogonal to the direction of wave propagation.

Since most microseismic background is of the Rayleigh type, it will exhibit elliptical polarization, but with little preferred directionality. Signal generated noise may also be polarized, but again the direction of polarization is random in nature. By using these various characteristics of polarized particle trajectories, filters may be designed which preserve motion if it satisfies specified conditions of polarization in a particular direction, and which attenuate motion that does not satisfy the desired criteria.

For example, a filter may be designed so that it passes only energy which exhibits a high degree of polarization (or high rectilinearity) in the direction of incident compressional pulses. In this case, P-type motion would be preserved. On the other hand, high rectilinearity in a direction perpendicular to the direction of propagation of the seismic waves might be of interest, so that a filter could be designed to pass motion which is SV in nature. Both of these filters, of course, would attenuate signal which was not highly rectilinear in the specified direction.

We see then, that the more or less randomly polarized microseismic background and signal generated noise would be attenuated, as well as the elliptically polarized Rayleigh waves and the transversely polarized Love phases. P and S body wave phases would be preserved.

For applications where the main interest might be in surface Rayleigh and Love type arrivals, similar filters may be designed. These filters do not require the high degree of linear polarization displayed by the body wave filters, but rather weight the input according to how closely the particle motion trajectory corresponds to theoretical Love and Rayleigh wave motion arriving from some pre-assigned direction. Simons (1968) for example, considers rectilinearity of Rayleigh waves based on a theoretical horizontal/

vertical displacement ratio of about 0.8 (Dorman and Prentiss, 1960).

1.3 Polarization Filters

Considering these patterns of particle motion, various workers have designed polarization filters for the enhancement of seismic data. Shimshoni and Smith (1964) suggest that the time averaged cross product of vertical and radial components of ground motion may be used as a measure of rectilinearity. The radial trace is obtained from a rotation of the two horizontal components into a path corresponding to the great circle azimuth from source to receiver, and the computed cross product is multiplied by the original signal. A function of ground motion which enhances rectilinearly polarized signal is thus obtained.

Another process described by the same workers decomposes the vertical and radial motions into their Fourier components and computes the parameters of an equivalent ellipse at each instant in time. Eccentricity, major axis, and angle of inclination of the ellipse from the vertical are displayed for the frequency at which maximum power is arriving. This information is used to provide criterion for the identification of P and SV type motion. In both processes described, no use is made of the transverse component of ground motion.

A particular polarization filter known as REMODE (REctilinear MOtion DEtection) which has received considerable attention was originally developed by Mims and Sax (1965) at Teledyne Industries, with subsequent work by Griffin (1966a, b). This process uses the highly rectilinear properties of P and SV motion to discriminate against the elliptically or randomly polarized nature of signal generated noise. Inputs Z (vertical) and R (radial) are rotated so that the expected direction of incident body waves bisects the angle between the two orthogonal components (Figure 1.1). In this way, all P and SV motion is represented in total by these two rotated components so that a similar shape of the Z and R waveforms (signal), contrasts with dissimilar shape if noise is present.

An estimate of these similarities is obtained by computing the cross-correlation function C(T), of Z(t) and R(t), over a specified window centered at some time t on the record. If the polarization in the R-Z plane is predominantly rectilinear, the even part of C(T) will be large relative to the odd part. If motion of elliptical and random polarization prevails, the even part of C(T) will be small relative to the odd part. By convolving the even part of C(T) with the original time series R(t) and Z(t), motion of high rectilinearity is enhanced and elliptically polarized motion is attenuated.

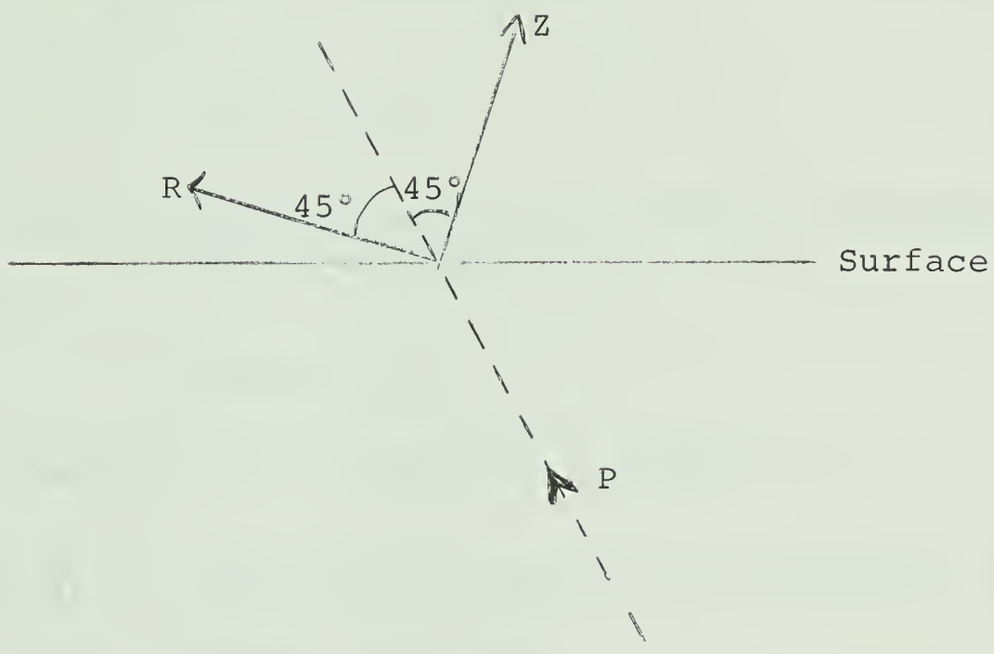

Figure 1.1. Rotation of Z (vertical) and R (radial) components for REMODE processing (after Fuchs 1969).

REMODE as described above will pass both the linearly polarized P and SV type motion. Fuchs (1969) and Basham (1967) describe a modification originally suggested by Griffin, which serves to "tune" the filter for P or SV phases. With the configuration of the rotated Z and R components as in figure 1.1 we find that for P or compressional motion,

$$R(t)Z(t) \geq 0 \tag{1.1}$$

and for SV motion perpendicular to the direction of energy propagation,

$$R(t)Z(t) \leq 0 \tag{1.2}$$

These relationships are illustrated in figure 1.2.

Thus, if compressional motion is of interest, an operator O_p may be defined such that

$$\begin{aligned} O_p &= 1, \quad R(t)Z(t) \geq 0 \\ O_p &= 0, \quad R(t)Z(t) < 0 \end{aligned} \tag{1.3}$$

and applied to the REMODE filtered traces for the preservation of P-motion. Conversely, an operator O_{SV} defined so that

$$\begin{aligned} O_{SV} &= 1, \quad R(t)Z(t) \leq 0 \\ O_{SV} &= 0, \quad R(t)Z(t) > 0 \end{aligned} \tag{1.4}$$

may be applied to the filtered components if SV-type motion

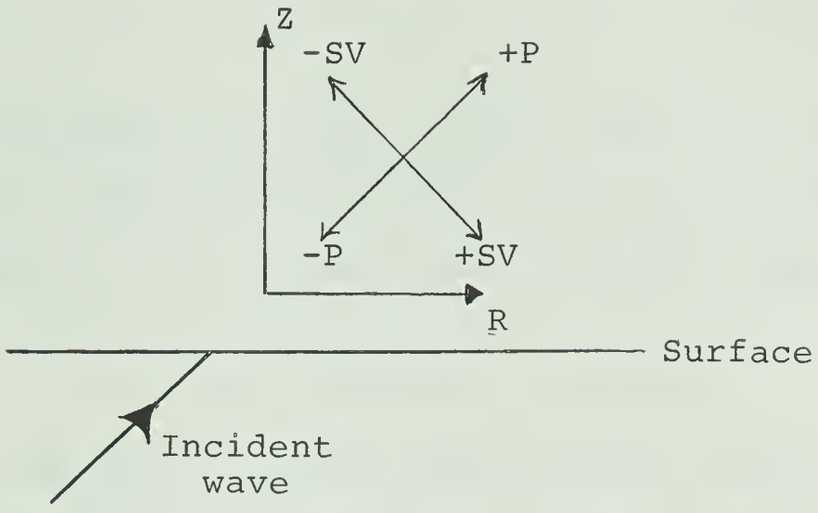

SIGNS OF COMPONENTS

Phase	Z	R	ZR
+P	+	+	+
-P	-	-	+
+SV	-	+	-
-SV	+	-	-

Figure 1.2 Detection of P and SV motion by the product of the Z and R components of motion (after Basham 1967).

is desired.

Archambeau and Flinn (1965) point out that a REMODE filter of the type described above can be approximated in the frequency domain by a cosine function of the form

$$\Phi(\omega) \simeq \cos[\phi_R(\omega) - \phi_Z(\omega)] \qquad (1.5)$$

where $\phi_R(\omega)$ and $\phi_Z(\omega)$ are the phase angles for the frequency components $R(\omega)$ and $Z(\omega)$ of the original traces. This filter function will admit displacements in phase or 180° out of phase on the vertical and radial components so that purely rectilinear motion has unit gain and other motion is attenuated. Elliptically polarized motion however may still be passed, as for example $\phi_R(\omega)-\phi_Z(\omega) = 60°$, in which case $\Phi(\omega) = 0.5$. Higher order REMODE filters with responses approximated by

$$\Phi(\omega) \simeq \cos^n[\phi_R(\omega)-\phi_Z(\omega)] \qquad (1.6)$$

have also been investigated (Fuchs 1969).

Flinn (1965) describes a processor for three component seismic records which considers not only rectilinearity, as does REMODE and the earlier filter described by Shimshoni and Smith, but also rectilinearity in some particular direction in three dimensional space. The two horizontal components of ground motion are rotated so that the radial component corresponds with the expected great circle

azimuth from source to receiver and the transverse component is orthogonal to this. Over a specified time window of length $N\Delta t$, where Δt is the digitizing interval of the data, parameters of an equivalent ellipsoid are calculated in the time domain from the covariance matrix for the set of N points (Z_i, R_i, T_i) $i = 1 \cdots N$. Z(vertical), R(radial) and T(transverse) represent the three orthogonal components of ground motion.

The ratio of the lengths of the major and secondary axes of the ellipsoid is used as a measure of rectilinearity and the orientation in space of the major axis is used to determine the direction of polarization. Appropriate functions of these two properties (rectilinearity and direction) are then applied to each of the three orthogonal records.

If for example, rectilinearity is high and the major axis of the ellipsoid is found to lie in the Z direction, motion on this component will be preserved when the filtering is applied, while the radial and transverse motions will be attenuated. Noise, of course, since it can be expected to display neither a high degree of polarization, nor any preferred direction will be attenuated on all three records.

Unlike REMODE or the process described by Shimshoni and Smith, this particular polarization filter also considers

the transverse component of ground motion. Although the information contained by the transverse record is not as useful as that contained by the vertical and radial components, it might be valuable for gaining information about local conditions near the recording station. This could especially be the case if local conditions give rise to large horizontally polarized shear phases (SH) due to reflection and refraction of P and SV body waves.

Polarization filters of the type described above can be more useful than frequency filters for enhancement of signal to noise ratio particularly when the signal and noise have similar spectral characteristics. It must be remembered however, that these types of filters are time-varying nonlinear processors and their applications require more computer time than for example a digital frequency filter whose response does not change with time, and which may be applied recursively in the time domain.

1.4 Some Applications of Polarization Filters

Various workers have applied polarization filtering techniques to recorded seismic data for improvement of the signal to noise ratio. Lewis and Meyer (1968) apply a phase filter of the REMODE type as described by Archambeau and Flinn (1965) to data recorded during the Early Rise experiment in the summer of 1966. The filtering

is applied to the vertical and radial components of ground motion and used to enhance body phases at both the compressional and shear wave portions of the seismogram.

Fourier transforms $F_Z(\omega)$ and $F_R(\omega)$ of the vertical and horizontal motion respectively are computed and used to form a function $F_{ZR}(\omega) = F_Z(\omega)\ F_R(\omega)^*$, (*denoting the complex conjugate of $F_R(\omega)$). The argument of $F_{ZR}(\omega)$ will be 0 or π if the spectral components of the vertical and radial motion are in phase or out of phase and will be $\pi/2$ for Rayleigh type motion. The enhancement of body phases then is obtained by considering a filter function $F_f(\omega)$ equal to the cosine of the argument of $F_{ZR}(\omega)$. That is:

$$F_f(\omega) = \frac{\mathrm{Re}[F_{ZR}(\omega)]}{\mathrm{ABS}[F_{ZR}(\omega)]} \tag{1.7}$$

or

$$\begin{aligned} F_f(\omega) &= \cos\phi \\ \phi &= \mathrm{ARG}[F_{ZR}(\omega)] \end{aligned} \tag{1.8}$$

This function is now multiplied by the original Fourier transforms so that

$$\begin{aligned} F_Z'(\omega) &= F_Z(\omega) \cdot F_f(\omega) \\ F_R'(\omega) &= F_R(\omega) \cdot F_f(\omega) \end{aligned} \tag{1.9}$$

and the inverse Fourier transform is taken to obtain the filtered record in the time domain.

In the application by Lewis and Meyer, the filter function was raised to the seventh power and applied to data digitized at 100 samples/second. A 1 or 2 second window moved along the record in steps of several tenths of a second was used for this analysis.

In another application, Basham and Ellis (1969) use a REMODE filter designated as a P-Detection, (P-D) filter to process P-wave codes of numerous seismic events recorded in western Alberta. Data is digitized at 16.6 samples/second and first bandpass filtered 0.25-2Hz to remove microseismic and cultural noise. The polarization filter applied to 25 seconds of record following the P onset allows identification of numerous compressional wave arrivals including P, pP and sP. P_cP and PKP phases for events at appropriate epicentral distances are also detected. Determination of P-pP times permits focal depth calculations.

Simons (1968) describes a process which examines three component particle motion trajectories of longer period Love and Rayleigh waves. Apparent horizontal azimuth, eccentricity and phase difference between the vertical and radial components is computed in the frequency domain from the

discrete Fourier coefficients of the data traces considered over a specified time window. The amplitude coefficients are then modified by appropriate functions of eccenticity, apparent azimuth and vertical-radial phase difference according to how closely each particular component satisfies expected theoretical patterns for Love and Rayleigh wave motion. Using these modified amplitude coefficients, the time series is reconstructed so that the filtered trace is obtained over the original time window. The window is then advanced along the record and the calculations are repeated.

Chapter 4 describes this process in more detail. The polarization filter described by Flinn (1965) is considered in Chapter 3. Examples of records processed by these methods are presented. A new seismic system developed at the University of Alberta which records directly onto digital tape, is described in Chapter 2. Examples of three component recordings from this system are also given.

CHAPTER 2

A WIDE-BAND SEISMOGRAPH SYSTEM

2.1 Characteristics of Standard Seismographs

The wide-band spectral characteristics of seismic arrivals from earthquakes as well as the dominant peak in microseismic background level for the 5 - 8 second period range was described in section 1.1. A seismograph system which has broad-band frequency characteristics and which at the same time attenuates energy in the region of major microseisms is thus most desirable for any seismological observatory.

To meet these criteria, many seismograph stations employ both a short and a long period recording system. The instruments are designed so that the long period end of the short period system, and the short period cut-off of the long period system attenuate the major microseismic band. In most cases, seismometer output is recorded on photographic paper by means of a light spot deflection of a galvanometer. The frequency characteristics of such systems are dependent entirely on the natural resonant period and damping constants of both the seismometer and the galvanometer.

Although the short period instrumentation is

generally found to be adequate, realization of mechanical constants required to obtain long period operation of galvanometers and seismometers make it difficult to extend the long period sensitivity much higher than about 150 seconds. Such low frequency characteristics necessitate the use of large and heavy galvanometer coils requiring great amounts of power to produce a given deflection, or seismometers with very large masses.

2.2 Use of Feedback

Electrical feedback may be used to alter the characteristics of a seismograph. Many methods utilize an electromagnetic transducer which couples the seismometer frame and suspended mass (Tucker, 1958; Willmore, 1961; de Bremaecker et al, 1962; Sutton and Lathan, 1964). The feedback current, i, flowing in the transducer coil causes a mass motion equivalent to a ground acceleration gi/m where g is the transducer constant and m the suspended mass. The effect of this simulated ground acceleration is an alteration of the characteristics of the system, the extent of the alteration being dependent upon the transfer function of the feedback loop as well as the transfer function of the system without feedback.

Willmore (1961) describes a system in which the natural periods of the seismometer and galvanometer are close

together near the center of the total response curve. The desired bandwidth is obtained by means of negative electrical feedback to the seismometer. The amount of this feedback is proportional to the velocity of the galvanometer spot deflection. A seismograph constructed with this type of feedback using a seismometer and galvanometer each with a natural period of 20 seconds is shown to have an almost flat velocity response from 0.5 to 800 seconds.

Russell et al (1968) eliminate the need of a transducer as input terminals for the application of negative feedback by incorporating the seismometer in a balanced Maxwell impedance bridge. Voltage applied to the bridge input terminals simulates a ground acceleration and allows the introduction of a feedback loop. This applied voltage is the output of the seismometer modified by the transfer function of the feedback loop. Such feedback may be used to control individually the mass, spring constant and damping constants of the seismometer. The feedback arrangement is shown to increase the resonant period of a Willmore Mark I seismometer from 1 to nearly 5 seconds. It should be pointed out however, that although these methods may be effectively used to alter the transfer characteristics of a seismograph system, no improvement in signal to noise ratio is possible through the use of such feedback.

2.3 Wideband Response By Filtering

Wideband frequency characteristics may also be realized by filtering the seismometer output. Pomeroy et al (1969) describe a system in which the motion of a pendulum with a natural period of 34 seconds, critically damped, is monitored by an electromagnetic (velocity) transducer which drives a galvanometer-phototube amplifier system. The galvanometer (also critically damped) has a natural period of 100 seconds. The amplified output is filtered and recorded photographically as well as by a strip chart recorder. Two different filters may be used.

Comparison is made with records of an event recorded by a conventional electromagnetic seismograph at the same location. The mechanical constants of this system are the same, but no amplification is used. The higher gain system is shown to have recorded several long period body phases not detected by the conventional seismograph. Rigid environmental control however, is required for the high gain, long period operation and the system is enclosed in an air-tight chamber in a deep mine.

At this university, an amplifier has been designed by M. D. Burke in the Geophysics electronic laboratories for use with a Willmore Mark II seismometer. The usable velocity sensitivity of the seismometer having a natural period of 1.5

seconds and damping 0.6 critical is extended out to the 40 second period range under normal environmental conditions.

The desired system response is obtained by the use of second order active R-C network filters following a design criterion described by Sallen and Key (1955). Employing low noise operational amplifiers, a differential filtering technique is used to separate broad-band and long period data, amplify the long period data to compensate for the drop in sensitivity due to the seismometer, and then recombine the signals. The two signals may be summed in phase or 180° out of phase so that microseismic enhancement or attenuation can be obtained.

Figure 2.1 shows the measured frequency and phase response of the amplifier itself. The dashed line indicates the case of "in phase" summation while the solid curve displays the attenuation available in the region of peak microseismic background when the two signals are summed in opposition. With appropriate choice of circuit components this summation point may be placed at any particular period, thus adapting the amplifier to the predominant background present at one particular recording site.

In figure 2.2 we see theoretical asymptotes for the velocity sensitivity of the complete system (seismometer and amplifier). Comparison is made with the calibra-

Figure 2.1 Tripartite system amplifier frequency and phase response. The dotted line indicates the case of 'in phase' summations, the solid line the case of 'out of phase' summation for microseismic attenuation.

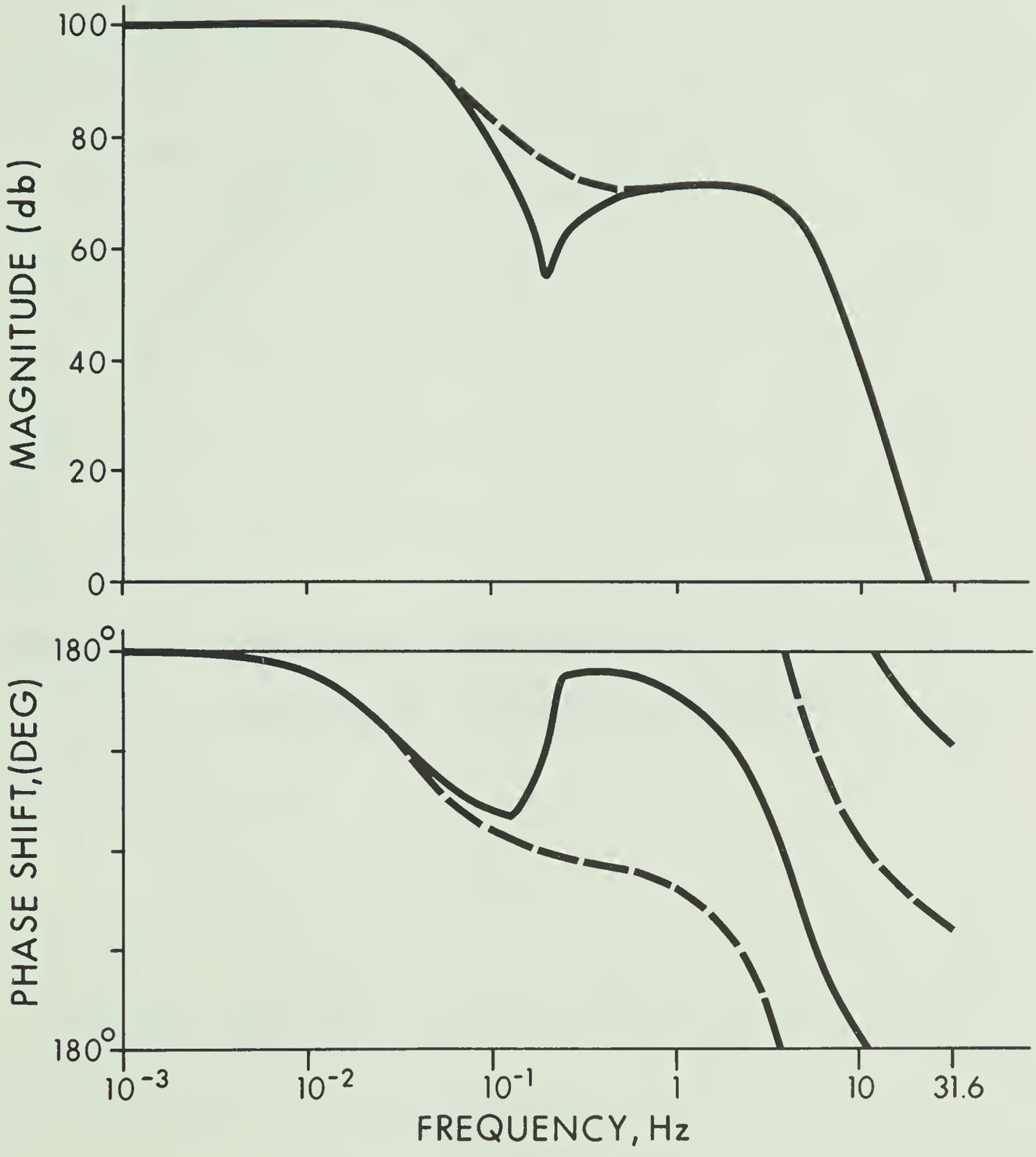
100
80
60
40
20
0
MAGNITUDE (db)
180°
180°
PHASE SHIFT,(DEG)
10 -3
10 -2
10 -1
1
10
31.6
FREQUENCY, Hz

Figure 2.2 Theoretical asymptotes for the tripartite seismometer - amplifier combination.

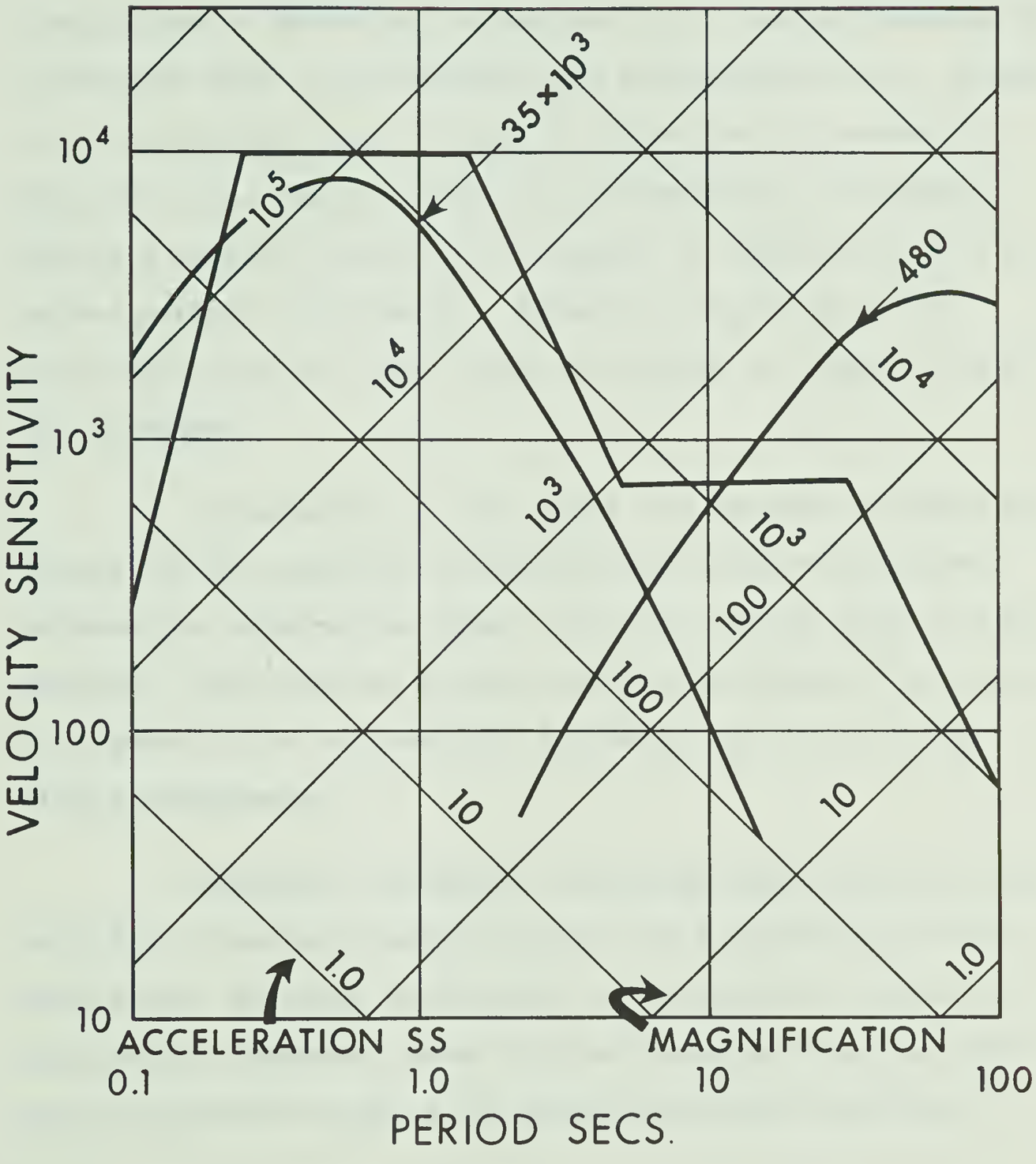
VELOCITY SENSITIVITY
10^4
10^3
100
10
35×10^3
10^5
480
10^4
10^4
10^3
10^3
100
100
10
10
1.0
1.0
ACCELERATION SS
MAGNIFICATION
0.1
1.0
10
100
PERIOD SECS.

tion curves of the Edmonton seismograph station operated as part of the Dominion Observatory network. Instrumentation in this case consists of the standard seismometer-galvanometer combination as described in Section 2.1. Natural periods of a Willmore Mark II seismometer and galvanometer are 1 second and 0.24 seconds respectively for short period recording, while for long period operation a Press-Ewing seismometer having a natural period of 29 seconds is combined with a 95 second period galvanometer. Extension of the Willmore characteristics for long period operation is exemplified by this diagram.

Intersection of the short and long period response curves for the Edmonton station indicate the microseismic attenuation obtained at about 7 seconds period using the two systems. With the new system, similar attenuation as shown in figure 2.1 is available by filtering the output of a single seismometer.

Appendix I presents a detailed description of the amplifier transfer function as well as a derivation of the theoretical velocity sensitivity curve shown in figure 2.2. Theoretical response curves for the transfer function have been calculated using an APL program and are also given.

2.4 Digital Recording System

A field operable digital recording system designed

for three data channels has also been developed in the Geophysics electronic laboratories at this university, for use in conjunction with the analog instrumentation just described. Figure 2.3 shows a block diagram of the system.

A successive approximation analog to digital convertor is used to produce an 11 bit binary word, including sign, from the input voltage. When conversion is complete, the binary word is transferred to a storage register and an end of conversion (E.O.C.) pulse is used to switch to the next data channel. The next conversion is made while the previous word is being written onto digital tape. After A-D conversion of the third channel signal, an end of frame pulse (E.O.F.) generates a flag bit which is written, as the 12th bit, onto tape with the binary word. This flag bit is used for channel identification when the tape is processed.

The recording is made on a seven track incremental transport. Two seven bit characters are written for each conversion. The first character consists of six bits of the binary word (most significant bits, including sign) and a parity bit. The last five bits of the binary word, channel identification and parity bit are written as the second character. Odd parity is used.

A crystal oscillator whose output is divided down

Figure 2.3 Block diagram of the digital recording system.

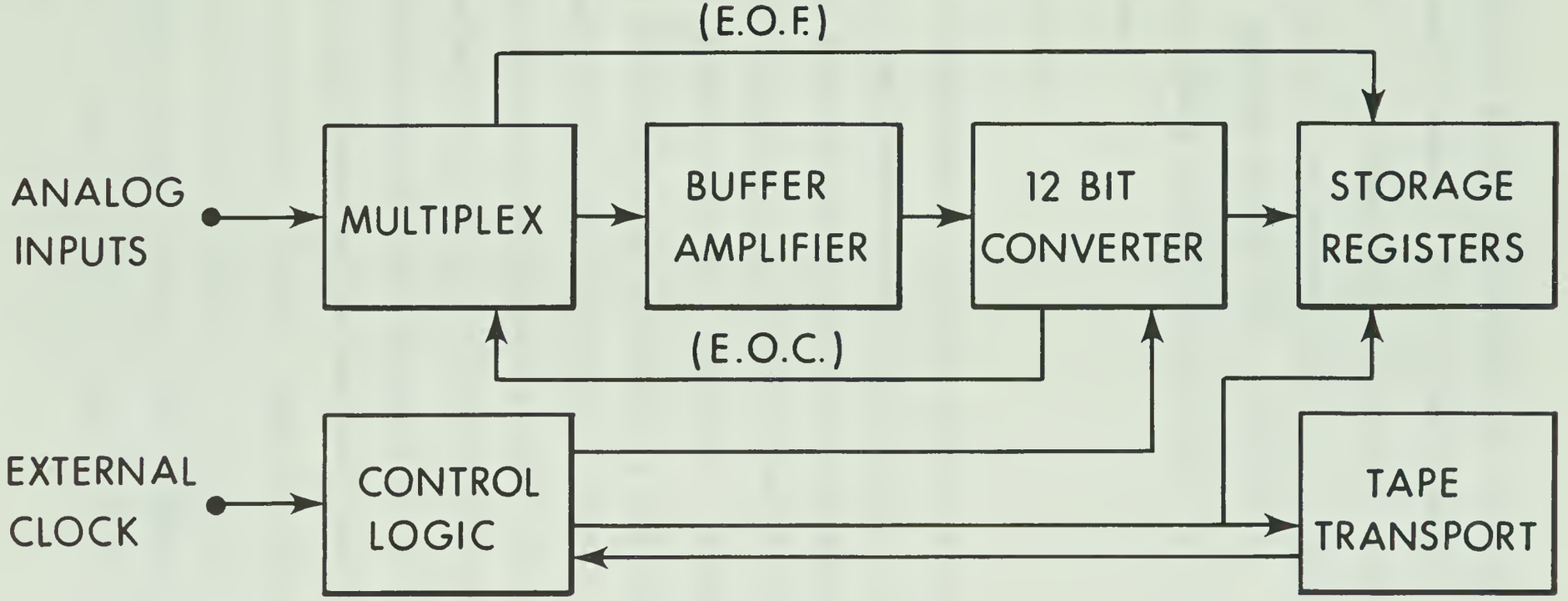
(E.O.F.)
ANALOG INPUTS
MULTIPLEX
BUFFER AMPLIFIER
12 BIT CONVERTER
STORAGE REGISTERS
(E.O.C.)
EXTERNAL CLOCK
CONTROL LOGIC
TAPE TRANSPORT

to 400 Hz controls pulse switching and was used to drive the incremental tape transport at 50 steps/second. With the two character word, 25 conversions/second are made so that a sampling rate of 8.33/second/channel is obtained. An inter-record gap is written every 6144 conversions. Write-time for this gap is short enough so that only one data point per channel is lost.

2.5 Recorded Data

Three components of ground motion (vertical, east-west horizontal and north-south horizontal) for a number of seismic events were obtained while the system described above was operated over a period of several months at the seismological observatory near Edmonton. Recording at 556BPI with a Digi-Data tape transport, the system could operate unattended for approximately 3 days. Helicorder records of the vertical component served as an analog monitor for determining which of the digitized data was to be used. Initial processing consisted of an unpacking procedure which transferred the sampled data from seven track field tape to nine track digital tape for use with an IBM 360/67 computer at the University of Alberta Computing Center. A Calcomp plotter output of the three component records was then produced so that a visual display of the digitized data was obtained.

Figure 2.4 illustrates such an event from a magnitude 5.9 earthquake which occurred near Taulaud Island in the Philippines on January 30, 1969. Universal time is indicated on the record. An epicentral distance of 103° was calculated using CGS preliminary co-ordinates. Arrival times of body phases as predicted by the Jeffreys-Bullen tables were determined. A well defined P-coda is indicated on the Z component, followed by good quality PP and PPP arrivals. The CGS depth determination of 70 kilometers was used for pP time.

Events indicated in the figure as P_1, P_2 and P_3 show good correlation with their respective pP, PP and PPP arrivals. At an epicentral distance of 103°, the original compressional pulse undergoes diffraction at the earth's core. The PP phase since it does not penetrate as deeply, but rather is reflected once at the surface, is not diffracted. Scattering of energy due to the diffraction is illustrated by the initial P phase and its coda which exhibit lower amplitude than the later PP phases which traverse the crust and mantle.

The SKS-SKKS-S group of waves are easily identified on the North and East horizontal components. Multiply reflected PKKP, PKKS and a particularly clear SKKKS arrival on the East component, as well as SS and PPS phases, are indicated on the record. The onset of

Figure 2.4 Digital recording of a magnitude 5.9 earthquake which occurred in the Philippines on January 30, 1969. Δ = 103°. Universal time is indicated in the figure. Various events have been identified on the basis of predicted travel-times.
Δt = 0.12 seconds.

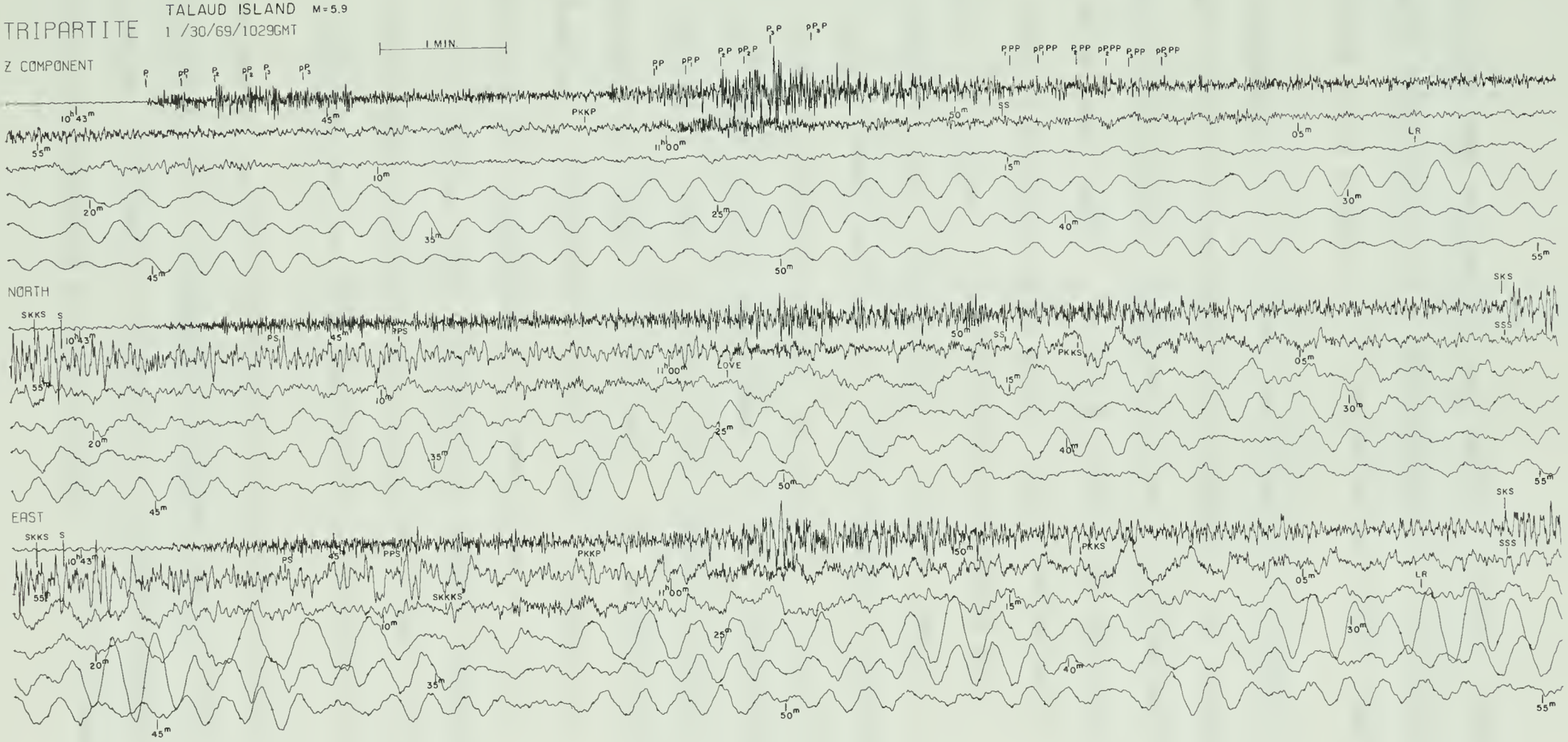
TRIPARTITE
TALAUD ISLAND M=5.9
1 /30/69/1029GMT
1 MIN.
Z COMPONENT
NORTH
EAST
PKKP
SS
LR
LOVE
SKKS
PS
PPS
SKS
SSS
PKKS

long period Love and Rayleigh (LR) waves are also shown. Periods range from about 35 - 40 seconds at the beginning of the surface wave train to 20 seconds at later times.

A comparison of another earthquake detected by this system with the same event recorded by the standard seismometer-galvanometer combination onto photographic paper has also been made. In this case, the data was first processed with a digital zero phase shift Butterworth filter using a Fortran IV subroutine developed by T. Alpasan (1968) at this university. A short period (0.25 - 5 seconds) and a long period (5 - 150 seconds) pass-band have been used in order to match as closely as possible the short and long period responses of the conventional system. Figures 2.5 and 2.6 show the impulse and amplitude response of these two filters. In actual practice, the gain factor introduced by the filter process is removed so that the response is normalized to unity. Figure 2.7 illustrates the theoretical system response obtained using these filters and compares these curves with the calibration for the conventional instrumentation.

The short period seismogram from the standard system and the 0.25 - 5 seconds filtered record from the digital system is shown in figure 2.8 (traces marked U.A.). The event is a magnitude 5.4 earthquake at an epicentral

Figure 2.5 Impulse and amplitude response of a 0.2-4.0 Hz digital zero phase shift Butterworth filter. The impulse response has been computed for 512 points. $\Delta t=0.12$ seconds.

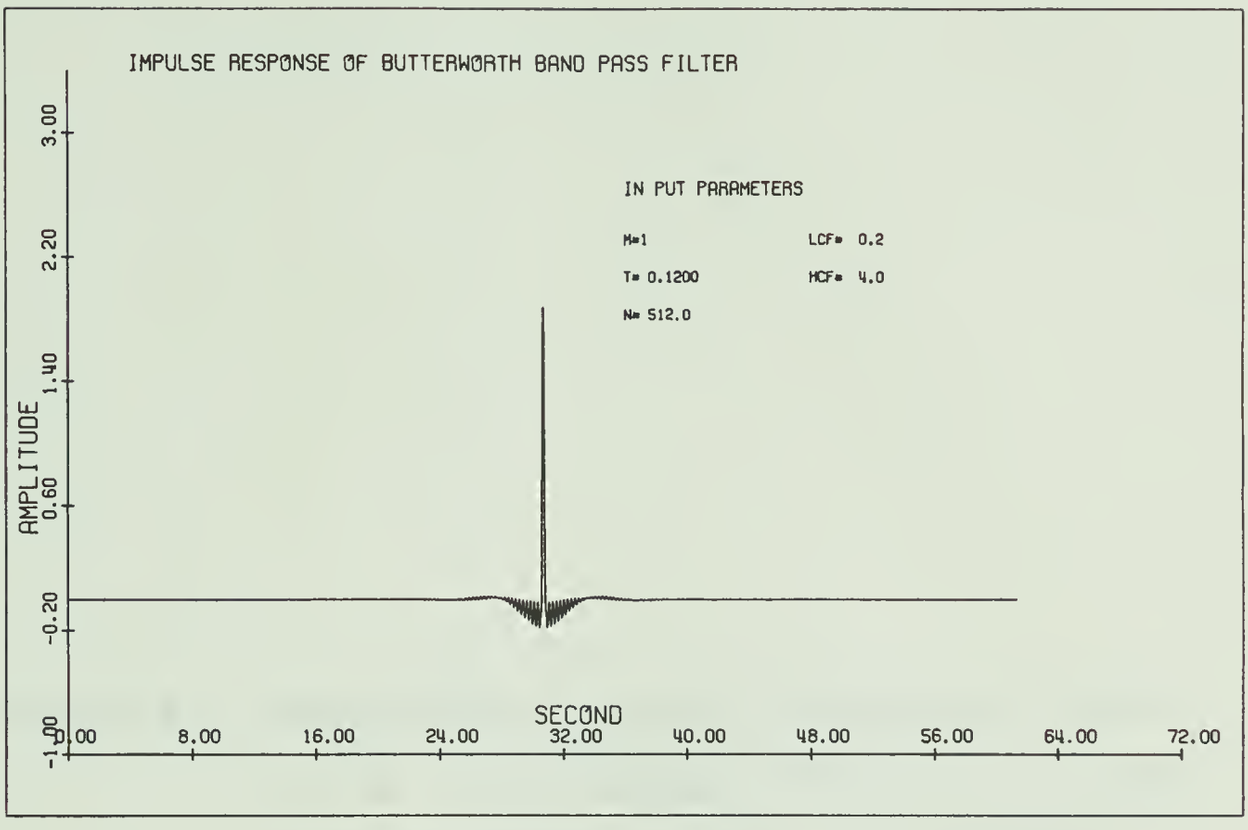
IMPULSE RESPONSE OF BUTTERWORTH BAND PASS FILTER
IN PUT PARAMETERS
M=1
LCF= 0.2
T= 0.1200
HCF= 4.0
N= 512.0
AMPLITUDE
3.00
2.20
1.40
0.60
-0.20
-1.00
SECOND
0.00
8.00
16.00
24.00
32.00
40.00
48.00
56.00
64.00
72.00

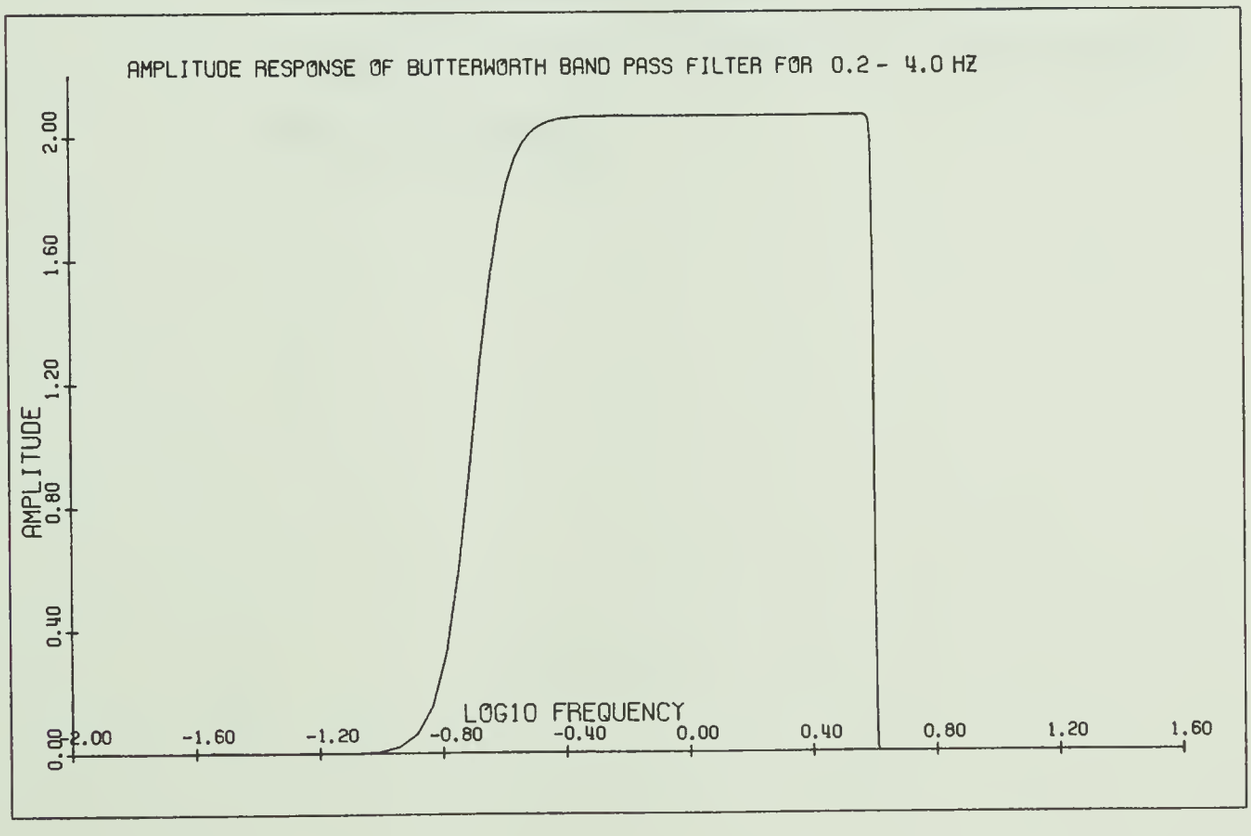
AMPLITUDE RESPONSE OF BUTTERWORTH BAND PASS FILTER FOR 0.2 - 4.0 HZ
AMPLITUDE
2.00
1.60
1.20
0.80
0.40
0.00
LOG10 FREQUENCY
-2.00
-1.60
-1.20
-0.80
-0.40
0.00
0.40
0.80
1.20
1.60

Figure 2.6 Impulse and amplitude response of a 0.007-0.2 Hz (5-150 seconds) digital zero phase shift Butterworth filter. The impulse response has been computed for 2048 points. Δt=0.12 seconds.

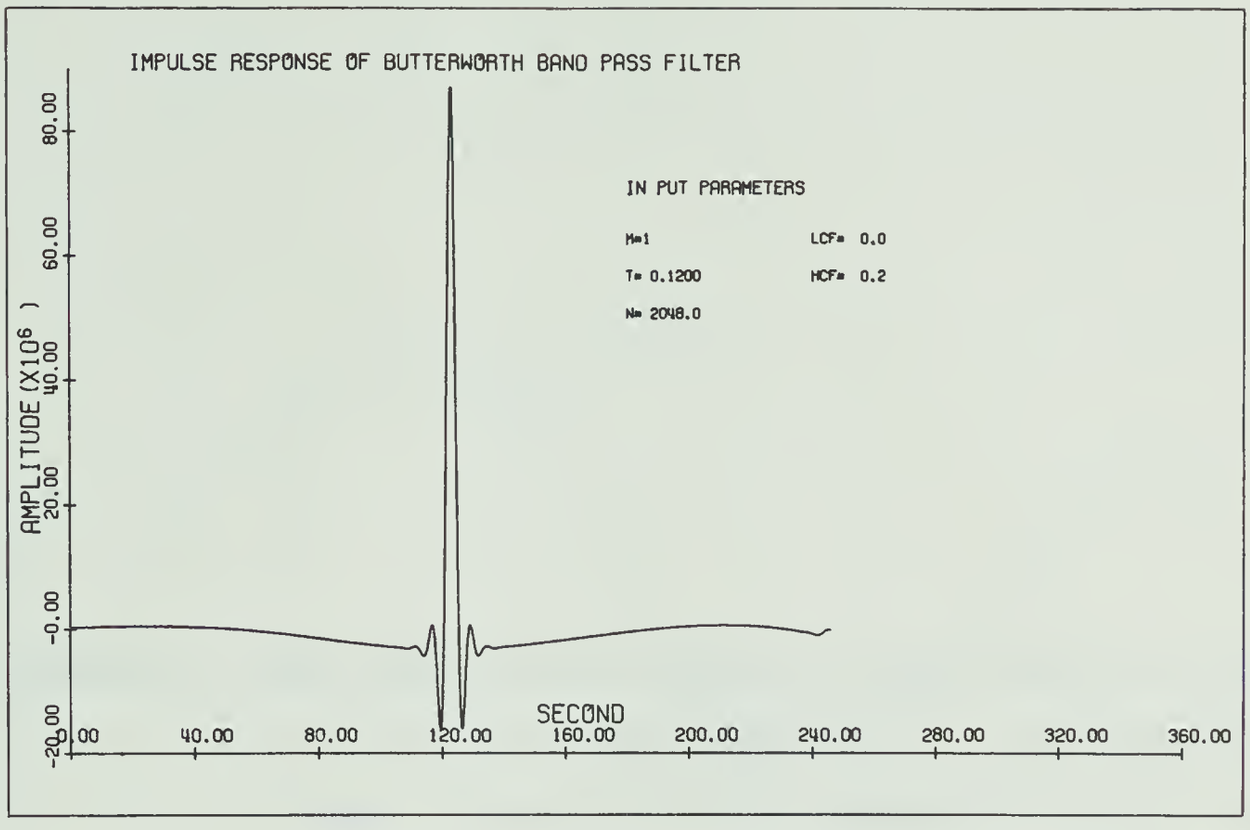
IMPULSE RESPONSE OF BUTTERWORTH BAND PASS FILTER
IN PUT PARAMETERS
M=1
LCF= 0.0
T= 0.1200
HCF= 0.2
N= 2048.0
AMPLITUDE (X10^6)
80.00
60.00
40.00
20.00
-0.00
-20.00
SECOND
0.00
40.00
80.00
120.00
160.00
200.00
240.00
280.00
320.00
360.00

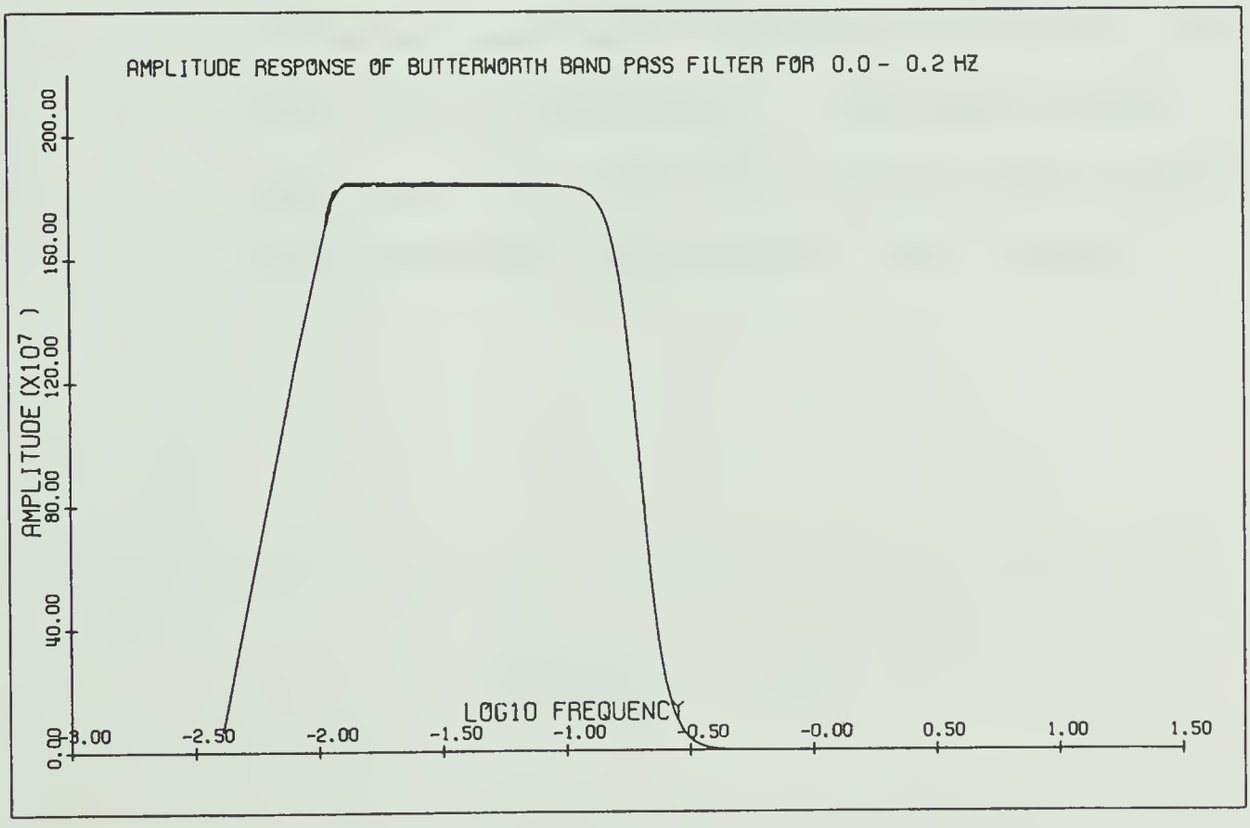
AMPLITUDE RESPONSE OF BUTTERWORTH BAND PASS FILTER FOR 0.0 - 0.2 HZ
AMPLITUDE (X10^7)
200.00
160.00
120.00
80.00
40.00
0.00
LOG10 FREQUENCY
-3.00
-2.50
-2.00
-1.50
-1.00
-0.50
-0.00
0.50
1.00
1.50

Figure 2.7 The effect of the digital filters shown in figures 2.5 and 2.6 on the asymptotes for the tripartite system. The solid curve marked T.S. is for the 0.2-4 Hz pass-band; the dashed curve for the 0.007-0.2 Hz pass-band. The smooth curves represent the calibration of the short period (Willmore) and long period (P-E) systems.

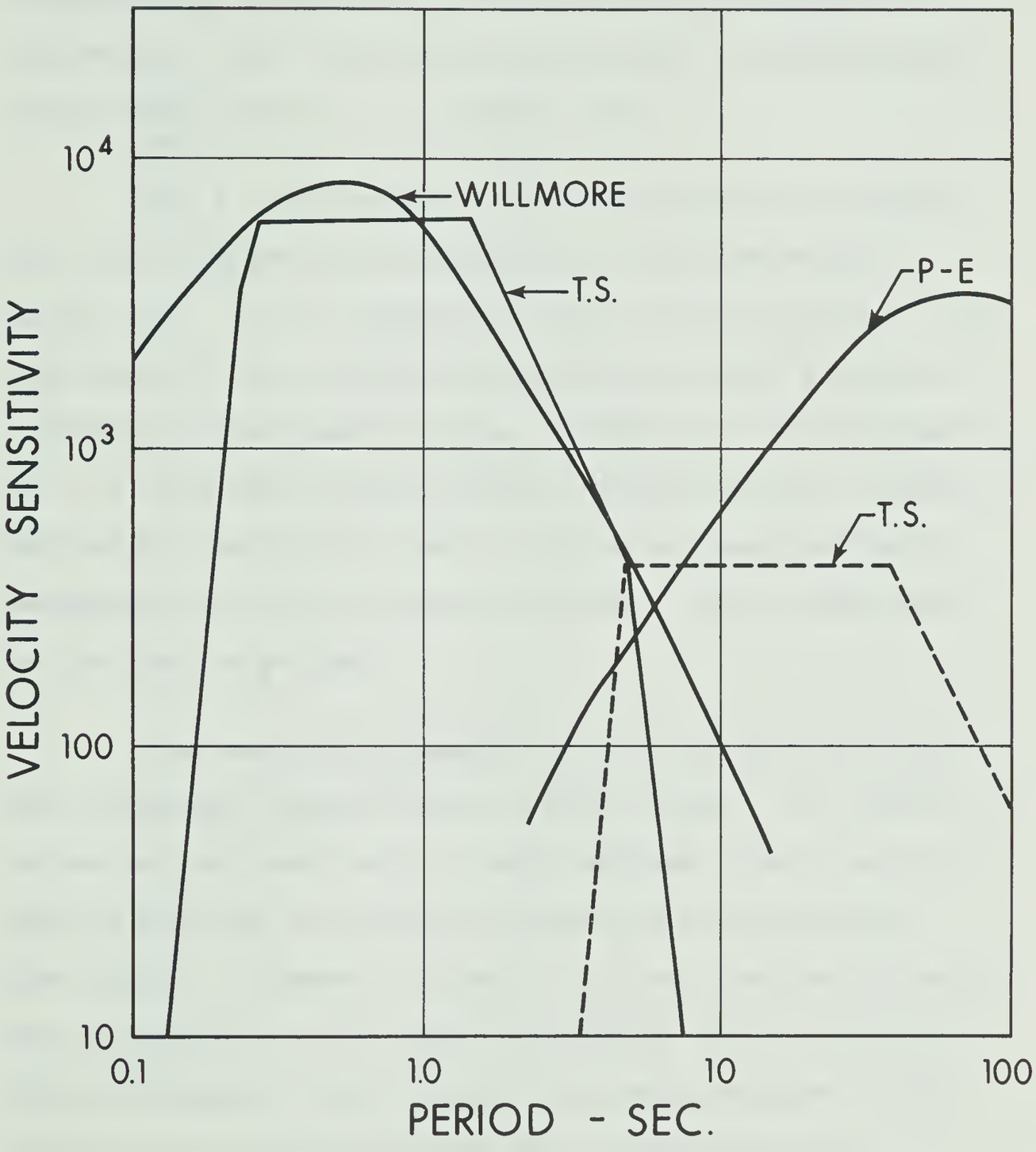
VELOCITY SENSITIVITY
10^4
10^3
100
10
WILLMORE
T.S.
P-E
T.S.
0.1
1.0
10
100
PERIOD - SEC.

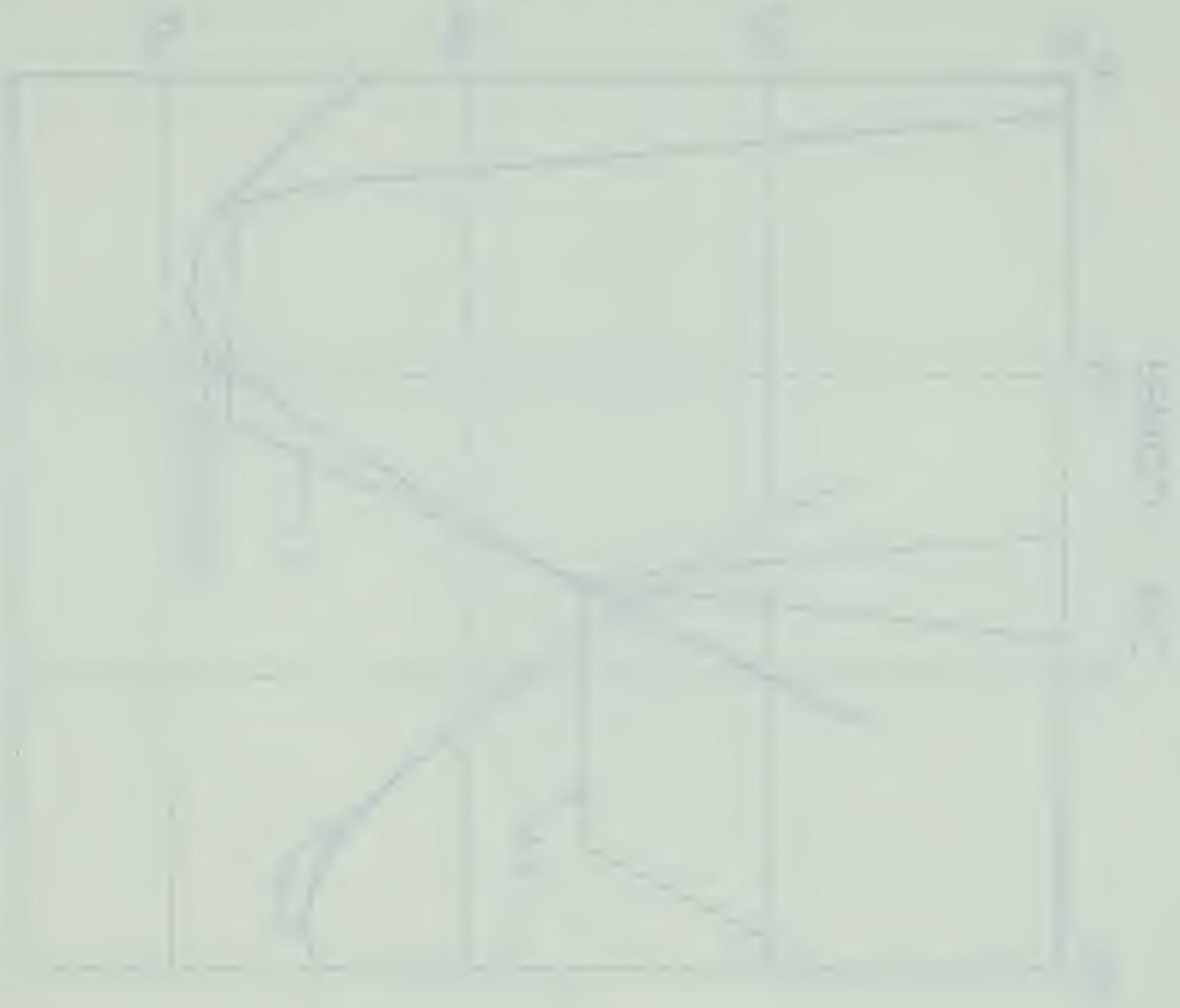

distance of 22° which occurred in the Gulf of California on March 21, 1969. Predicted arrival times of P, PP and PPP compressional phases for a surface-focus earthquake are indicated. Since the depth of the event is undetermined, these times may be 2 - 5 seconds late.

The 5 - 150 seconds filtered record is compared with the long period seismogram for the same event in figure 2.9. To aid comparison, the original vertical (Z) component of the conventional system is shown along with tracings of the three records. Predicted arrival times of P, S, P_cP and S_cS body phases are indicated. A well defined LR (Rayleigh) onset is shown on the Z and North components and the LQ (Love) surface train is indicated on the East recording.

The examples presented here illustrate the wide-band recording capabilities of this system. In figure 2.4 we see on the same record a well defined, short period P-coda as well as long period surface Love and Rayleigh wave trains. Figures 2.8 and 2.9 illustrate how filtering may be applied to the wide-band digital data so that any desired frequency band within the total response of the system may be extracted from the original record. Although this system does not extend out to the very long periods, the wide-band frequency characteristics and good

Figure 2.8 Comparison of the conventional short period seismogram with the 0.2-4 Hz filtered digital record indicated by the traces marked U.A. Three components of ground motion are shown. The earthquake of magnitude 5.4 occurred in the Gulf of California on March 21, 1969 at $04^{h}56^{m}20^{s}$ UT. Universal time is indicated. $\Delta=22°$.

GULF OF CALIFORNIA M=5.4, MARCH 21, 1969

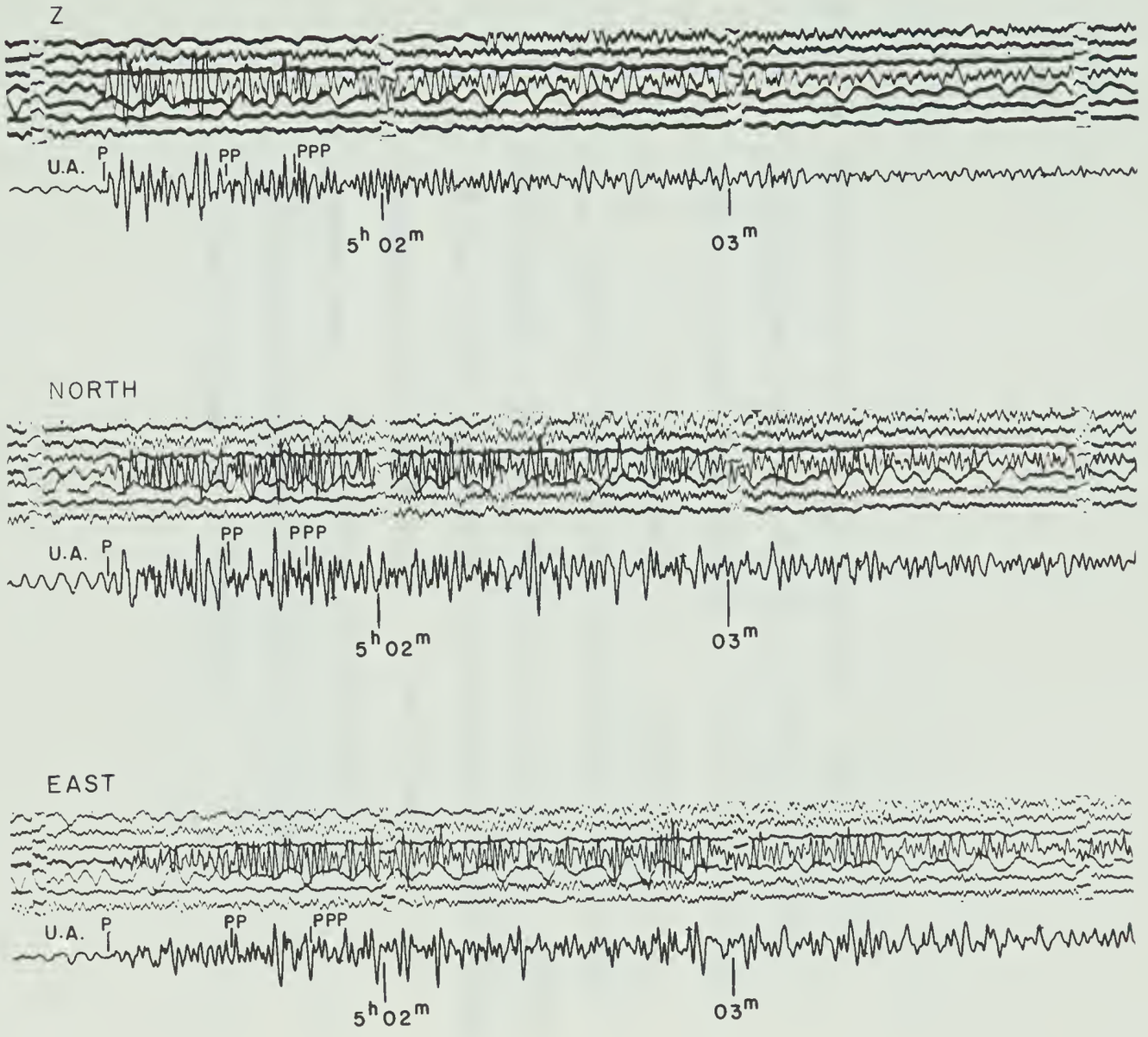

Figure 2.9 Comparison of the conventional long period seismogram with the 5-150 second filtered digital record indicated by the traces marked U.A. The first record is a reproduction of the original vertical photographic recording. The second, fourth and sixth traces are copies of the three component photographic seismograms presented beside the U.A. recordings to aid comparison. The event is the same Gulf of California earthquake shown in figure 2.8. Universal time is indicated.

GULF OF CALIFORNIA M=5.4, MARCH 21, 1969

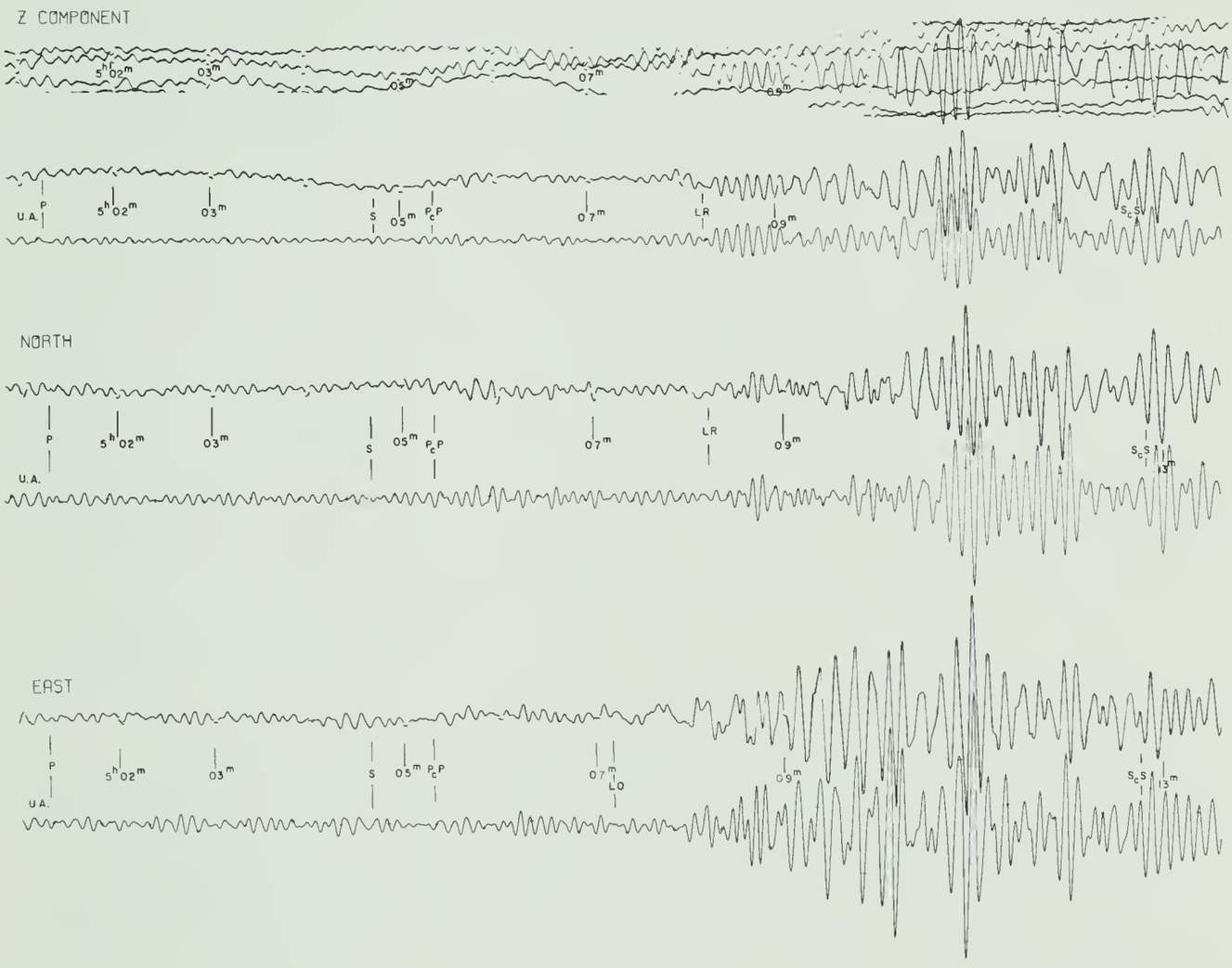

dynamic range available, along with its adaptability for operation in the field show it to be very valuable for the detection and interpretation of seismic events.

CHAPTER 3

A TIME DOMAIN POLARIZATION FILTER

3.1 Introduction

Particle motion trajectories, and the polarization characteristics of body phases and surface wave groups have been discussed in Chapter 1. A number of time-varying nonlinear processors which utilize these polarization properties to enhance the signal to noise ratio of a seismogram have been described (Shimshoni and Smith, 1964; Mims and Sax, 1965; Flinn, 1965; Fuch, 1969). In this chapter, a processor which can be particularly useful for enhancement of the shorter period body phases is discussed in more detail, and examples of records processed with this filter are presented.

Since the data was recorded using vertical, east-west and north-south horizontal detectors as described in the previous chapter, the two horizontal components of ground motion were first rotated so that a radial and a transverse record were obtained. To do this, the expected great circle azimuth from source to receiver was computed and a transformation applied to the data. If ϕ is the expected azimuth measured clockwise from North, then the transformation of co-ordinates is given by

$$R = E \sin \phi + N \cos \phi$$
$$T = -E \cos \phi + N \sin \phi \qquad (3.1)$$

where E and N represent the east-west and north-south components of ground motion respectively. Figure 3.1 illustrates this transformation. The new co-ordinate system is right-handed so that R x T = Z, with Z up being positive.

3.2 The Covariance Matrix

Adopting the method described by Flinn (1965), a polarization filter that considers both rectilinearity and direction of particle motion has been developed. In order to obtain measures of these two quantities, the covariance matrix for a set of N points taken over each of the three orthogonal components of ground motion, R, T and Z, is computed. A specified time window of length $N\Delta t$, where Δt is the sampling interval, is thus considered. To determine the covariance matrix for this set of observations, the means, variances and covariances must be calculated for the three variables R, T and Z.

We define the mean or expected value of N observations of the random variable W as

$$\mu_W = \frac{1}{N} \sum_{i=1}^{N} w_i = E(W) \qquad (3.2)$$

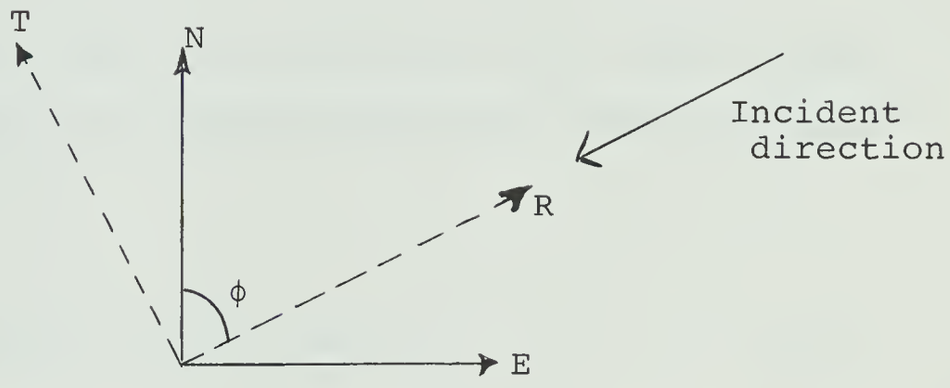

Figure 3.1 Illustration of the transformation of seismometer co-ordinates so that the east-west and north-south components of ground motion are rotated into a radial-transverse configuration. The expected great circle azimuth is the angle ϕ measured clockwise from North.

The covariance between N observations of two variables x_1 and x_2 is given by

$$\mathrm{Cov}[X_1, X_2] = E[\,(X_1 - E(X_1))(X_2 - E(X_2))\,] \tag{3.3}$$

which by equation 3.2 can be written

$$\mathrm{Cov}[X_1, X_2] = \frac{1}{N} \sum_{i=1}^{N} (x_{1i} - \mu_1)(x_{2i} - \mu_2) \tag{3.4}$$

It is evident that $\mathrm{Cov}[X_1, X_2] = \mathrm{Cov}[X_2, X_1]$. The quantity $\mathrm{Cov}[X_1, X_1]$ is defined as the variance of x_1 and by equation 3.4 may be written as

$$\mathrm{Var}[X_1] = \frac{1}{N} \sum_{i=1}^{N} (x_1 - \mu_1)^2 \tag{3.5}$$

The matrix with $\mathrm{Cov}[X_\gamma, X_s]$ in its γ^{th} row and s^{th} column ($\gamma, s = 1, 2, \cdots n$) is the covariance matrix for the set of n random variables X_j, $j = 1, 2, \cdots n$. If $\bar{X}$ is the vector of the random variables and $\bar{\mu}$ the vector of means for each of these variables, the covariance matrix V is defined by (Jenkins and Watts, Chapter 3)

$$V = E[\,(\bar{X} - \bar{\mu})(\bar{X} - \bar{\mu})^t] \tag{3.6}$$

The superscript t indicates the column transpose of the vector. This can be written as

$$V = \begin{bmatrix} \mathrm{Var}[X_1] & \mathrm{Cov}[X_1,X_2] & \cdots & \mathrm{Cov}[X_1,X_n] \\ \mathrm{Cov}[X_2,X_1] & \mathrm{Var}[X_2] & \cdots & \mathrm{Cov}[X_2,X_n] \\ \vdots & & & \\ \mathrm{Cov}[X_n,X_1] & \mathrm{Cov}[X_n,X_2] & \cdots & \mathrm{Var}[X_n] \end{bmatrix} \qquad (3.7)$$

where the covariances and variances are defined in equations 3.4 and 3.5. As $\mathrm{Cov}[X_i,X_j] = \mathrm{Cov}[X_j,X_i]$ this matrix is symmetric about the main diagonal. For our case of three variables R, T and Z considered over the time window $N\Delta t$, equation 3.7 is written

$$V = \begin{bmatrix} \mathrm{Var}[R] & \mathrm{Cov}[R,T] & \mathrm{Cov}[R,Z] \\ \mathrm{Cov}[R,T] & \mathrm{Var}[T] & \mathrm{Cov}[T,Z] \\ \mathrm{Cov}[R,Z] & \mathrm{Cov}[T,Z] & \mathrm{Var}[Z] \end{bmatrix} \qquad (3.8)$$

3.3 Measures of Rectilinearity and Direction

If the covariance matrix given by equation 3.8 is diagonalized, an estimate of the rectilinearity of particle motion trajectory over the specified time window can be obtained from the ratio of the principal axes of this matrix. The direction of polarization may be measured by considering the eigenvector of the largest principal axis. Since the eigenvalues of V will lie along the principal axes, by computing the eigenvalues and their corresponding eigenvectors, the appropriate functions of rectilinearity

and directionality can be determined. To this end it was considered that if λ_1 is the largest eigenvalue, and λ_2 the next largest eigenvalue of the covariance matrix, then a function of the form

$$F(\lambda_1,\lambda_2) = 1-(\frac{\lambda_2}{\lambda_1})^n \qquad (3.9)$$

would be close to unity when rectilinearity is high ($\lambda_1 >> \lambda_2$) and close to zero when the two principal axes approach one another in magnitude (low rectilinearity). The direction of polarization can be determined by considering the components of the eigenvector associated with the largest eigenvalue with respect to the co-ordinate directions R, T and Z.

To illustrate this, figures 3.2a-d show some computations applied to sets of data in two dimensions. These points were computed for an ellipse and then perturbed by the addition of random noise. In 3.2b and 3.2d, the data points were generated from a 45° rotation of the original ellipse determined for 3.2a and 3.2b respectively. The computed covariance matrix, correlation coefficient ρ, $F(\lambda_1,\lambda_2)$ for n = 1, and the eigenvector of the principal axis, $\bar{E}$, is shown for each case. The correlation coefficient is determined from the usual definition (Jenkins and Watts, Chapter 3)

$$\rho_{12}^{2} = \frac{(\mathrm{Cov}[X_1, X_2])^2}{\mathrm{Var}[X_1]\mathrm{Var}[X_2]} \qquad (3.10)$$

Comparing 3.2a and 3.2b we see that in the first case, $\mathrm{Cov}[X_1, X_2]$ is small with respect to the variance terms on the main diagonal, and the eigenvector $\bar{E}$ indicates a preferred direction along the X_2-axis. In the second case, $\mathrm{Cov}[X_1, X_2]$ is larger and $\bar{E}$ = (0.726, 0.689) shows no preferred direction along either the X_1 or X_2 co-ordinate axis. In both instances, $F(\lambda_1, \lambda_2)$ is approximately the same. Similar properties of the covariance matrix and the eigenvector $\bar{E}$ are indicated by figures 3.2c and 3.2d, but here the rectilinearity, $F(\lambda_1, \lambda_2)$, is low in both cases. We see then that when the off-diagonal terms of the covariance matrix are significant, the diagonalization will introduce a rotation. After rotation, the orientation in space of the principal axis of the covariance matrix will be given by the components of its eigenvector relative to the original co-ordinate system. $F(\lambda_1, \lambda_2)$ will give an estimate of the degree of polarization along the major axis. In each of figures 3.2a-d, the data points could be considered as representing particle motion trajectory over a specified time in one of the orthogonal planes of the R, T, Z co-ordinate system.

Suppose now that in the matrix of equation 3.8, the covariance terms are small with respect to those on the

Figure 3.2 Computations of the covariance matrix, correlation coefficient ρ, $F(\lambda_1,\lambda_2)$ for n=1, and the eigenvector $\bar{E}$ of the principal axis of the covariance matrix for sets of 20 points in two dimensions. The data was generated by the addition of random noise to a perfect ellipse. Figures 3.2b and 3.2c represent rotations of the original ellipse by 45°.

3.2a

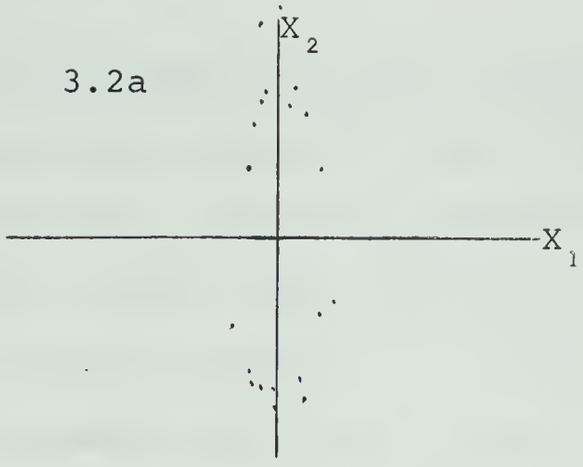

$$V = \begin{bmatrix} 1.317 & -0.237 \\ -0.237 & 26.510 \end{bmatrix}$$

$\rho = 0.040$

$F(\lambda_1, \lambda_2) = 0.950$

$\bar{E} = (-0.009, 0.999)$

3.2b

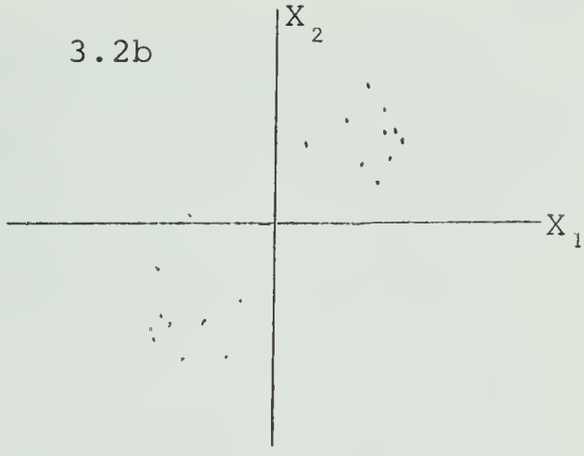

$$V = \begin{bmatrix} 13.775 & 11.756 \\ 11.756 & 12.519 \end{bmatrix}$$

$\rho = 0.895$

$F(\lambda_1, \lambda_2) = 0.945$

$\bar{E} = (0.726, 0.689)$

3.2c

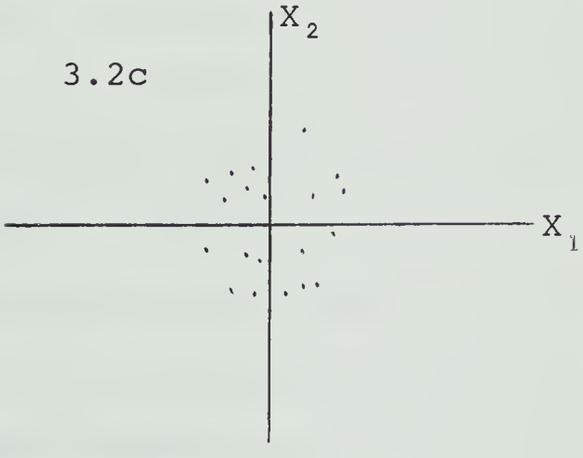

$$V = \begin{bmatrix} 2.416 & 0.221 \\ 0.221 & 3.426 \end{bmatrix}$$

$\rho = 0.077$

$F(\lambda_1, \lambda_2) = 0.318$

$\bar{E} = (0.205, 0.979)$

3.2d

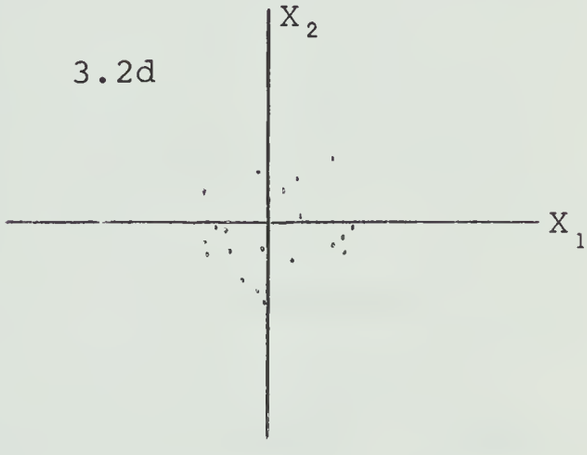

$$V = \begin{bmatrix} 2.803 & 0.420 \\ 0.420 & 3.085 \end{bmatrix}$$

$\rho = 0.143$

$F(\lambda_1, \lambda_2) = 0.262$

$\bar{E} = (0.584, 0.812)$

main diagonal, on which, Var[R]>Var[T]>Var[Z]. The two principal axes would thus correspond very closely to Var[R] and Var[T], and the eigenvector associated with the major axis, Var[R], would have its largest component in the R co-ordinate direction. If Var[R]>>Var[T], then $F(\lambda_1,\lambda_2)$ in equation 3.9 would be close to unity and we would have high rectilinearity in the R direction. If Var[R]$\sim$Var[T], then the direction of polarization would still be predominantly along the R co-ordinate axis, but the rectilinearity would be low. If the off-diagonal terms of the matrix were significant, the diagonalization would introduce a rotation, and the orientation in space of the major axis would be given by the components of its eigenvector relative to the original R, T, Z co-ordinate system. Depending on the amount of rotation necessary to produce this diagonalization, the rectilinearity would exhibit either a preferred direction or no preferred direction. By combining $F(\lambda_1,\lambda_2)$ and the appropriate eigenvector, we see that measures of rectilinearity and directionality can be obtained. Determination of a suitable filter function is then possible.

3.4 The Polarization Filter

Applying this analysis to the digital seismograms, the covariance matrix is computed for a specified time window of length $N\Delta t$ centered about t_o, where t_o is allowed to range over the entire record length of interest.

Eigenvalues and the corresponding eigenvectors of this matrix are then determined. The measure of rectilinearity for the time t_o is given by

$$RL(t_o) = [F(\lambda_1,\lambda_2)]^J \tag{3.11}$$

where $F(\lambda_1,\lambda_2)$ is defined in equation 3.9. If we represent the eigenvector of the principal axis with respect to the R, T, Z co-ordinate system by $\bar{E} = (e_1,e_2,e_3)$ then the direction functions at time t_o are given by

$$\begin{aligned} D_R(t_o) &= (e_1)^K \\ D_T(t_o) &= (e_2)^L \\ D_Z(t_o) &= (e_3)^M \end{aligned} \tag{3.12}$$

Since the eigenvector is normalized ($|\bar{E}| = 1$), we see that for each of these functions D_i

$$0 \leq D_i \leq 1 \tag{3.13}$$

The exponents J, K, L and M, as well as n (equation 3.9), are determined empirically. Once these functions are computed, the window is moved down the record one sample interval and the calculations are repeated. When the end of the desired record is reached, these quantities are then averaged over a window equal to about half the original window length. This has the effect of "smoothing" these operators so that contributions due to any anomolous spikes are subdued. If this time window consists of M points, the

gain functions are given by

$$RL^*(t_o) = \frac{1}{M} \sum_{\tau=-L}^{L} R(t_o+\tau)$$

$$D_i^*(t_o) = \frac{1}{M} \sum_{\tau=-L}^{L} D_i(t_o+\tau), i=R,T,Z \qquad (3.14)$$

$$L = \frac{M-1}{2}$$

The resulting operators are then used as a point by point gain control to modulate the rotated records so that at any time t, the filtered seismograms are given by

$$\begin{aligned} R_f(t) &= R(t) \cdot RL^*(t) \cdot D_R^*(t) \\ T_f(t) &= T(t) \cdot RL^*(t) \cdot D_T^*(t) \qquad (3.15) \\ Z_f(t) &= Z(t) \cdot RL^*(t) \cdot D_Z^*(t) \end{aligned}$$

In most cases, the data was band-pass filtered with a zero phase shift digital filter before rotation so that the spectral content of the record was known. The window length could be specified so as to be consistent with one or two cycles of the dominant period. Values of J, K, L and M which appeared quite adequate were 1,2,2,2 respectively. For rectilinearity, n = 0.5 or 1 was used.

3.5 Application of the Polarization Filter

A Fortran IV program has been written for this

polarization filter. The program is arranged so that window length for both the covariance matrix (equation 3.8) and the smoothing process (equations 3.14), starting point of calculations, and the exponents J, K, L, M and n can be specified as input data. The option of frequency filtering is also available. Figures 3.3 and 3.4 show two events processed by this method. The first example is of a magnitude 5.9 earthquake which occurred in the Philippines on January 30, 1969 at a depth of 70 kilometers, while the second is the nuclear test shot 'Benham' of magnitude 6.3, detonated in Nevada on December 19, 1968. The first three traces represent the vertical, radial and horizontal components of ground motion after rotation (equation 3.1), followed by the filter functions as given by equations 3.14. The last three represent the records after applying these operators as in equations 3.15. The filter functions and the processed records are displayed from the point in time where calculations began.

Data in figure 3.3 was band-pass filtered 0.3-4Hz before rotation. We see a good separation of events labeled P_1, P_2 and P_3 in the P,PP and PPP codas of the processed seismogram. The good correlation of these events with their respective pP times suggests a multiplicity of sources at the same location rather than a single release of energy. Attenuation of the radial and transverse traces,

Figure 3.3 Example of a magnitude 5.9 earthquake which occurred in the Philippines on January 30, 1969, processed by the polarization filter with J=1, K,L,M=2 and $F(\lambda_1,\lambda_2)=1-(\frac{\lambda_2}{\lambda_1})^{\frac{1}{2}}$. The event occurred at $10^h29^m40^s$UT. Universal time is indicated along the top of the figure. For this event, $\Delta=103°$. The first three traces are the vertical, radial and horizontal components of ground motion respectively; the next four represent the computed filter operators; the last three are the filtered seismograms. Data was band-pass filtered 0.3-4 Hz before rotation.

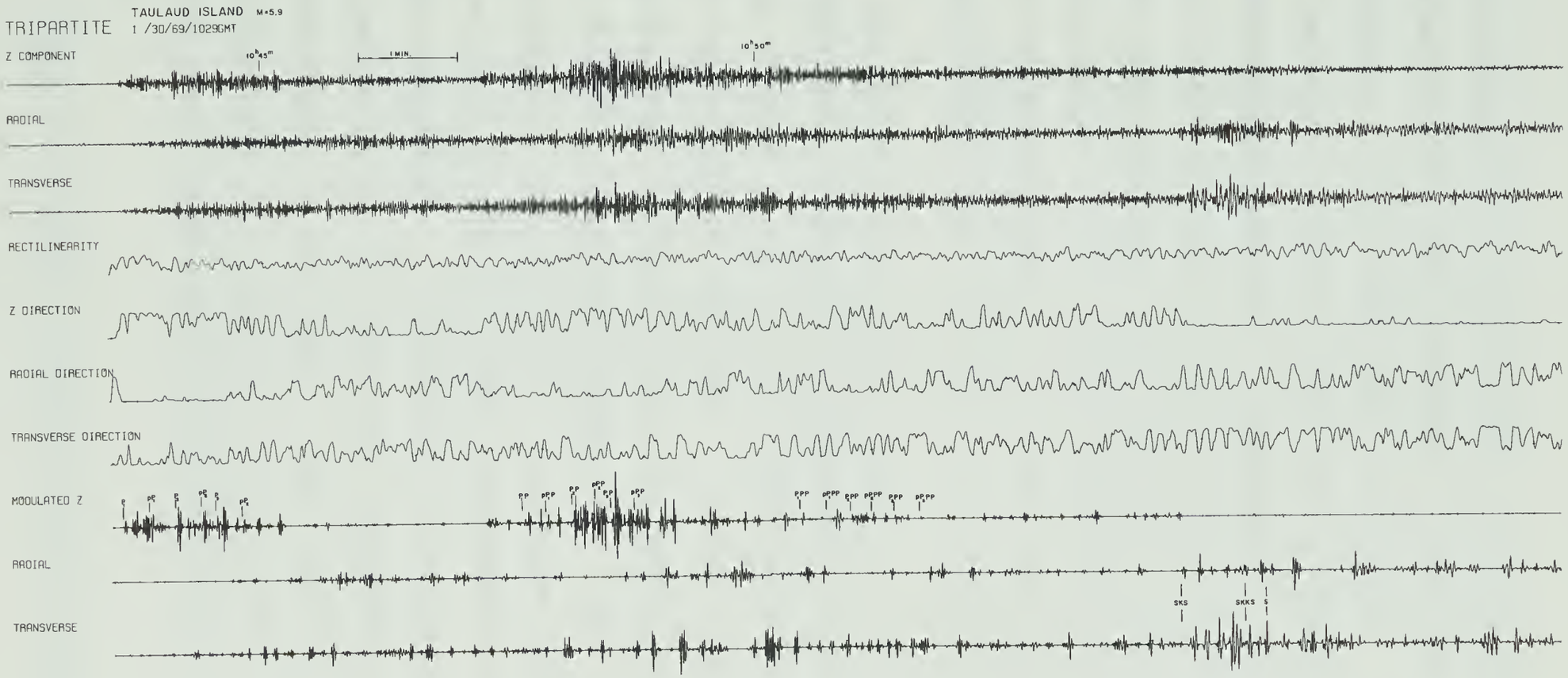
TRIPARTITE
TAULAUD ISLAND M=5.9
1 /30/69/1029GMT
Z COMPONENT
10h45m
1 MIN.
10h50m
RADIAL
TRANSVERSE
RECTILINEARITY
Z DIRECTION
RADIAL DIRECTION
TRANSVERSE DIRECTION
MODULATED Z
RADIAL
TRANSVERSE
SKS
SKKS
S

especially during the P and PP events illustrates how the filter enhances motion which exhibits a preferred direction of polarization, in this case, the Z direction. We note also the increase in signal on the two horizontal components and a corresponding decrease in the vertical trace at the beginning of the SKS-SKKS-S group of waves which has been identified using predicted times from the Jeffreys-Bullen travel-time curves. This is to be expected since little or no signal should be present on the vertical component of ground motion when shear (S) waves are predominant.

The nuclear test shot of figure 3.4 was recorded with microseismic attenuation as described in section 2.3. The effect of this is seen in the almost zero level signal before the beginning of the event. In this case, no digital filtering has been applied to the data before rotation. We see here that the processed records show a very simple P-coda, as would be expected from an explosive point source. Again, the shear phases (S,SS,SSS) are present only on the horizontal components. Of interest is the high level of activity exhibited by the radial and transverse records near the beginning of the event. These arrivals cannot be correlated with any predicted travel-times, but could possibly be due to body phase conversions near the recording station.

Figure 3.5 shows a particle motion diagram for the

Figure 3.4 The nuclear test shot 'Benham' detonated in Nevada at 16^h30^mUT on December 19, 1968, processed by the polarization filter with J=1, K,L,M=2 and $F(\lambda_1,\lambda_2)=1-(\frac{\lambda_2}{\lambda_1})^{\frac{1}{2}}$. Universal time is indicated along the top of the figure. The event was of magnitude 6.3, with $\Delta=16°$. The display of traces is the same as in figure 3.3. No band-pass filtering has been applied to the data.

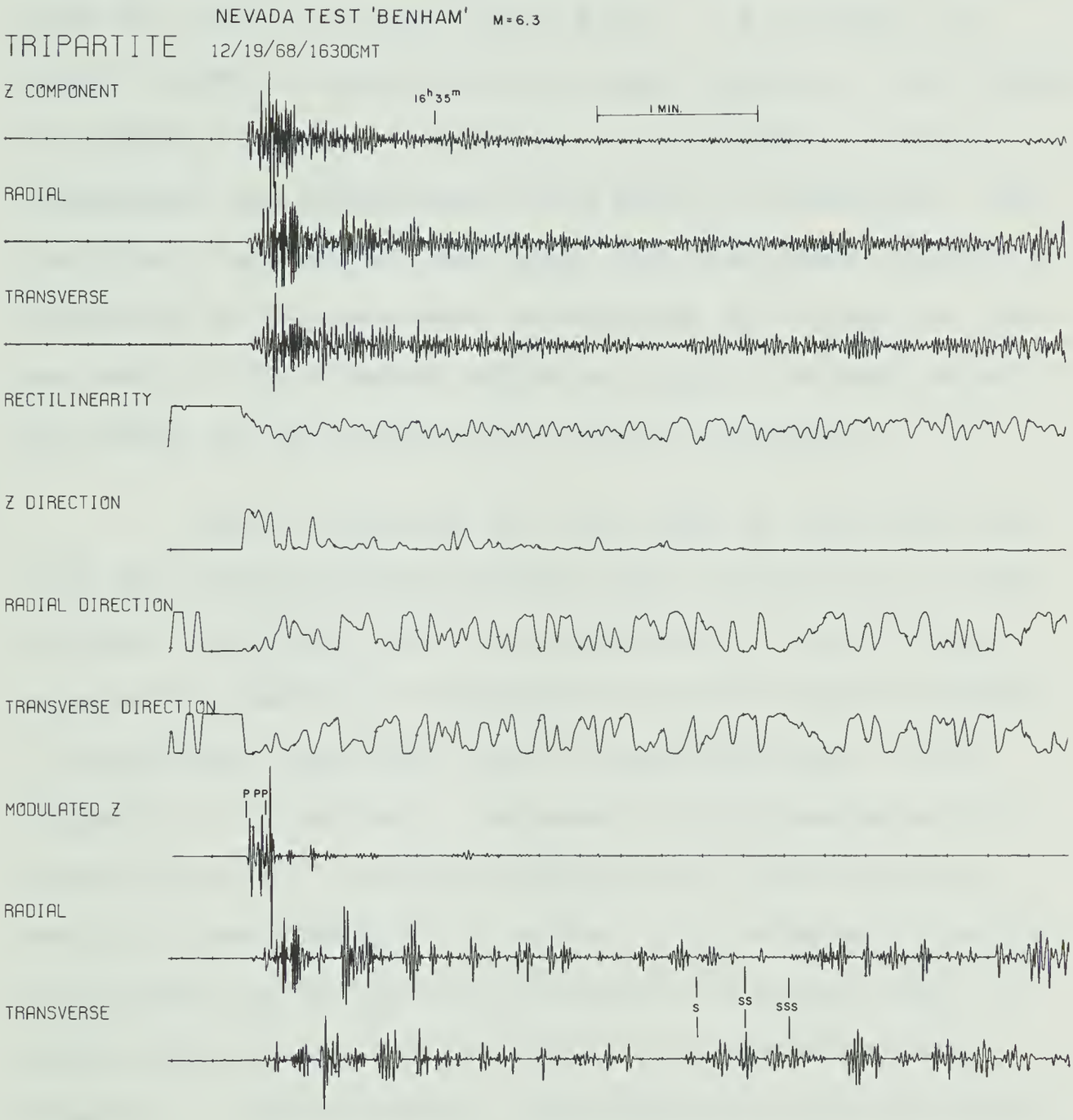
NEVADA TEST 'BENHAM' M=6.3
TRIPARTITE
12/19/68/1630GMT
Z COMPONENT
16h35m
1 MIN.
RADIAL
TRANSVERSE
RECTILINEARITY
Z DIRECTION
RADIAL DIRECTION
TRANSVERSE DIRECTION
MODULATED Z
P PP
RADIAL
TRANSVERSE
S
SS
SSS

vertical (R-Z) and horizontal (R-T) planes of the first 20 seconds of this event. The unfiltered portion of the three components of ground motion are shown with time in seconds from the onset indicated above each. A 2.5 second (21 point) window is represented by every diagram. This window is advanced in time 2.5 seconds for each plot so that a continuous representation of the event is displayed. The build-up of energy on the radial and transverse records indicated by the processed seismograms of figure 3.4, can be seen in this diagram beginning about 10 seconds after the onset and extending out to about 20 seconds.

The R-Z diagrams for the onset of the event show that the original compressional pulse is arriving at near vertical incidence, but the orientation of the principal axis of the particle trajectory in the R-T plane suggests a significant departure from the expected great circle azimuth (R^+ direction). Increase in the transverse component from 10-15 seconds indicates that the horizontal motion is not purely SV in nature, but contains a significant amount of horizontally polarized SH motion which is being detected by both the radial and transverse seismometers. Similar effects, particularly at this recording location, have been observed by Ellis and Basham (1968) and Basham and Ellis (1969) in a study of seismograms taken at various stations in central Alberta, and have been

Figure 3.5 Particle motion diagrams for the first 22.5 seconds of the nuclear test shot 'Benham'. The unfiltered portions of the vertical, radial and transverse records are shown with time in seconds from the onset of the event indicated above each. Sign convention is indicated for the R-Z and R-T planes in the first diagram. A 21 point (2.5 seconds) window is represented by each diagram with "1" representing the first point and "21" the last point so that the direction of motion can be seen. The beginning of each diagram is separated by one sample interval from the last point of the preceeding plot. Time for point "1" is indicated along the diagrams. As in figure 3.4, no band-pass filtering has been applied to the data before rotation.

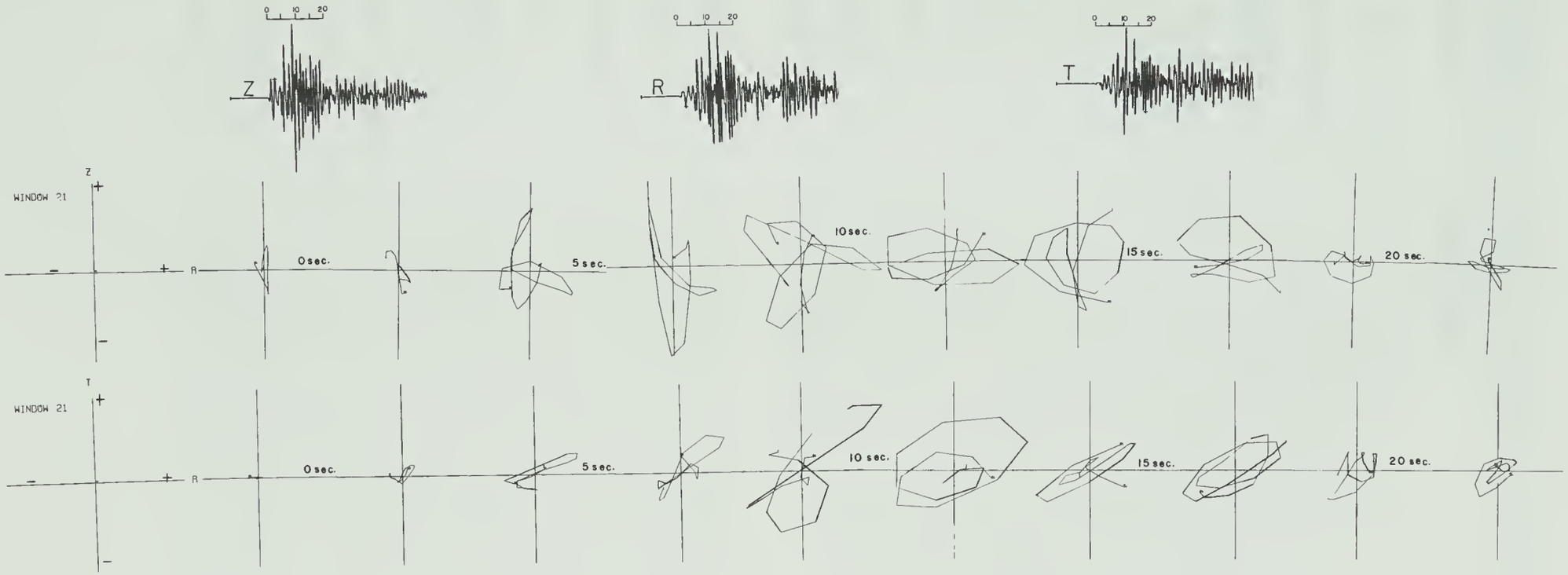
0 10 20
Z
0 10 20
R
0 10 20
T
Z
WINDOW 21
+
−
+
−
R
0 sec.
5 sec.
10 sec.
15 sec.
20 sec.
T
WINDOW 21
+
−
+
−
R
0 sec.
5 sec.
10 sec.
15 sec.
20 sec.

suggested as being the result of body wave conversions at or near the base of the sediments.

In the course of the present study, it was apparent that a larger increase in transverse energy following the original compressional pulse was associated with events arriving at azimuths between about 180-270 degrees. This suggests that the observed transverse motion might be generated by body phase conversions at major topological features in the vicinity of the recording station, rather than at the base of the sediments. Analysis of events arriving from various azimuths using an array arranged around the present recording site would permit a more reliable interpretation of these observations.

Although the particle motion diagram of figure 3.5 shows that the original compressional pulse is arriving at near vertical incidence, this of course may not necessarily be the case for all events. If the angle of incidence were inclined appreciably from the vertical, then pure P or SV motion would be present on both the vertical and radial components, and separation of the two types would not be as efficient. By considering a unit vector $\bar{A} = (a_1, a_2, a_3)$, which is orientated at the observed inclination from the vertical in the R,T,Z co-ordinate system, direction functions of the form

$$D_R = e_1 \cdot a_1$$

$$D_T = e_2 \cdot a_2 \qquad (3.16)$$

$$D_Z = e_3 \cdot a_3$$

where $\bar{E} = (e_1, e_2, e_3)$ is the eigenvector of the principal axis of the covariance matrix, could be obtained. Rotation of the Z and R components of motion about the transverse horizontal direction so that the former vertical instrument lies in the P direction and the former radial instrument in the SV direction could be accomplished. Application of the direction operators 3.16 might then more effectively separate pure P and SV motion. Transverse motion on the original radial trace would also be eliminated by virtue of the rotation in the vertical-radial plane. One method of determining the apparent direction of incidence is by fitting a straight line to the vertical-radial particle motion considered over the first few seconds of the P-coda (Fuchs 1969).

A comparison of filtered and unfiltered records from three events, A,B,C, all within 11 kilometers of each other, is shown in figures 3.6 and 3.7. The earthquakes, of magnitude 5.3, 5.4 and 5.5 respectively occurred in the Gulf of California within about a 3 hour period on March 21, 1969. In each case, the data was band-pass filtered 0.3-4Hz before rotation. On the seismograms processed with the polarization filter, a good correlation from record to record is evident

Figure 3.6 Vertical, radial and transverse components of ground motion for three events which occurred in the Gulf of California on March 21, 1969. Magnitudes of each event A, B and C are 5.3, 5.4 and 5.5 respectively. For each, Δ=22°. Universal time is indicated on each record. Digital band-pass filtering of 0.3-4 Hz has been applied before rotation.

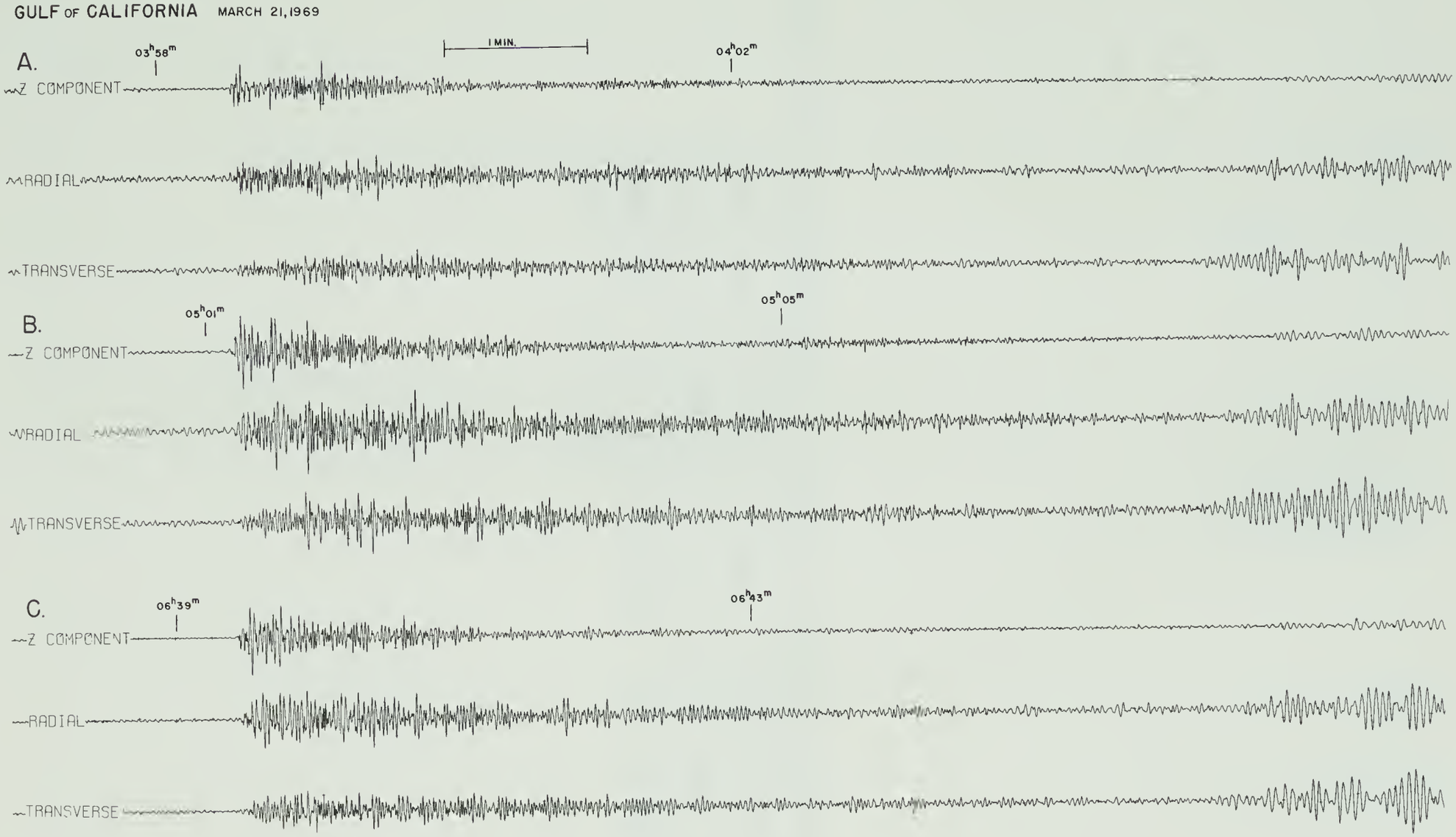
GULF OF CALIFORNIA MARCH 21, 1969
1 MIN.
A.
03h58m
04h02m
Z COMPONENT
RADIAL
TRANSVERSE
B.
05h01m
05h05m
Z COMPONENT
RADIAL
TRANSVERSE
C.
06h39m
06h43m
Z COMPONENT
RADIAL
TRANSVERSE

Figure 3.7 The seismograms of figure 3.6 after processing with the polarization filter. Identification of events from predicted P and S travel times is indicated. For these records: J=1, K,L,M=2 and $F(\lambda_1,\lambda_2)= 1-(\frac{\lambda_2}{\lambda_1})$.

GULF OF CALIFORNIA MARCH 21, 1969

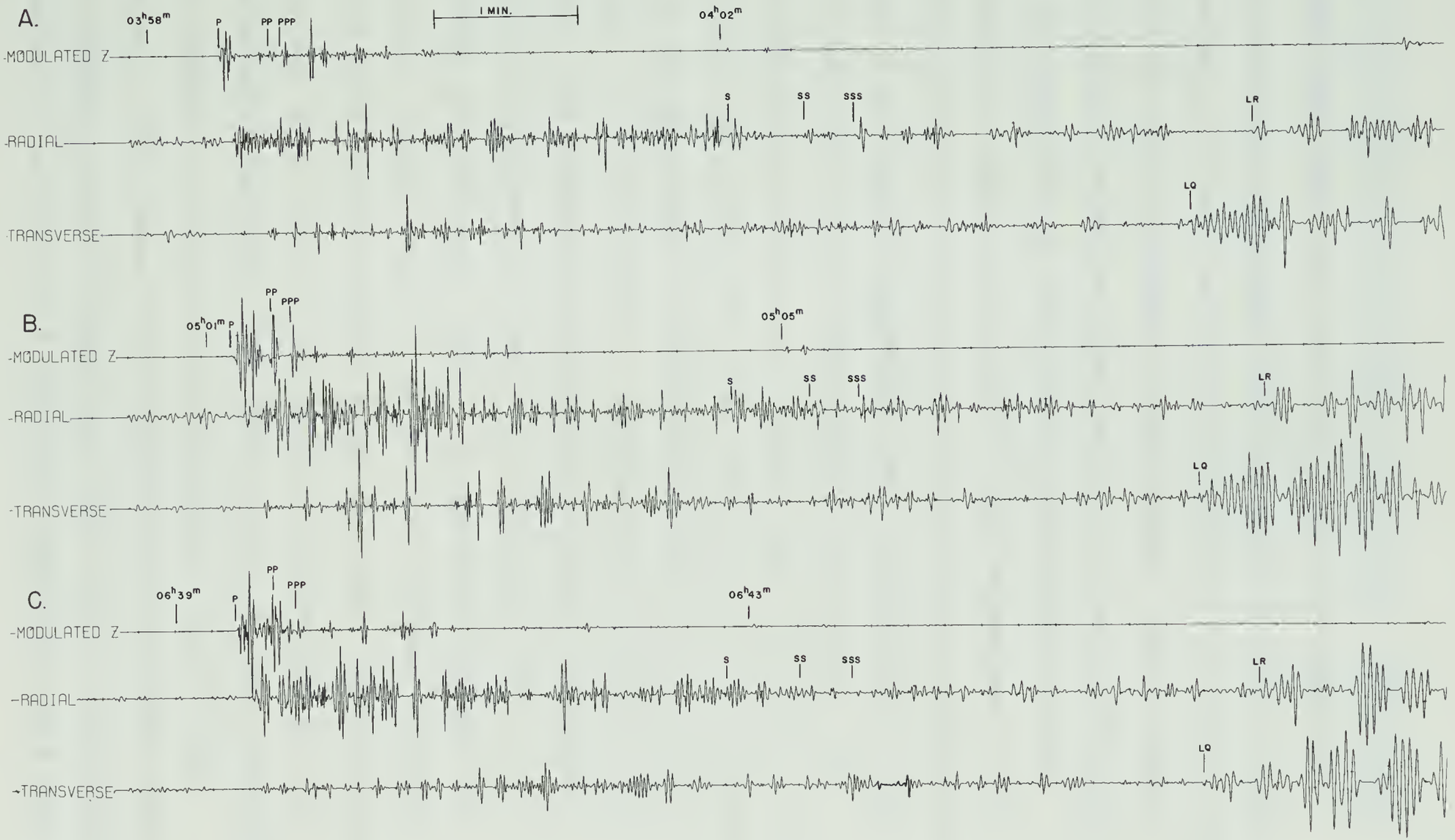

for the P-PP-PPP and S-SS-SSS wave groups. Since these events have been identified from predicted times for a surface-focus earthquake, and the depth of each is undetermined, at least part of the variations in arrival time could be due to different focal depths. The increase in horizontally polarized shear motion is clearly displayed at the beginning of the Love (LQ) wave train on the transverse component of each filtered seismogram. The onset of Rayleigh (LR) waves is also clearly indicated on each of the radial components, and a separation of dominant Love and Rayleigh type motion can be seen. The absence of any vertical (Z) motion over the portion of the filtered seismogram following the arrival of LR indicates that the major axis of polarization never lies predominantly in this direction. Assuming the Gutenberg earth model, the theoretical horizontal/vertical displacement ratio for fundamental long period Rayleigh waves is 0.8 (Dorman and Prentiss, 1960). We would thus expect the vertical ground motion to be dominant for such arrivals. Since this does not appear to be the case, indications are that the major axis of the particle trajectory for the fundamental Rayleigh waves does not lie in the Z direction, but rather is inclined at some angle to the vertical. Haskell (1953) shows that transmission of Rayleigh waves in imperfect elastic medium can give rise to such effects. Whether or not this is a localized condition could only be

determined by comparison with seismograms from other recording sites.

The examples shown here illustrate how this type of polarization filter can be applied to enhance motion which is rectilinear in a preferred direction. Future applications of this processor to data sets from an array of recording instruments could be valuable in interpretation of both source characteristics and localized conditions near the receiver. It is evident however, that particle trajectories of arrivals such as Rayleigh surface waves which exhibit motion more elliptical in nature, will be subject to attenuation along one of the major axes. This is seen to be the case in figure 3.7 when strong Love waves exhibiting high rectilinearity in the transverse direction arrive at about the same time as the Rayleigh phases. The filter thus appears to be most useful for the enhancement of P and S body waves.

CHAPTER 4

A FREQUENCY DOMAIN SURFACE WAVE DISCRIMINATION FILTER

4.1 Introduction

The arrival of Love and Rayleigh surface waves from a teleseismic event is generally characterized on a seismogram by an increase in long period signal. Since the group velocity of the fundamental Rayleigh mode is less than that of the Love mode (Grant and West, Chapter 3), the Rayleigh waves will generally arrive behind the Love waves. Most often however, this time difference is not sufficient to separate the Rayleigh and Love groups so that at the same time, motion which is elliptical in nature will be present in the vertical-radial plane due to the Rayleigh waves, and linearly polarized SH motion from the Love waves will be present in the horizontal plane. As the SH polarized Love groups exhibit higher rectilinearity than the Rayleigh waves, the effect of a particle motion filter which enhances motion displaying high rectilinearity will be to preserve the SH phases, but attenuate the vertical-radial Rayleigh wave motion. This effect is seen in the filtered seismograms of figure 3.7. Since the surface wave trains are dispersive however, different group maxima will arrive at different times so that the spectral content of each

component of ground motion over a particular time interval might be used to separate Love and Rayleigh wave-trains.

Simons (1968), describes a process in which frequency filtering using measurements on particle motion to shape the filter response is used to enhance the signal to noise ratio of surface wave groups. The discrete Fourier series of the three components of ground motion are computed, and then each harmonic is treated independently. Amplitude coefficients at each frequency are weighted according to how closely the three dimensional particle motion trajectory at that frequency corresponds to theoretical Love or Rayleigh wave patterns arriving from a specified direction. These modified coefficients are then used to reconstruct the trace in the time domain. In the band around the microseismic peak (5-8 seconds period), interfering effects of the background will cause attenuation at those frequencies, but the remainder of the spectrum will be enhanced by the filter process. Band-pass filtering to eliminate the microseisms can of course be applied before the Fourier transforms are computed.

4.2 The Filter Function

If the data traces are rotated as in equations 3.1 and then considered over simultaneous time segments of length $N\Delta t$, where Δt is the sampling interval, then for

each component of ground motion, the amplitude and phase of each harmonic is given in terms of the discrete Fourier coefficients a(nf) and b(nf) by

$$A_i(nf) = [a_i^2(nf) + b_i^2(nf)]^{\frac{1}{2}}$$

$$\Phi(nf) = \arctan \frac{b_i(nf)}{a_i(nf)} \tag{4.1}$$

where i = Z,R,T corresponds to the vertical, radial or transverse component of motion and

$$n = 0,1,2,\cdots\frac{N}{2}$$

$$\frac{Nf}{2} = \text{Nyquist frequency} = \frac{1}{2\cdot\Delta t}$$

$$f = \frac{1}{N\Delta t} \tag{4.2}$$

$$= \text{fundamental harmonic of the Fourier series}$$

A measure of the apparent horizontal azimuth can be obtained from the function

$$\beta(nf) = \arctan \frac{A_T(nf)}{A_R(nf)} \tag{4.3}$$

and an estimate of eccentricity of the particle motion ellipse is represented by

$$\psi(nf) = \arctan \frac{A(nf)}{A_Z(nf)}$$

$$A(nf) = [A_R^2(nf) + A_T^2(nf)]^{\frac{1}{2}} \tag{4.4}$$

The geometrical relationship represented by equations 4.3 and 4.4 is shown in figure 4.1. We see from the diagram that if motion at a particular frequency is purely radial then $A_T(nf) = 0$ implies $\beta(nf) = 0$; while motion which is purely transverse ($A_R(nf) = 0$) gives $\beta(nf) = \frac{\Pi}{2}$. As far as eccentricity is concerned, if motion is in the horizontal plane only, $A_Z(nf) = 0$ and $\psi(nf) = \frac{\Pi}{2}$, while a predominant vertical component ($A(nf) \sim 0$) yields $\psi(nf) = 0$. If $A(nf) = A_Z(nf)$, the eccentricity exhibits no preferred direction and $\psi(nf) = \frac{\Pi}{4}$. The phase difference between vertical and radial components is also determined as

$$\alpha(nf) = \Phi_R(nf) - \Phi_Z(nf) \tag{4.5}$$

Functions of α, β and ψ are then used to weight the amplitude coefficients according to the following equations

$$A'_Z(nf) = A_Z(nf) \cdot \cos^M[\beta(nf)] \cdot \cos^K[\psi(nf)-\theta] \cdot \sin^N[\alpha(nf)]$$

$$A'_R(nf) = A_R(nf) \cdot \cos^M[\beta(nf)] \cdot \cos^K[\psi(nf)-\theta] \cdot \sin^N[\alpha(nf)] \tag{4.6}$$

$$A'_T(nf) = A_T(nf) \cdot \sin^M[\beta(nf)] \cdot \sin^K[\psi(nf)]$$

The exponents M,K and N are determined empirically. We see that the Z and R components receive identical weights, and that each function of α, β and ψ lies in the range (0,1).

Keeping in mind the limiting cases of $\beta(nf)$ and

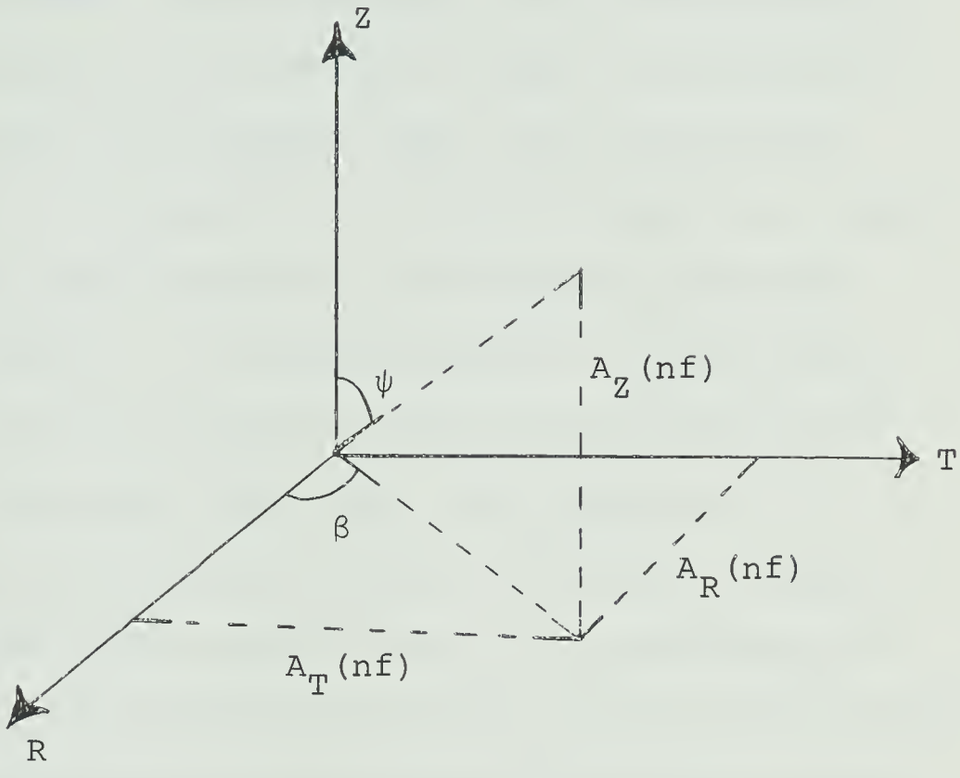

Figure 4.1 A representation of the amplitude coefficients calculated for the three orthogonal components of ground motion illustrating how measures of apparent horizontal azimuth and eccentricity of the particle motion trajectory can be obtained for each frequency component.

$\psi(nf)$ discussed above, it is evident that if at a particular frequency motion in the horizontal plane is purely radial ($\beta(nf)=0$), $A_Z(nf)$ and $A_R(nf)$ are preserved and $A_T(nf)$ is attenuated. Motion which is purely transverse in nature ($\beta(nf)=\frac{\Pi}{2}$) will, on the other hand, be attenuated in the vertical-radial plane. The parameter θ in the equations for $A'_Z(nf)$ and $A'_R(nf)$ can be chosen so that a particular horizontal/vertical displacement ratio for the particle motion trajectory is preserved. If $\psi(nf)=\theta$ then the radial and vertical amplitudes receive unit weighting from the function $\cos^K[\psi(nf)-\theta]$. For motion which is purely horizontal $\psi(nf)=\frac{\Pi}{2}$, and the function $\sin^K[\psi(nf)]$ applies unit weight to the transverse amplitude. The function $\sin^N[\alpha(nf)]$ will attenuate the radial and vertical amplitudes by an amount which varies from 1 to 0 according to how closely the phase difference between radial and vertical components departs from the theoretical $\frac{\Pi}{2}$ value for fundamental retrograde Rayleigh waves.

The combined effect of these weighting factors is thus seen to enhance pure Rayleigh or pure Love waves of some particular period arriving at the recording station. If for example, motion in the horizontal plane is predominantly radial, the horizontal/vertical displacement ratio corresponds to the specified θ, and the phase difference between radial and vertical components is $\frac{\Pi}{2}$, then the Z

and R coefficients will be preserved and the transverse component attenuated. This corresponds to the case of pure Rayleigh motion. Conversely, a dominant arrival at some particular period on the transverse component along with little or no amplitude on the vertical record corresponds to a Love phase so that the amplitude coefficient for the transverse trace will be preserved and the Z-R motion will be attenuated. Particle trajectories which lie between these limits will be subject to varying degrees of attenuation. It is evident that this process, since it considers the particle motion patterns over all harmonics contained in the time window chosen to compute the Fourier coefficients, will not be efficient if surface Rayleigh and Love waves of similar periods and comparable amplitudes arrive in the same time segment. In this case, the interfering effects of the simultaneous arrivals will result in a mutually confusing particle motion pattern so that little or no output from the filter will be obtained. A further condition on the Z-R amplitudes can be specified as

$$\sin[\alpha(nf)] \equiv 0, \quad \Pi \leq \alpha(nf) \leq 2\Pi \tag{4.7}$$

so that prograde Rayleigh type motion will also be attenuated.

4.3 Application of the Filter

A Fortran IV program has been written which can be used to process the three component records from the digital system described in Chapter 2. In practice, the Fourier coefficients are determined over the specified window and then modified using the weighting functions as in equation 4.6. As no modification is applied to the phase angles of each Fourier component, these are used along with the modified amplitude coefficients to reconstruct the trace in the time domain. The window is then moved down the record some fraction of the original window length and calculations are repeated. The final output is the arithmetic average of all overlapping time segments at any particular point on the seismogram.

Fourier transforms and their inverses were computed using a high-speed algorithm developed by Gentleman and Sande (1966). It was found that a cosine taper applied to about the first and last 10% of the data points in each window was required to reduce slight phasing effects introduced by the discontinuities in the original time series at the beginning and end of each window. With a window length of 512 points, an increment of 16 points ($\frac{1}{32}$) was found to give the best results. As the sampling interval of the data was 0.12 seconds, this corresponds to a time window of 61.4 seconds with a 1.9 second overlap.

The program was arranged so that any window from 128 to 1024 points, in multiples of 2, as well as the increment, could be specified on card input. The factors of 2 were required for application of the particular fast Fourier algorithm that was used. It is evident that choice of window length should be consistent with the spectral content of the seismogram over the region of interest so that the fundamental harmonic of the Fourier series corresponds to at least a single cycle of the longest period present on the record. Following the suggestions of Simons (1968), values of M,K and N (equations 4.6), were chosen as 8, 8 and 4 respectively, and θ corresponded to a horizontal/vertical displacement ratio of 0.8.

A portion of a seismogram from a magnitude 5.4 earthquake which occurred in the Gulf of California on March 21, 1969 is shown in figure 4.2 before and after this filter has been applied. The data was digital band-pass filtered 0.007-0.2 Hz (5-150 seconds) before rotation. Predicted arrival times of LQ and LR for a surface focus earthquake are indicated on the processed records. Although good Love-type arrivals are evident on the transverse component, the vertical and radial traces show little signal except for one well-defined group. It is thus apparent that motion in the vertical-radial plane did not satisfy the theoretical pattern chosen for surface Rayleigh waves, in

Figure 4.2 Portion of a seismogram processed with the surface wave discrimination filter. For this record: M,K = 8; N = 4; θ corresponds to a horizontal/vertical displacement ratio of 0.8. A 61.4 second window with a 1.9 second increment was used. Digital band-pass filtering 0.007-0.2 Hz was applied to the data before rotation. The event, of magnitude 5.4, occurred in the Gulf of California on March 21, 1969. Δ = 22°.

GULF OF CALIFORNIA MARCH 21, 1969

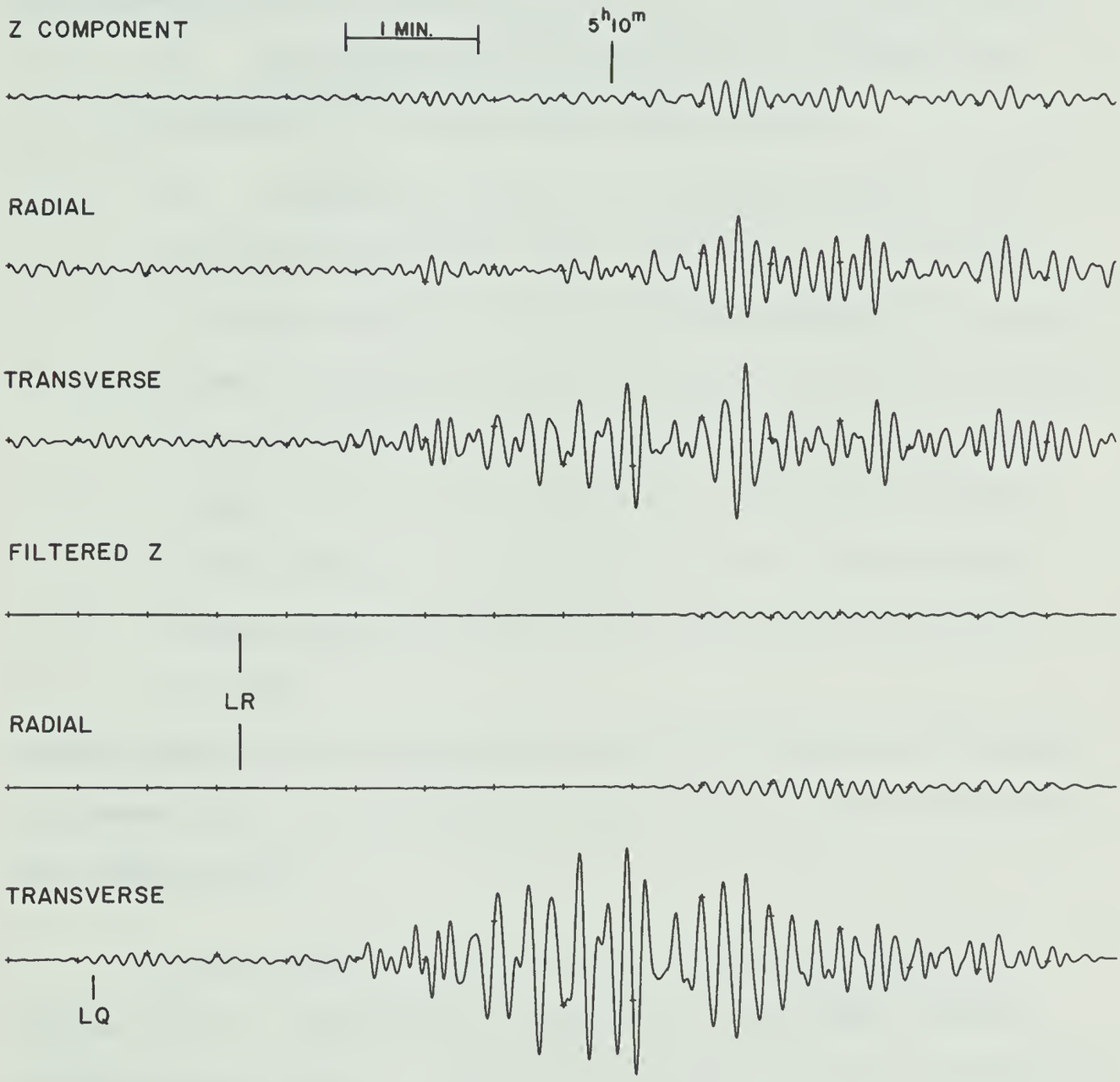

particular, the expected horizontal/vertical displacement ratio of 0.8. An examination of the unfiltered Z and radial components suggests that the apparent ratio might be >1. Interpretation of this observation has two possibilities:

1. Few well-defined Rayleigh wave groups are arriving from this particular event.

2. Conditions near the recording station, or the average effect over the entire, or at least a large portion of the crustal waveguide, are such that the major axis of the particle motion ellipse for the Rayleigh wave groups is inclined at some large angle to the vertical. This would result in an apparent horizontal/vertical displacement ratio quite different from the specified value of 0.8.

A more definite interpretation could of course be obtained by comparison of seismograms taken with an array of recording instruments.

The example however, does illustrate that this filter can be successfully applied to the longer period surface wave groups. Data from an array, once processed by this method, might then be digitally filtered with narrow pass-band zero phase shift filters so that group and phase velocity studies of surface Love and Rayleigh waves could be pursued.

Conclusion

In the course of this study, it has been shown how digital techniques can be applied to three-component seismograms for enhancement of the signal to noise ratio. If the spectral characteristics of signal and noise are different, zero phase shift band-pass filters can be effectively used to improve the quality of the records. If signal and noise exhibit similar spectral characteristics, the availability of three component seismograms permits determination of filter functions which use the polarization properties of both body waves and longer period surface waves to enhance the arrival of various phases. Two such filters, one particularly suited for the study of body waves, and the other which can be applied as a surface wave discrimination process have been considered in Chapters 3 and 4. With three component data recorded directly onto digital tape using broad-band instrumentation as described in Chapter 2, seismic energy covering a wide spectrum can be obtained for immediate application of digital processing techniques. It is hoped that future applications of the polarization filters studied to data taken with an array of these instruments will prove valuable in the interpretation of seismic events.

BIBLIOGRAPHY

Alpasan, T., 1968. *Spectral behaviour of short period body waves and the synthesis of crustal structure in Western Canada*, M.Sc. thesis, University of Alberta, Department of Physics, Edmonton, Alberta.

Archambeau, C. B. and E. A. Flinn, 1965. Automated analysis of seismic radiation for source characteristics: *Proc. of the IEEE*, v. 53, p. 1876-1884.

Basham, P. W., 1967. *Time domain studies of short period teleseismic P phases*, M.Sc. thesis, University of British Columbia, Department of Geophysics, Vancouver, B.C.

Basham, P. W. and R. M. Ellis, 1969. The composition of P-codas using magnetic tape seismograms: *Bull. Seism. Soc. Am.*, v. 59, p. 473-486.

Brune, J. N. and J. Oliver, 1959. The seismic noise of the earth's surface: *Bull. Seism. Soc. Am.*, v. 49, p. 349-353.

De Bremaecker, J. Cl., P. Donoho and J. G. Michel, 1962. A direct digitizing seismograph: *Bull. Seism. Soc. Am.*, v. 52, p. 661-672.

Burr-Brown, 1963. *Handbook of operational amplifier applications*, Burr-Brown Research Corp., Tuscon, Arizona.

Dettman, J. W., 1962. *Mathematical methods in physics and engineering*, Toronto: McGraw-Hill.

Dorman, J., and D. Prentiss, 1965. Particle amplitude profiles for Rayleigh waves on a heterogeneous earth: *J. Geophys. Res.*, v. 65, p. 3805-3816.

Ellis, R. M. and P. W. Basham, 1968. Crustal characteristics from short-period P waves: *Bull. Seism. Soc. Am.*, v. 58, p. 1681-1700.

Flinn, E. A., 1965. Signal analysis using rectilinearity and direction of particle motion: *Proc. of the IEEE*, v. 53, p. 1874-1876.

Frantti, G. E., D. E. Willis and J. T. Wilson, 1962. The spectrum of seismic noise: *Bull. Seism. Soc. Am.*, v. 52, p. 113-121.

Fuchs, J. P., 1969. *Evaluation of a rectilinear motion detector*, M.Sc. thesis, University of British Columbia, Department of Geophysics, Vancouver, B.C.

Gentleman, W. M. and G. Sande, 1966. Fast Fourier transforms - for fun and profit: *Proc. of the Fall Joint Computer Conference*, San Francisco, p. 563-578.

Grant, F. S. and G. F. West, 1965. *Interpretation theory in applied geophysics*, Toronto: McGraw-Hill.

Graybill, F. A., 1961. *An introduction to linear statistical models*, v. 1, Toronto: McGraw-Hill.

Griffin, J. N., 1966a. *Application and development of polarization (REMODE) filters:* Seismic Data Laboratory Report 141, Teledyne, Inc., Alexandria, Va.

Griffin, J. N., 1966b. *REMODE signal/noise tests in polarized noise:* Seismic Data Laboratory Report 162, Teledyne, Inc., Alexandria, Va.

Haskell, N. A., 1953. The dispersion of surface waves on a multilayered media: *Bull. Seism. Soc. Am.*, v. 43, p. 17-34.

Hilger and Watts Ltd., 1964. *Instruction manual for the Willmore seismometer Mk II*, London, England.

Jenkins, G. M. and D. G. Watts, 1968. *Spectral analysis and its applications*, San Francisco: Holden-Day.

Lewis, B. T. R. and R. P. Meyer, 1968. A seismic investigation of the upper mantle to the west of Lake Superior: *Bull. Seism. Soc. Am.*, v. 58, p. 565-596.

Mims, C. H. and R. L. Sax, 1965. *Rectilinear motion detection (REMODE):* Seismic Data Laboratory Report 118, Teledyne, Inc., Alexandria, Va.

Pomeroy, P. W., G. Hade, J. Savino and R. Chander, 1969. Preliminary results from high-gain, wide-band long-period electromagnetic seismograph systems: *J. Geophys. Res.*, v. 74, p. 3295-3298.

Richter, C. F., 1958. *Elementary Seismology*, San Francisco: W. H. Freeman and Co.

Russell, R. D., R. D. Meldrum and O. G. Jensen, 1968. The Maxwell bridge as a circuit element in electromagnetic feedback seismographs: *Bull. Seism. Soc. Am.*, v. 58, p. 1621-1630.

Sallen, R. P. and E. L. Key, 1955. Practical method of designing R-C active filters: *Inst. Radio Engrs.-Trans. on Circuit Theory*, v. CT-2, p. 74-85.

Shimshoni, M. and S. W. Smith, 1964. Seismic signal enhancement with three component detectors: *Geophysics*, v. 29, p. 664-671.

Simons, R. S., 1968. A surface wave particle motion discrimination process: *Bull. Seis. Soc. Am.*, v. 58, p. 629-637.

Sutton, G. H. and G. V. Latham, 1964. Analysis of a feedback-controlled seismometer: *J. Geophys. Res.*, v. 69, p. 3865-3882.

Tucker, M. J., 1958. An electronic feedback seismometer: *J. Sci. Instr.*, v. 35, p. 167-179.

Willmore, P. L., 1961. Some properties of heavily damped electromagnetic seismographs: *Geophys. J.*, v. 4, p. 389-404.

APPENDIX 1

A1.1 The Amplifier Transfer Function

A circuit diagram of the analog amplifier described in Chapter 2 is shown in figure A1.1. A derivation of the complete transfer function is presented by considering the separate transfer characteristics of each operational amplifier stage. The input resistance of the first amplifier is determined from technical specifications for the Willmore Mark II seismometer as given in the Hilger and Watts operational manual (1964). If n is some multiple of the coil resistance of the seismometer then we have for the Willmore Mark II

$$n+1 = 1.7 \frac{T}{D} \qquad \text{(A1.1)}$$

where T is the natural period of the seismometer and D the damping factor. With T = 1.5 seconds and D = 0.6, n = 3.25. With a coil resistance of 3300Ω, the input resistance for the first stage is given by

$$\begin{aligned} R_{in} &= 3300 \times 3.25 \\ &= 10.72 \text{ K}\Omega \end{aligned} \qquad \text{(A1.2)}$$

so that R_{in} = 10 KΩ is used.

Figure A1.1 Circuit diagram of the analog amplifier for the Tripartite system.

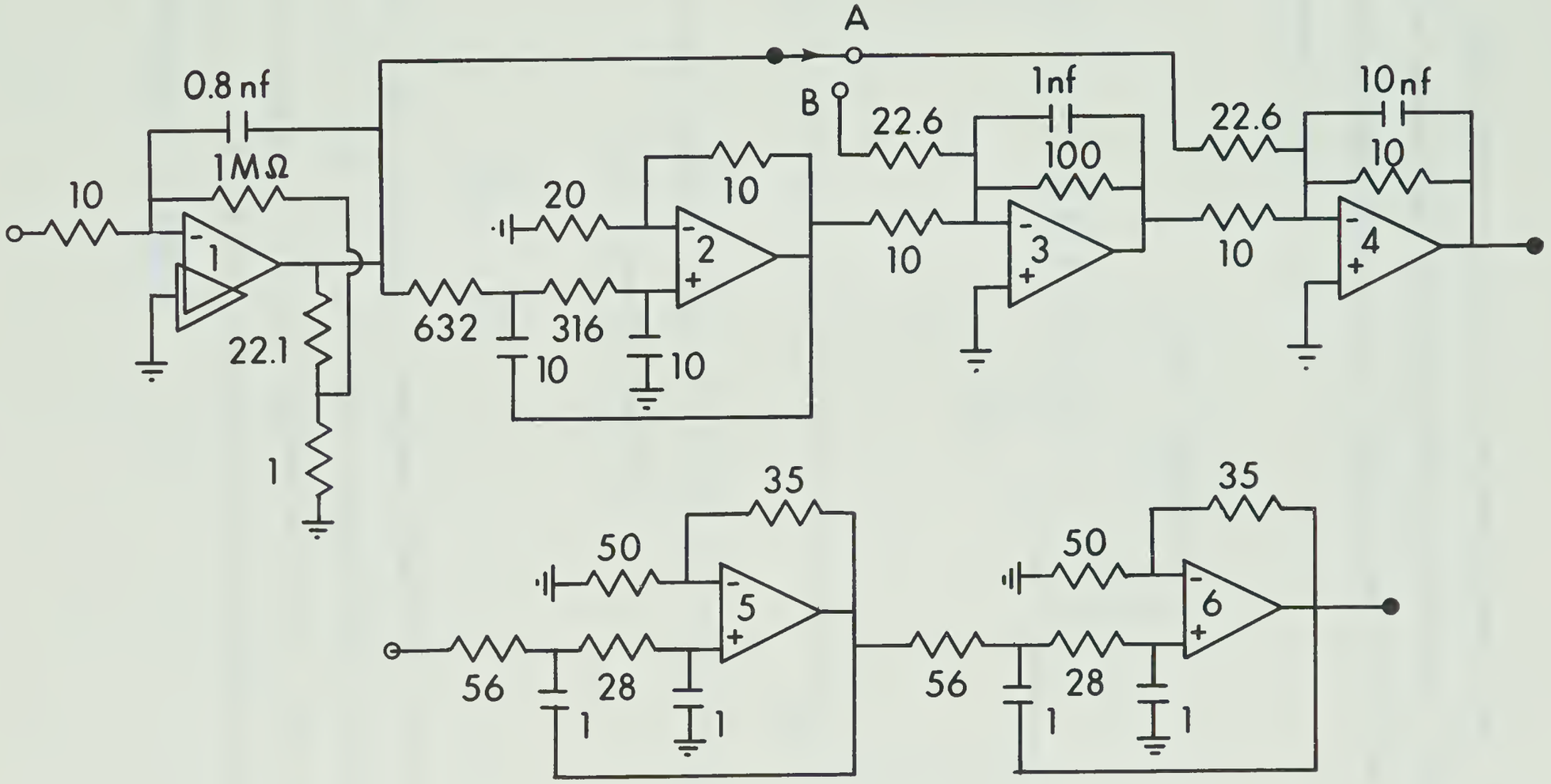
A
B
0.8 nf
1MΩ
10
1
22.1
1
632
316
10
10
20
10
2
10
22.6
1nf
100
3
10
22.6
10nf
10
4
10
35
50
5
56
28
1
1
35
50
6
56
28
1
1

For simplification of the development that follows, use of an operational amplifier with differential input as an inverting amplifier will be represented as follows (Burr-Brown, 1963)

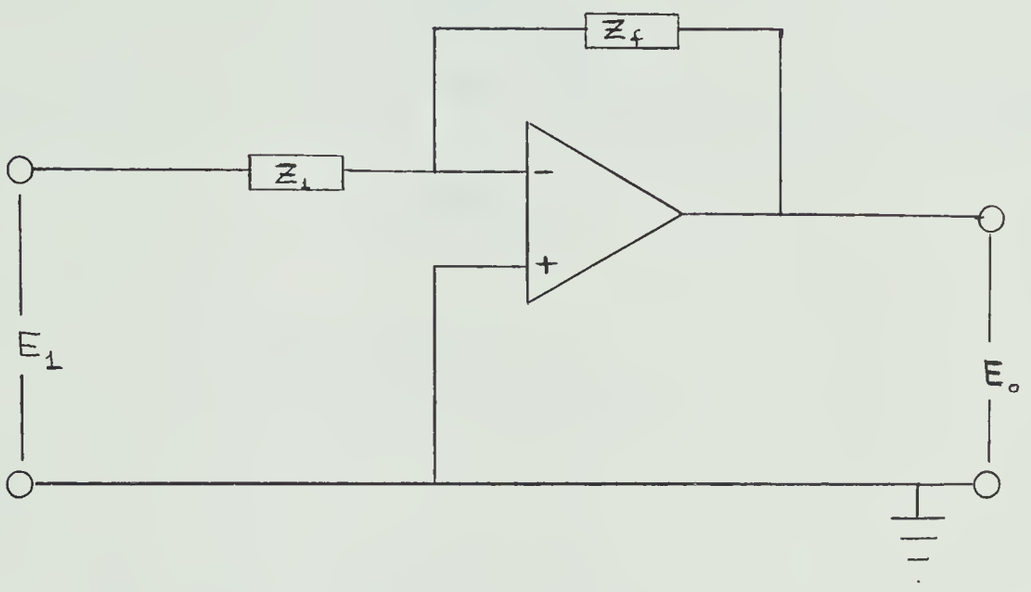

Figure A1.2 General Form of the Inverting Amplifier with transfer function

$$\frac{E_o}{E_1} = - \frac{Z_f}{Z_1} \qquad \text{(A1.2)}$$

Z_f and Z_1 are, in general, complex impedances. As a matter of notation, and when necessary, output from a particular amplifier stage i, will be represented by E_{oi}, and input by E_{1i}, E_{2i}.... The same convention will hold for circuit components R_i, C_i etc.

Amplifier 1

Following figure A1.2 and equation A1.2, we have for the first stage

$$Z_f = \frac{R_{eq}/j\omega c_1}{R_{eq} + \frac{1}{j\omega c_1}} = \frac{R_{eq}}{1 + j\omega\tau_1} \qquad (A1.3)$$

$$Z_1 = R_{in}$$

so that

$$\frac{E_{o1}}{E_{11}} = - \frac{R_{eq}}{R_{in}} \cdot \frac{1}{1 + j\omega\tau_1} \qquad (A1.4)$$

$$\tau_1 = R_{eq} C_1$$

R_{eq} is determined from considerations of D-C feedback in the amplifier stage with the following configuration

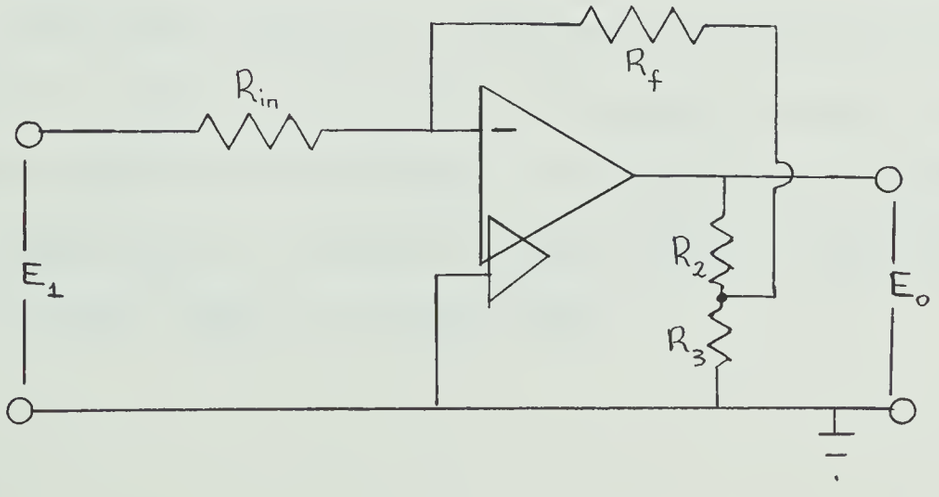

for which

$$\frac{E_o}{E_1} = -\frac{R_f}{R_{in}} \cdot \left[\frac{R_2 + R_3}{R_3}\right]$$

$$\frac{E_o}{E_i} = -\frac{R_{eq}}{R_{in}} \qquad \text{(A1.5)}$$

Substituting the values of the actual circuit components as given in figure A1.1 we have by A1.4 and A1.5

$$R_{eq} = 23.1 \text{ M}\Omega$$

$$\tau = 1.85 \times 10^{-2} \text{ seconds}$$

$$R_{in} = 10 \text{ K}\Omega \qquad \text{(A1.6)}$$

$$\frac{E_{o_1}}{E_{i_1}} = \frac{-2.31 \times 10^{3}}{1 + 1.85 \times 10^{-2}\, j\omega}$$

The transfer function has a high frequency cut-off at $\omega = \frac{1}{\tau} =$ 8.6 Hz.

Amplifier 2

The second stage is a low pass active R-C network filter with a corner at 0.033 Hz (30 second period) and an attenuation rate of 12 db/octave. Following the design criterion described by Sallen and Key (1955), the transfer function of this stage is of the form

$$\frac{E_{o2}}{E_{i2}} = \frac{K}{(j\omega)^2 + d(j\omega) + 1} \qquad \text{(A1.7)}$$

K = gain factor

which for this stage is given by

$$\frac{E_{o2}}{E_{i2}} = \frac{1.5}{1 + \frac{1.4j\omega}{20.9x10^{-2}} + \frac{j\omega}{20.9x10^{-2}}^2} \qquad \text{(A1.8)}$$

Amplifiers 3 and 4

Two cases A and B, indicated by the circuit diagram, will be considered.

Case B

We have at stage 3, two inputs, so that the amplifier is used as a voltage adder. Following equation A1.2, the transfer function for this stage can be written

$$E_{o3} = - Z_{f3} \cdot \left[\frac{E_{i3}}{R_{i3}} + \frac{E_{23}}{R_{23}} \right]$$

$$Z_{f3} = \frac{R_{f3}}{1+j\omega\tau_3}, \quad \tau_{f3} = R_{f3}C_3 \qquad \text{(A1.9)}$$

If $T_2(j\omega)$ represents the right-hand side of equation A1.8

then $E_{23} = T_2(j\omega) \cdot E_{12}$ so that A1.9 becomes

$$E_{O3} = \frac{-R_{f3}}{1+j\omega\tau_3} \cdot \left[\frac{1}{R_{13}} + \frac{T_2(j\omega)}{R_{23}} \right] \cdot E_{O1} \qquad \text{(A1.10)}$$

where we have used $E_{13} = E_{12} = E_{O1}$ (output of first stage). At amplifier 4 we have

$$\frac{E_{O4}}{E_{14}} = -\frac{Z_{f4}}{R_{24}}$$

$$Z_{f4} = \frac{R_{f4}}{1+j\omega\tau_4}, \quad \tau_4 = R_{f4}C_4 \qquad \text{(A1.11)}$$

Combining A1.10 and A1.11 with $E_{14} = E_{O3}$ we write

$$E_{O4} = \frac{-R_{f3}}{1+j\omega\tau_3} \cdot \left[\frac{1}{R_{13}} + \frac{T_2(j\omega)}{R_{23}} \right] \cdot \left[\frac{-R_{f4}}{R_{24}} \cdot \frac{1}{1+j\omega\tau_4} \right] \cdot E_{O1} \qquad \text{(A1.12)}$$

Substituting values of circuit components:

$$R_{13} = 226K\Omega \quad \tau_3 = \tau_4 = 10^{-4} \text{ seconds}$$

$$R_{f3} = 100K\Omega \quad R_{23} = R_{24} = R_{f4} = 10K\Omega$$

equation A1.12 yields

$$E_{O4} = \left[\frac{0.443}{1+10^{-4}(j\omega)} + \frac{10}{1+10^{-4}(j\omega)} T_2(j\omega) \right] \cdot \left[\frac{1}{1+10^{-4}(j\omega)} \right] \cdot E_{O1} \qquad \text{(A1.13)}$$

Case A

Following a similar development as for case B, the circuit configuration at amplifier 3 now gives

$$E_{o3} = \frac{-R_{f3}}{R_{23}} \cdot \frac{T_2(j\omega)}{1+j\omega\tau_3} \cdot E_{o1} \qquad \text{(A1.14)}$$

Amplifier 4 is now in a summation mode so that

$$\begin{aligned} E_{o4} &= \frac{-R_{f4}}{1+j\omega\tau_4} \cdot \left[\frac{E_{o1}}{R_{14}} + \frac{E_{o3}}{R_{24}}\right] \\ &= \frac{-R_{f4}}{1+j\omega\tau_4} \cdot \left[\frac{1}{R_{14}} - \frac{R_{f3}}{R_{24}R_{23}} \cdot \frac{T_2(j\omega)}{1+j\omega\tau_3}\right] \cdot E_{o1} \end{aligned} \qquad \text{(A1.15)}$$

Substituting the values of circuit components:

$$R_{14} = 22.6K\Omega \qquad \tau_3 = \tau_4 = 10^{-4} \text{ seconds}$$

$$R_{f3} = 100K\Omega \qquad R_{23} = R_{24} = R_{f4} = 10K\Omega$$

equation A1.15 yields

$$E_{o4} = \left[\frac{-0.443}{1+10^{-4}(j\omega)} + \frac{10}{1+10^{-4}(j\omega)} \cdot \frac{T_2(j\omega)}{1+10^{-4}(j\omega)}\right] \cdot E_{o1} \qquad \text{(A1.16)}$$

Contributions from the term $10^{-4}(j\omega)$ which corresponds to a high frequency corner at about 1500 Hz are negligible so that equations A1.13 and A1.16 may be written

$$E_{o^4} = \left[+0.443 + 10\ T_2(j\omega)\right] \cdot E_{o^1}, \text{ Case B}$$

$$E_{o^4} = \left[-0.443 + 10\ T_2(j\omega)\right] \cdot E_{o^1}, \text{ Case A} \qquad \text{(A1.17)}$$

We see then that case A corresponds to "out of phase" summation and case B to "in phase" summation which can be used for microseismic attenuation.

Amplifiers 5 and 6

Amplifiers 5 and 6 are aliasing filters each with a double corner at 4.3 Hz. Their transfer functions are the same type as that given in equation A1.7 so that for these two stages we have

$$E_{o^6} = \left[\frac{1.7}{1 + \frac{1.2}{27}(j\omega) + \frac{j\omega}{27}^2}\right]^2 \cdot E_{o^4} \qquad \text{(A1.18)}$$

Combining equations A1.6, A1.13, A1.18 and the expression for $T_2(j\omega)$ we have the complete transfer function for case B. Equations A1.6, A1.16 and A1.18 yield the complete transfer function for case A. These expressions are given in figure A1.3. An APL program has been used to evaluate the amplitude and phase responses of the complete transfer functions and these are shown in figure A1.4.

Figure A1.3 The complete transfer functions for the circuit diagram of figure A1.1. Case A is the case of "out of phase" summation, Case B the case of "in phase" summation for microseismic attenuation.

CASE A

$$\frac{E_o}{E_{in}} = - \left[\frac{2.31\times10^{3}}{1+1.85\times10^{-2}(j\omega)}\right] \cdot \left[\frac{1.5}{1+\frac{1.4(j\omega)}{20.9\times10^{-2}}+\frac{j\omega}{20.9\times10^{-2}}^{2}} \cdot \frac{10}{1+10^{-4}(j\omega)} \cdot \frac{1}{1+10^{-4}(j\omega)} - \frac{0.443}{1+10^{-4}(j\omega)}\right] \cdot \left[\frac{1.7}{1+\frac{1.2}{27}(j\omega)+\frac{j\omega}{27}^{2}}\right]^{2}$$

CASE B

$$\frac{E_o}{E_{in}} = - \left[\frac{2.31\times10^{3}}{1+1.85\times10^{-2}(j\omega)}\right] \cdot \left[\frac{1.5}{1+\frac{1.4(j\omega)}{20.9\times10^{-2}}+\frac{j\omega}{20.9\times10^{-2}}^{2}} \cdot \frac{10}{1+10^{-4}(j\omega)} + \frac{0.443}{1+10^{-4}(j\omega)}\right] \cdot \left[\frac{1}{1+10^{-4}(j\omega)}\right] \cdot \left[\frac{1.7}{1+\frac{1.2}{27}(j\omega)+\frac{j\omega}{27}^{2}}\right]^{2}$$

Figure A1.4 Calculated phase and amplitude responses for the transfer functions shown in figure A1.3. The two cases, A and B, are indicated.

Case B
Case A

A1.2 Theoretical Asymptotes for Seismometer and Amplifier.

Consider the following situation:

Let x be the position of the center of mass of a seismometer relative to an inertial reference.

Let y be the position of a point on seismometer frame relative to the same inertial reference.

K = spring constant

M = mass of seismometer

B = sum of viscous and electrical damping factors

The second order linear differential equation for the motion of the seismometer mass is given by (Richter, Chapter 15)

$$\frac{1}{\omega_n^2}\frac{d^2x}{dt^2} + \frac{2\zeta}{\omega_n}\frac{dx}{dt} + x = \frac{M}{K}\frac{d^2y}{dt^2} \qquad \text{(A1.19)}$$

$$\omega_n = \sqrt{\frac{K}{M}} = \text{natural period of seismometer}$$

$$\zeta = \frac{B}{2\sqrt{MK}}$$

Adopting Laplace transform notation (Dettman, Chapter 6) so that $L[f(x)] = F(s)$, $s = j\omega$, we have from equation A1.19

$$\frac{s^2}{\omega_n^2} X(s) + \frac{2\zeta}{\omega_n} sX(s) + X(s) = \frac{M}{K} s^2 Y(s) \qquad \text{(A1.20)}$$

The output voltage generated by the seismometer coil is given by

$$e_o = - G \frac{dx}{dt} \qquad \text{(A1.21)}$$

where G is the transducer constant. In terms of the Laplace transform, this can be written

$$E_o(s) = - G(s)\ sX(s) \qquad \text{(A1.22)}$$

Combining A1.20 and A1.22 we have as the transfer function of the seismometer:

$$\frac{E_o(s)}{Y(s)} = - \frac{GMs^3}{K\left[1+\frac{2\zeta}{\omega_n} s+ \frac{s^2}{\omega_n^2}\right]} = T(s) \qquad \text{(A1.23)}$$

Considering velocity sensitivity, we are interested in $E_o(s)/s\ Y(s)$ so that A1.23 yields, with $s = j\omega$,

$$T(j\omega) = - \frac{GM}{K} \cdot \frac{(j\omega)^2}{1+\frac{2\zeta}{\omega_n}(j\omega)+\left(\frac{j\omega}{\omega_n}\right)^2} \qquad \text{(A1.24)}$$

This expression may be easily evaluated for the three cases $\omega << \omega_n$, $\omega = \omega_n$, $\omega >> \omega_n$ to obtain the theoretical asymptotes for the velocity sensitivity of the seismometer. We have

$$\left|T(j\omega)\right| \longrightarrow \frac{GM}{K}\,\omega^2 \quad , \ \omega << \omega_n \quad \text{(12db/octave slope)}$$

$$\left|T(j\omega)\right| = \frac{GM}{B}\,\omega_n \ , \quad \omega = \omega_n \quad \text{(a point)} \qquad \text{(A1.25)}$$

$$\left|T(j\omega)\right| \longrightarrow G \quad , \quad \omega >> \omega_n \quad \text{(a constant)}$$

Considerations of the theoretical asymptotes for the amplifier show that the two aliasing filters give a cut-off of 80db/decade from a 4.3 Hz corner and the filter in stage 2 has a double corner at 0.033 Hz (40db/decade slope). Figure A1.5 shows the asymptotic response of the seismometer, amplifier and the combination of the two. The figure serves only to illustrate the bandwidth available from this system so that the amplitude scale is not absolute.

Figure A1.5 Theoretical asymptotes for the velocity sensitivity of the seismometer and the transfer function of the amplifier showing how the two curves are combined to attain the desired bandwidth. S marks the curve for the seismometer, A the amplifier, and S-A the seismometer-amplifier combination.

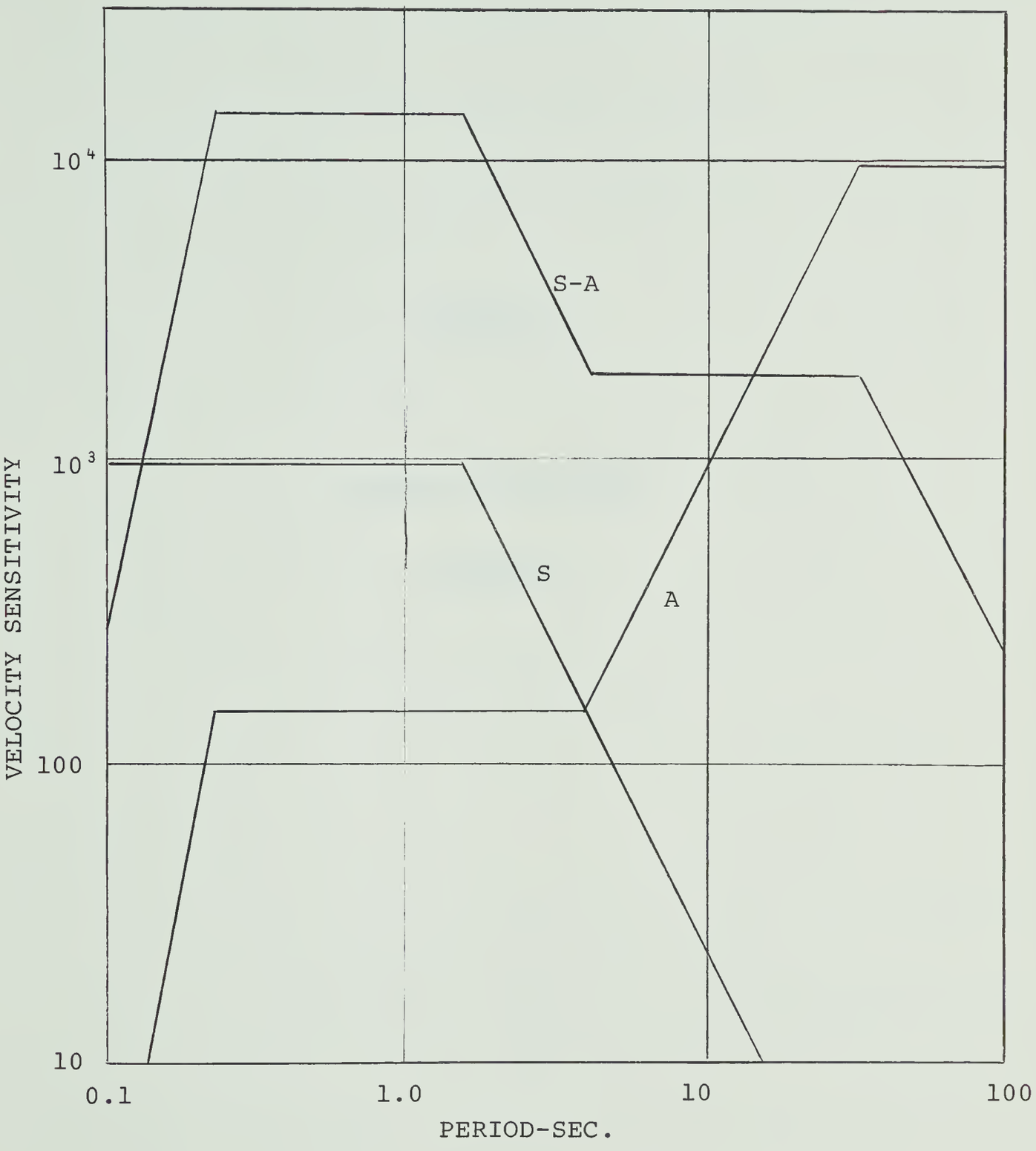
VELOCITY SENSITIVITY
10^4
10^3
100
10
S-A
S
A
0.1
1.0
10
100
PERIOD-SEC.

APPENDIX 2

LISTING OF COMPUTER

PROGRAMS

```
C  TIME DOMAIN POLARIZATION FILTER
C  CALCULATES RECTILINEARITY AND DIRECTION GAIN CONTROLS
C  DATA MAY BE FILTERED
C  IE,IP,ISV,ISH...EXPONENTS FOR GAIN FUNCTIONS
C  NWIN...WINDOW LENGTH FOR SMOOTHING AS IN
C  SUBROUTINE GAINAV.
C  EXP...EXPONENT USED FOR RATIO OF EIGENVALUES
C  THETA...GREAT CIRCLE AZIMUTH IN DEGREES AND
C  DECIMAL PARTS OF DEGREES
C  IB...BLKS SKIPPED IF ISKIP.EQ.1
C  IF IZS(#ZBLKS).NE.ZERO FILTER
C  ISTART=POINT OF FIRST CALCULATION
C  NBLKS=#BLKS PROCESSED
C  MAXIMUM BLKS PROCESSED IF FILTERED =5
C  IBLK=BLKLENGTH/CHANNEL
C  LWIN=WINDOW LENGTH(MUST BE ODD INTEGER)
C  LREC=PARAMETER FOR SUBROUTINE READSK
C  =LENGTH (IN BLKS OF 2048 WORDS OF RECORD DESIRED)
C  READ NBK.=1+NPLKS ONTO DISK FOR
C  PURPOSES OF WINDOW.
C  TWO BLKS ARE READ AT ONE TIME SO
C  POINTS AT BEGINNING OF LAST BLOCK MAY BE INCLUDED
C  IN WINDOW
C  SUBROUTINE EIGEN IS A LIBRARY PROGRAM FROM
C  THE SCIENTIFIC SUBROUTINE PACKAGE
C  CALCULATES EIGENVALUES AND EIGENVECTORS
C  OF A REAL SYMMETRIC MATRIX
CCCCCCCCCCCCCCCCCCCCCCCCCCCCCCCCCCCCCCCCCCCCCCCCCCCCCCCCCCCCCCCCCCCCC
    95 FORMAT(4F10.0,I5)
    96 FORMAT(4F10.0)
    97 FORMAT(5X,F10.0)
    98 FORMAT(3I5)
    99 FORMAT(5I5,F10.0)
   100 FORMAT('0POINT OF FIRST GAIN ='I5,' WINDOW ='I5,' PROCESSED BLKS =
      .'I5//' POINTS/CHANNEL =' I5,' LREC ='I5)
   101 FORMAT('0POINT'I5,' ERROR PARAMETER IS'I4)
   102 FORMAT('0RECTILINEARITY EXPN='I5,' DIRECTION P EXPN='I5//
      .' DIRECTION SV EXPN.='I5,' DIRECTION SH EXPN='I5)
   103 FORMAT('0WINDOW FOR GAIN AVERAGING='I5)
   104 FORMAT('0POWER OF AXES RATIO='F7.2)
   105 FORMAT(4X,10F10.3)
   106 FORMAT('0BLKS SKIPPED ='I5,' ZEROS FOR FILTER ='I5)
   107 FORMAT(5X,3F10.3)
   114 FORMAT('1RECTILINEARITY')
   115 FORMAT('1DIRECTION SV')
   116 FORMAT('1DIRECTION SH')
   117 FORMAT('1DIRECTION P')
   118 FORMAT('1Z')
   119 FORMAT('1RADIAL')
   120 FORMAT('1TRANSVERSE')
```

```
  121 FORMAT('1P')
  122 FORMAT('1SV')
  123 FORMAT('1SH')
  124 FORMAT('0AZIMUTH ='F10.3)
  125 FORMAT('0PTS/INCH ='F7.2,' AMP/INCH ='F7.2,' SAMPLES/SEC ='F7.2,
     .' PTS/SYMBOL ='I5)
  126 FORMAT('CALL PLOTS TO 999 COMPLETE')
  127 FORMAT('0MONTH ='F10.0,' DAY ='F10.0,' YEAR ='F10.0,
     .' OUT ='F10.0)
  128 FORMAT('0AMP/INCH AFTER MODULATION='F7.2)
  200 FORMAT(5X,F10.3)
  201 FORMAT('0SCALE FACTOR'F10.2)
      COMMON/TEMP/IDAT(6144)
      COMMON/FIL/FI(8)
      COMMON/DISKS/CHAN1(2048),CHAN2(2048),CHAN3(2048)
      COMMON/OFSET/DC(3)
      DIMENSION X(2050)
      DIMENSION XX(12438)
      COMMON/STORAC/DAT(3,4096)/BLK/IBLK
      COMMON/GAINS/RL(2050),DSV(2050),DSH(2050),DP(2050)
      COMMON/ANGLE/THETA
      DIMENSION Z(2050),R(2050),T(2050)
      DIMENSION EIGV(9),QUAD(6)
      EQUIVALENCE(XX(1),IDAT(1)),(XX(6145),Z(1)),(XX(8195),R(1)),
     .(XX(10245),T(1))
      COMMON/DATE/SMONTH,DAY,YEAR,TIME
      DIMENSION BUFF(512)
C  OPEN PLOTTAPE FILE
      CALL PLOTS(BUFF(1),2048)
      READ(5,99) IB,IP,ISV,ISH,NWIN,EXR
      READ(5,97)THETA
      READ(5,98) ISKIP,IB,IZ$
      READ(5,99) ISTART,LWIN,NBLKS,IBLK,LREC
      READ(5,200)SCAL
C  LABELS AND SCALES FOR PLOTTING
      READ(5,96) SMONTH,DAY,YEAR,TIME
      READ(5,95) TIN,AMP1,AMP2,SPS,IUNIT
      IF(LREC.NE.2)LREC=2
      IF(ISTART.LT.((LWIN+1)/2))ISTART=0
      IF(ISKIP.EQ.1)CALL SKIP(IB)
      WRITE(6,106) IB,IZ$
      WRITE(6,106) ISTART,LWIN,NBLKS,IBLK,LREC
      WRITE(6,103) NWIN
      WRITE(6,104) EXR
      WRITE(6,124) THETA
      WRITE(6,201)SCAL
      WRITE(6,102) IB,IP,ISV,ISH
      WRITE(6,127) SMONTH,DAY,YEAR,TIME
      WRITE(6,125) TIN,AMP1,SPS,IUNIT
      WRITE(6,128) AMP2
```

```
      PI=3.1415926536
      THETA=THETA*PI/180.00
      DELT=1.0/SPS
      WIN=DELT*FLOAT(LWIN)
C  SETTING SCALE FACTORS FOR PLOTTING
      TPI=TIN*DELT
      DELX=FLOAT(IBLK)/TIN
      RL(2049)=0.0
      RL(2050)=1.0
      DP(2049)=0.0
      DP(2050)=1.0
      DSV(2049)=0.0
      DSV(2050)=1.0
      DSH(2049)=0.0
      DSH(2050)=1.0
      Z(2049)=0.0
      R(2049)=0.0
      T(2049)=0.0
C  ABSCISSA VALUES FOR PLOT
      X(2049)=0.0
      X(2050)=TPI
C
      DO 16 JJ=1,IBLK
      X(JJ)=FLOAT(JJ-1)*DELT
   16 CONTINUE
      CALL LABELS(WIN,TPI)
C  READ TAPE AND FLOAT DATA
      KKK=0
      NNN=1+NBLKS
      IFIL=0
      IF(IZS.NE.0)IFIL=1
      CALL READTP(NNN)
C  FILTER IF NECESSARY
      IF(IFIL.EQ.1)CALL BUT(NNN,IZS,XX)
      CALL READSK(LREC,KKK,SCAL)
C  IF NOT FILTERED,REMOVE DC
      IF(IFIL.EQ.0)CALL REMOVE(LREC)
C  FILL GAIN VECTORS WITH ZEROS TO STARTING POINT
      CALL CAINST(ISTART,LWIN,INDEX,IB,IC)
C  BEGIN CALCULATIONS
      DO 14 KKK=1,NBLKS
      IF(KKK.NE.1)CALL SET(IB,IC,LWIN)
   15 CONTINUE
      DO 10 I=IB,IC
      ISTOP=INDEX+LWIN
      INDEX=INDEX+1
C  READ IN WINDOW
      CALL WINDOW(INDEX,ISTOP)
C  CALCULATE COVARIANCE MATRIX
      CALL COVAR(LWIN,QUAD)
```

```
C  CALCULATE EIGENVALUES AND EIGENVECTORS
      CALL EIGEN (QUAD,EIGV,3,0)
C  FORM GAIN FUNCTIONS
      RL(I)=(1.0-(QUAD(3)/QUAD(1))**EXR)**IR
      DSV(I)=(ABS(EIGV(1)))**ISV
      DSH(I)=(ABS(EIGV(2)))**ISH
      DP(I)=(ABS(EIGV(3)))**IP
   10 CONTINUE
      IF(IC-IBLK)12,13,13
   12 CONTINUE
C  IF AT END OF BLK,READ IN MORE DATA
      CALL READSK(LREC,KKK,SCAL)
      IF(IFIL.EQ.0)CALL REMOVE(LREC)
      INDEX=0
      IB=(LWIN+1)/2
      IC=IBLK
      GO TO 15
   13 CONTINUE
C  SMOOTH GAIN FUNCTIONS
      IF(NPIN.NE.0)CALL GAINAV(LWIN,XX)
C  ROTATE INTO R,T,Z CO-ORDINATE SYSTEM
      CALL ROTATE(R,T,Z)
      Z(2050)=AMP1
      R(2050)=AMP1
      T(2050)=AMP1
C  PLOTS
      IF(KKK.NE.1)GO TO 17
      CALL PLOT(0.0,25.0,-3)
      GO TO 18
   17 CALL PLOT(DELX,22.5,-3)
   18 CONTINUE
      CALL LINE (X,Z,IBLK,1,IUNIT,3)
      CALL PLOT(0.0,-2.5,-3)
      CALL LINE (X,R,IBLK,1,IUNIT,3)
      CALL PLOT(0.0,-2.5,-3)
      CALL LINE (X,T,IBLK,1,IUNIT,3)
      CALL PLOT(0.0,-2.5,-3)
      CALL LINE (X,RL,IBLK,1,IUNIT,3)
      CALL PLOT(0.0,-2.5,-3)
      CALL LINE (X,DP,IBLK,1,IUNIT,3)
      CALL PLOT(0.0,-2.5,-3)
      CALL LINE (X,DSV,IBLK,1,IUNIT,3)
      CALL PLOT(0.0,-2.5,-3)
      CALL LINE (X,DSH,IBLK,1,IUNIT,3)
      CALL GAIN (R,T,Z)
      Z(2050)=AMP2
      R(2050)=AMP2
      T(2050)=AMP2
      CALL PLOT(0.0,-2.5,-3)
      CALL LINE (X,Z,IBLK,1,IUNIT,3)
```

```
      CALL PLOT(0.0,-2.5,-3)
      CALL LINE (X,R,IBLK,1,IUNIT,3)
      CALL PLOT(0.0,-2.5,-3)
      CALL LINE (X,T,IBLK,1,IUNIT,3)
   14 CONTINUE
      CALL PLOT (0.0,0.0,999)
      WRITE(6,126)
      WRITE(6,126)
      STOP
      END
      SUBROUTINE LABELS(WIN,TPI)
C  LABEL PLOTS
      COMMON/DATE/SMONTH,DAY,YEAR,TIME
      CALL SYMBOL(0.0,3.5,0.30,'TRANSVERSE',0.0,10)
      CALL SYMBOL(0.0,6.0,0.30,'RADIAL',0.0,6)
      CALL SYMBOL(0.0,8.5,0.30,'MODULATED Z',0.0,11)
      CALL SYMBOL(0.0,11.0,0.30,'TRANSVERSE DIRECTION',0.0,20)
      CALL SYMBOL(0.0,13.5,0.30,'RADIAL DIRECTION',0.0,16)
      CALL SYMBOL(0.0,16.0,0.30,'Z DIRECTION',0.0,11)
      CALL SYMBOL (0.0,18.5,0.30,'RECTILINEARITY',0.0,14)
      CALL SYMBOL (0.0,21.0,0.30,'TRANSVERSE',0.0,10)
      CALL SYMBOL (0.0,23.5,0.30,'RADIAL',0.0,6)
      CALL SYMBOL (0.0,26.0,0.30,'Z COMPONENT',0.0,11)
      CALL SYMBOL (0.0,27.0,0.50,'TRIPARTITE',0.0,10)
      CALL NUMBER (5.0,27.0,0.30,SMONTH,0.0,-1)
      CALL SYMBOL(5.50,27.0,0.40,97,0.0,-1)
      CALL NUMBER(5.80,27.0,0.30,DAY,0.0,-1)
      CALL SYMBOL (6.30,27.0,0.40,97,0.0,-1)
      CALL NUMBER (6.60,27.0,0.30,YEAR,0.0,-1)
      CALL SYMBOL(7.10,27.0,0.40,97,0.0,-1)
      CALL NUMBER (7.40,27.0,0.30,TIME,0.0,-1)
      CALL SYMBOL (8.40,27.0,0.30,'GMT',0.0,3)
      CALL NUMBER(9.40,27.2,0.20,TPI,0.0,2)
      CALL SYMBOL (10.50,27.20,0.20,'SEC/INCH',0.0,8)
      CALL NUMBER (9.40,26.8,0.20,WIN,0.0,2)
      CALL SYMBOL (10.50,26.80,0.20,'SEC WINDOW',0.0,10)
      RETURN
      END
      SUBROUTINE READSK(LREC,KKK,SCAL)
C  READS DATA FROM DISKS FOR COMPUTATIONS
C  TWO BLKS AT ONE TIME
      COMMON/STORAG/DAT(3,4096)
      COMMON/BLK/IBLK
      COMMON/DISKS/CHAN1(2048),CHAN2(2048),CHAN3(2048)
      IF(KKK.EQ.0)GO TO 4
      LJ=KKK-1
      DO 3 JJ=1,LJ
      READ(1)
      READ(2)
      READ(3)
```

```
    3 CONTINUE
    4 CONTINUE
      I=0
      DO 1 L=1,LREC
      READ(1) CHAN1
      READ(2) CHAN2
      READ(3) CHAN3
      DO 2 J=1,IBLK
      I=I+1
      DAT(1,I)=CHAN1(J)/SCAL
      DAT(2,I)=CHAN2(J)/SCAL
      DAT(3,I)=CHAN3(J)/SCAL
    2 CONTINUE
    1 CONTINUE
      REWIND 1
      REWIND 2
      REWIND 3
      RETURN
      END
      SUBROUTINE REMOVE(LREC)
C  REMOVES DC IF DATA NOT FILTERED
      COMMON/STORAG/DAT(3,4096)/OFSET/DC(3)
      COMMON/BLK/IBLK
      NTOT=LREC*IBLK
      DO 1 I=1,NTOT
      DAT(1,I)=DAT(1,I)-DC(1)
      DAT(2,I)=DAT(2,I)-DC(2)
      DAT(3,I)=DAT(3,I)-DC(3)
    1 CONTINUE
      RETURN
      END
      SUBROUTINE GAINST(ISTART,LWIN,INDEX,IB,IC)
C  FILL IN ZEROS AND SET INDICES FOR FIRST PASS
      COMMON/GAINS/RL(2050),DSV(2050),DSH(2050),DP(2050)
      COMMON/BLK/IBLK
      IF(ISTART.NE.0)GO TO 51
      IA=(LWIN-1)/2
      DO 70 I=1,IA
      RL(I)=0.0
      DSV(I)=0.0
      DSH(I)=0.0
      DP(I)=0.0
   70 CONTINUE
      INDEX=0
      IB=(LWIN+1)/2
      GO TO 52
   51 CONTINUE
      IA=ISTART-1
      DO 71 I=1,IA
      RL(I)=0.0
```

```
      OSV(I)=0.0
      OSH(I)=0.0
      DP(I)=0.0
   71 CONTINUE
      INDEX=(ISTART-(LWIN+1)/2)
      IB=ISTART
   52 CONTINUE
      IC=IBLK
      RETURN
      END
      SUBROUTINE SET(IB,IC,LWIN)
C  SETS INDICES FOR BEGINNING OF BLOCK ON SUBSEQUENT PASSES
      IB=1
      IC=(LWIN-1)/2
      RETURN
      END
      SUBROUTINE WINDOW(INDEX,ISTOP)
C  FILLS VECTOR OVER WINDOW FOR CALCULATIONS
      COMMON/STORAG/DAT(3,4096)
      COMMON/DISKS/CHAN1(2048),CHAN2(2048),CHAN3(2048)
      COMMON/ANGLE/THETA
      JJ=0
      DO 1 J=INDEX,ISTOP
      JJ=JJ+1
      CHAN1(JJ)=DAT(1,J)
      CHAN2(JJ)=DAT(2,J)*SIN(THETA)-DAT(3,J)*COS(THETA)
      CHAN3(JJ)=DAT(3,J)*SIN(THETA)+DAT(2,J)*COS(THETA)
    1 CONTINUE
      RETURN
      END
      SUBROUTINE COVAR(LWIN,QUAD)
C  CALCULATES COVARIANCE MATRIX OVER SPECIFIED WINDOW
      COMMON/DISKS/CHAN1(2048),CHAN2(2048),CHAN3(2048)
      REAL*4 MNX,MNY,MNZ
      DIMENSION QUAD(6)
      PTS=FLOAT(LWIN)
      MNX=0.0
      MNY=0.0
      MNZ=0.0
      DO 1 J=1,LWIN
      MNX=MNX+CHAN3(J)
      MNY=MNY+CHAN2(J)
      MNZ=MNZ+CHAN1(J)
    1 CONTINUE
      MNX=MNX/PTS
      MNY=MNY/PTS
      MNZ=MNZ/PTS
      VAR1=0.0
      VAR2=0.0
      VAR3=0.0
```

```
      COV12=0.0
      COV13=0.0
      COV23=0.0
      DO 2 J=1,LWIN
      VAR1=VAR1+(CHAN3(J)-MNX)*(CHAN3(J)-MNX)
      VAR2=VAR2+(CHAN2(J)-MNY)*(CHAN2(J)-MNY)
      VAR3=VAR3+(CHAN1(J)-MNZ)*(CHAN1(J)-MNZ)
      COV12=COV12+(CHAN3(J)-MNX)*(CHAN2(J)-MNY)
      COV13=COV13+(CHAN3(J)-MNX)*(CHAN1(J)-MNZ)
      COV23=COV23+(CHAN2(J)-MNY)*(CHAN1(J)-MNZ)
    2 CONTINUE
      PPTS=FLOAT(LWIN)
      VAR1=VAR1/PPTS
      VAR2=VAR2/PPTS
      VAR3=VAR3/PPTS
      COV12=COV12/PPTS
      COV13=COV13/PPTS
      COV23=COV23/PPTS
      QUAD(1)=VAR1
      QUAD(2)=COV12
      QUAD(3)=VAR2
      QUAD(4)=COV13
      QUAD(5)=COV23
      QUAD(6)=VAR3
      RETURN
      END
      SUBROUTINE GAINAV(MWIN,XX)
C  AVERAGES THE GAIN FUNCTIONS OVER A SPECIFIED WINDOW LENGTH
      COMMON/BLK/IBLK
      COMMON/GAINS/RL(2050),DSV(2050),DSH(2050),DP(2050)
      DIMENSION XX(10)
      K=2*IBLK
      KK=3*IBLK
      PTS=FLOAT(MWIN)
      INDEX=0
      NST=(MWIN+1)/2
      NEND=IBLK-(MWIN-1)/2
      NST1=NST-1
      NPLUS=NEND+1
      DO 1 I=NST,NEND
      IC=INDEX+MWIN
      INDEX=INDEX+1
      AV1=0.0
      AV2=0.0
      AV3=0.0
      AV4=0.0
      DO 2 J=INDEX,IC
      AV1=AV1+RL(J)
      AV2=AV2+DSV(J)
      AV3=AV3+DSH(J)
```

```
      AV4=AV4+DP(J)
    2 CONTINUE
      AV1=AV1/PTS
      AV2=AV2/PTS
      AV3=AV3/PTS
      AV4=AV4/PTS
      XX(I)=AV1
      XX(I+IBLK)=AV2
      XX(I+K)=AV3
      XX(I+KK)=AV4
    1 CONTINUE
C   FILL GAINS WITH AVERAGES
C   BEGINNING
      DO 3 I=1,NSTM1
      RL(I)=XX(NST)
      DSV(I)=XX(NST+IBLK)
      DSH(I)=XX(NST+K)
      DP(I)=XX(NST+KK)
    3 CONTINUE
C   END
      DO 4 I=NPLUS,IBLK
      RL(I)=XX(NEND)
      DSV(I)=XX(NEND+IBLK)
      DSH(I)=XX(NEND+K)
      DP(I)=XX(NEND+KK)
    4 CONTINUE
C   MIDDLE
      DO 5 I=NST,NEND
      RL(I)=XX(I)
      DSV(I)=XX(I+IBLK)
      DSH(I)=XX(I+K)
      DP(I)=XX(I+KK)
    5 CONTINUE
      RETURN
      END
      SUBROUTINE ROTATE (R,T,Z)
C   ROTATES ORIGINAL DATA TRACES INTO AN
C   R,T,Z CO-ORDINATE SYSTEM
      COMMON/STORAG/DAT(3,4096)
      COMMON/BLK/IBLK/ANGLE/THETA
      DIMENSION R(10),T(10),Z(10)
      DO 1 L=1,IBLK
      R(L)=DAT(3,L)*SIN(THETA)+DAT(2,L)*COS(THETA)
      T(L)=DAT(2,L)*SIN(THETA)-DAT(3,L)*COS(THETA)
      Z(L)=DAT(1,L)
    1 CONTINUE
      RETURN
      END
      SUBROUTINE GAIN(R,T,Z)
C   APPLIES GAIN FUNCTIONS TO THE DATA
```

```
      COMMON/GAINS/RL(2050),DSV(2050),DSH(2050),DP(2050)
      COMMON/BLK/IBLK
      DIMENSION R(10),T(10),Z(10)
      DO 1 L=1,IBLK
      Z(L)=Z(L)*RL(L)*DP(L)
      R(L)=R(L)*RL(L)*DSV(L)
      T(L)=T(L)*RL(L)*DSH(L)
    1 CONTINUE
      RETURN
      END
      SUBROUTINE READTP(NBLK)
C  MOUNT DATA TAPE ON FT04
C  DISKS 1-3 FOR CHANNELS 1-3
C  READS # BLKS DESIRED AND PUTS ONTO DISK
C CALCULATE DC
      COMMON/TEMP/IDAT(6144)/OFSET/DC(3)
      COMMON/BLK/IBLK
      COMMON /DISKS/CHAN1(2048),CHAN2(2048),CHAN3(2048)
      DC(1)=0.0
      DC(2)=0.0
      DC(3)=0.0
      PTS=FLOAT(IBLK*NBLK)
      DO 1 L=1,NBLK
      I=0
      READ(4) IDAT
      DO 2 J=1,6144,3
      I=I+1
      CHAN1(I)=FLOAT(IDAT(J))
      CHAN2(I)=FLOAT(IDAT(J+1))
      CHAN3(I)=FLOAT(IDAT(J+2))
      DC(1)=DC(1)+CHAN1(I)
      DC(2)=DC(2)+CHAN2(I)
      DC(3)=DC(3)+CHAN3(I)
    2 CONTINUE
      WRITE(1) CHAN1
      WRITE(2) CHAN2
      WRITE(3) CHAN3
    1 CONTINUE
      DC(1)=DC(1)/PTS
      DC(2)=DC(2)/PTS
      DC(3)=DC(3)/PTS
      WRITE(6,100) (DC(NN),NN=1,3)
  100 FORMAT('OFFSETS'3E20.7)
      REWIND 1
      REWIND 2
      REWIND 3
      RETURN
      END
      SUBROUTINE SKIP(N)
C  SKIPS DOWN THE TAPE
```

```
      DO 1 J=1,N
      READ(4)
    1 CONTINUE
      RETURN
      END
      SUBROUTINE OUT(NBLK,IZ$,XX)
C  READS DATA FROM DISK, BUTTERWORTH FILTERS
C  PUTS BACK ONTO DISK
      DIMENSION XX(1C)
      COMMON/DISKS/CHAN1(2048),CHAN2(2048),CHAN3(2048)
      COMMON/BLK/IBLK
      COMMCN /CFSET/DC(3)/FIL/FI(8)
      IX$=NBLK*IBLK
      IXZ$=IX$+IZ$
      II=IX$+1
      READ(5,80) FREQLC,FREQHC,G
      READ(5,81) FI
      WRITE(6,82) FREQLC,FREQHC,G
      DO 3 I=1,3
      DO 4 J=1,NBLK
      WRITE(6,1C1) I
      READ(I) CHAN1
      INDEX=IBLK*(J-1)
      DO 5 IK=1,IBLK
      INDEX=INDEX+1
      XX(INDEX)=CHAN1(IK)
    5 CONTINUE
    4 CONTINUE
      REWIND I
C  REMOVE DC.
      DO 2 K=1,IX$
      XX(K)=XX(K)-DC(I)
    2 CONTINUE
C  ADD ZEROS
      DO 1 K=II,IXZ$
      XX(K)=0.0
    1 CONTINUE
      CALL FILTER(IXZ$,XX)
      CALL REVERS(IXZ$,G,XX)
      CALL FILTER(IXZ$,XX)
      CALL REVERS(IXZ$,G,XX)
C  WRITE BACK ONTO DISK
      DO 6 J=1,NBLK
      INDEX=IBLK*(J-1)
      DO 7 IK=1,IBLK
      INDEX=INDEX+1
      CHAN1(IK)=XX(INDEX)
    7 CONTINUE
      WRITE(I) CHAN1
    6 CONTINUE
```

```
      REWIND I
      WRITE(6,100) I
    3 CONTINUE
  100 FORMAT('0FILTERING COMPLETE CHANNEL' I4)
  101 FORMAT('0I='I5)
   60 FORMAT(3F20.0)
   91 FORMAT(3F10.0)
   92 FORMAT('0BUTTERWORTH BANDPASS'2F10.3,' GAIN ='F10.2)
      RETURN
      END
      SUBROUTINE FILTER(I$,X)
C
C  BUTTERWORTH RECURSIVE SUBROUTINE WRITTEN
C  BY T. ALPASAN
C     FILTER VERSION 1 ************************************************
C
      DIMENSION X(10)
      COMMON/FIL/FI(8)
      REAL*4 C(3),D(3),E(3)
      MOD3(INDEX)=INDEX-((INDEX-1)/3)*3
      XIM2=X(1)
      XIM1=X(2)
      XI=X(3)
      C(1)=XIM2
      C(2)=XIM1-FI(1)*C(1)
      C(3)=XI-XIM2-FI(1)*C(2)-FI(2)*C(1)
      D(1)=C(1)
      D(2)=C(2)-FI(3)*D(1)
      D(3)=C(3)-C(1)-FI(3)*D(2)-FI(4)*D(1)
      E(1)=D(1)
      E(2)=D(2)-FI(5)*E(1)
      E(3)=D(3)-D(1)-FI(5)*E(2)-FI(6)*E(1)
      X(1)=E(1)
      X(2)=E(2)-FI(7)*X(1)
      X(3)=E(3)-E(1)-FI(7)*X(2)-FI(8)*X(1)
      DO 1 I=4,I$
      XIM2=XIM1
      XIM1=XI
      XI=X(I)
      IL=MOD3(I)
      IM1L=MOD3(I-1)
      IM2L=MOD3(I-2)
      C(IL)=XI-XIM2-FI(1)*C(IM1L)-FI(2)*C(IM2L)
      D(IL)=C(IL)-C(IM2L)-FI(3)*D(IM1L)-FI(4)*D(IM2L)
      E(IL)=D(IL)-D(IM2L)-FI(5)*E(IM1L)-FI(6)*E(IM2L)
      X(I)=E(IL)-E(IM2L)-FI(7)*X(I-1)-FI(8)*X(I-2)
    1 CONTINUE
      RETURN
      END
      SUBROUTINE REVERS(N,C,X)
```

```
C  REVERS ROUTINE FOR BUTTERWORTH FILTER
      DIMENSION X(10)
      NN=N/2
      DO 1 I=1,NN
      J=N-I
      TEMP=X(I)
      X(I)=X(J+1)/C
      X(J+1)=TEMP/C
    1 CONTINUE
      RETURN
      END
```

```
C   PARTICLE SURFACE WAVE DISCRIMINATION PROCESS
C   MAXIMUM BLKS PROCESSED ...4
C   DATA MAY BE FILTERED(SUBROUTINE BUT)
C   HI AND LO-CUT FREQ AND FILTER
C   COEFFICIENTS READ IN SUBROUTINE BUT
C   AZIMUTH FROM NORTH SPECIFIED IN DEGREES AND
C   DECIMAL PARTS OF DEGREES AS ANGLE THETA
C   COMPUTES FOURIER COEFFICIENTS OVER A SPECIFIED
C   WINDOW...LWIN, A POWER OF 2 FROM 2**7 TO 2**10
C   INCREMENTS DOWN RECORD AN AMOUNT 'INC' POINTS
C   FOR NEXT WINDOW
C   IR,IK,IN...EXPONENTS FOR WEIGHTING FUNCTIONS OF
C   AMPLITUDE COEFFICIENTS
C   RL...THEORETICAL HORIZONTAL/VERTICAL DISPLACEMENT
C   RATIO FOR RAYLEIGH WAVES
C   ISKIP...BLKS SKIPPED ON TAPE,IBLK...PTS/BLK/CHANNEL
C   NBLKS...NUMBER OF PROCESSED BLKS
C   IZS...ZEROS FOR FILTER,IZS.EQ.0...DO NOT FILTER
C   MAXIMUM IZS=300 FOR 4 BLKS
C   WFPTS...FRACTION OF POINTS IN WINDOW TAPERED
C   BEFORE TAKING FFT'S
C   SUBROUTINE STACK RECONSTRUCTS TRACE OVER THE
C   OVERLAPPING WINDOWS
C   SUBROUTINES USED HERE AND LISTED WITH
C   APPLICABLE PROGRAM INCLUDE:  SKIP,READTP,BUT,
C   FILTER,REVERS.
CCCCCCCCCCCCCCCCCCCCCCCCCCCCCCCCCCCCCCCCCCCCCCCCCCCCCCCC
   94 FORMAT(4F10.0,I5)
   95 FORMAT(4F10.0)
   96 FORMAT(3I5)
   97 FORMAT(5X,F10.0)
   98 FORMAT(7I5)
  100 FORMAT('0BLKS SKIPPED='I5,' BLKS PROCESSED='I5,'
     . ZEROS FOR FILTER='I5)
  101 FORMAT('0WINDOW LENGTH='I5,' INCREMENT=' I5,'
     . PTS/BLK=' I5)
  102 FORMAT('1Z COMPONENT')
  103 FORMAT('1RADIAL COMPONENT')
  104 FORMAT('1TRANSVERSE COMPONENT')
  105 FORMAT(4X,10F10.3)
  106 FORMAT('0BETA EXPONENT='I5,' PSI EXPONENT='I5,
     .' ALFA EXPONENT='I5)
  107 FORMAT('0HORIZONTAL/VERTICAL THEORETICAL
     . DISPLACEMENT RATIO =' F10.3)
  108 FORMAT(5X,10F10.2)
  109 FORMAT('0AZIMUTH='F10.2)
  110 FORMAT('0MONTH ='F10.0,' DAY ='F10.0,' YEAR ='F10.0,
     .' GMT ='F10.0)
  111 FORMAT('0PTS/INCH='F7.2,'AMP/INCH='F7.2,
     .' AMP/INCH AFTER MODULATION='F7.2//' SAMPLES/SEC='F7.2,
```

```
     .' PTS/SYMBOL='I5)
  112 FORMAT('CALL PLOTS TO 999 COMPLETE')
  115 FORMAT('FRACTION OF WINDOW TAPERED=1/'I5)
      DIMENSION XZ(8194),XR(8194),XT(8194)
      DIMENSION FZ(1024),FT(1024),FR(1024),DUMMY(1024)
      DIMENSION AR(513),AT(513),AZ(513)
      DIMENSION PHIR(511),PHIT(511),PHIZ(511)
      DIMENSION X(8194)
      COMMON/TEMP/IDAT(6144)
      COMMON/FIL/FI(8)
      COMMON/LISKS/CHAN1(2048),CHAN2(2048),CHAN3(2048)
      COMMON/OFSET/DC(3)
      DIMENSION XX(8192)
      COMMON/BLK/IBLK
      COMMON/ANGLE/THETA
      COMMON/EXPNT/IM,IK,IN
      COMMON/INV/DR
      COMMON/PIE/PI,TWOPI
      COMMON/DATE/SMONTH,DAY,YEAR,TIME
      DIMENSION BUFF(512)
      EQUIVALENCE(XZ(1),XX(1))
      EQUIVALENCE(FZ(1),CHAN1(1)),(FT(1),CHAN1(1025)),
     .(FR(1),CHAN2(1)),(DUMMY(1),CHAN2(1025)),
     .(AR(1),CHAN3(1)),(PHIR(1),CHAN3(514)),
     .(AT(1),CHAN3(1025)),(PHIT(1),CHAN3(1538))
      EQUIVALENCE(X(1),IDAT(1))
      READ(5,96) IM,IK,IN
      WRITE(6,106) IM,IK,IN
      READ(5,97) DR
      WRITE(6,107) DR
      READ(5,97) THETA
      WRITE(6,109) THETA
      READ(5,98) ISKIP,IZ$,LWIN,INC,NBLKS,IBLK,NFPTS
      WRITE(6,100) ISKIP,NBLKS,IZ$
      WRITE(6,101) LWIN,INC,IBLK
      WRITE(6,115) NFPTS
C  CONSTANTS FOR PLOT
      READ(5,95) SMONTH,DAY,YEAR,TIME
      READ(5,94) TIK,AMP1,AMP2,SPS,IUNIT
      WRITE(6,110) SMONTH,DAY,YEAR,TIME
      WRITE(6,111) TIK,AMP1,AMP2,SPS,IUNIT
C  OPEN PLOTTAPE FILE
      CALL PLOTS(BUFF(1),2048)
      DELT=1.0/SPS
      WIN=DELT*FLOAT(LWIN)
      TPI=TIK*DELT
      TINC=DELT*FLOAT(INC)
      IFIL=0
      IF(IZ$.NE.0)IFIL=1
      DR=ATAN(DR)
```

```
      PI=3.1415926536
      TWOPI=2.0*3.1415926536
      DELTA=THETA*(PI/180.00)
C  READ REQUIRED NUMBER OF BLKS OF DATA FROM TAPE
C  AND STORE ON DISK
      IF(ISKIP.NE.0)CALL SKIP(ISKIP)
      CALL READTP(NBLKS)
C  IFIL.EQ.1...FILTER
      IF(IFIL.EQ.1)CALL BUT(NBLKS,IZ,XX)
C  FILL VECTORS XZ,XT,XR, WITH ROTATED DATA Z,T,R
      KKK=NBLKS*IBLK
C  FILL ABSCISSA
      DO 3 J=1,KKK
      X(J)=FLOAT(J-1)*DELT
    3 CONTINUE
      X(KKK+1)=0.0
      X(KKK+2)=TPI
      XZ(KKK+1)=0.0
      XR(KKK+1)=0.0
      XT(KKK+1)=0.0
      CALL FILL(NBLKS,XZ,XT,XR)
C  PLOTTING INPUT
      XZ(KKK+2)=AMP1
      XR(KKK+2)=AMP1
      XT(KKK+2)=AMP1
      CALL PLOT(0.0,25.0,-3)
      CALL LINE(X,XZ,KKK,1,IUNIT,3)
      WRITE(6,102)
      WRITE(6,103)(XZ(I),I=1,KKK)
      CALL PLOT(0.0,-2.5,-3)
      CALL LINE(X,XR,KKK,1,IUNIT,3)
      WRITE(6,103)
      WRITE(6,108)(XR(I),I=1,KKK)
      CALL PLOT(0.0,-2.5,-3)
      CALL LINE(X,XT,KKK,1,IUNIT,3)
      WRITE(6,104)
      WRITE(6,108)(XT(I),I=1,KKK)
C  SET VALUE OF LOG2N FOR FFT'S
      IF(LWIN.EQ.128)LOG2N=7
      IF(LWIN.EQ.256)LOG2N=8
      IF(LWIN.EQ.512)LOG2N=9
      IF(LWIN.EQ.1024)LOG2N=10
      NNN=KKK-LWIN+1
C  PROCEED WITH ANALYSIS
      DO 2 I=1,NNN,INC
C  FILL VECTORS FOR TWO FFT
      CALL WINDOW(I,LWIN,XZ,XT,XR,FZ,FT,FR)
C  RADIAL...FR,TRANSVERSE...FT,Z...FZ
C  FILL DUMMY FOR TWO FFT
      DO 1 JJ=1,LWIN
```

```
      DUMMY(JJ)=1.0
    1 CONTINUE
C  TAPER
      CALL TAPER(LWIN,NPTS,FR,FT,FZ)
C  COMPUTE TRANSFORMS
      CALL TWOFFT(LOG2N,FZ,FR)
      CALL TWOFFT(LOG2N,FT,DUMMY)
C  NOW HAVE FOURIER TRANSFORMS OF Z,R,T
C  PERFORM SEPARATION
C  OUTPUT FROM SUBROUTINE SWAVE IS MODIFIED RECONSTRUCTED
C  TRACE OVER WINDOW IN TIME DOMAIN STORED
C  IN FR...RADIAL,FT...TRANSVERSE.FZ...Z
C  WRITE THESE SEGMENTS ON DISK
C
      CALL SWAVE(LWIN,LOG2N,FZ,FR,FT,AZ,AR,AT,PHIZ,PHIP,PHIT)
      WRITE(1) FZ
      WRITE(2) FT
      WRITE(3) FR
    2 CONTINUE
      REWIND 1
      REWIND 2
      REWIND 3
C  RECONSTRUCT ENTIRE TRACE
      CALL STACK(NBLKS,LWIN,INC,XZ,XT,XR,FZ,FT,FR)
C  PLOTTING OUTPUT
      XZ(KKK+2)=AMP2
      XR(KKK+2)=AMP2
      XT(KKK+2)=AMP2
      CALL PLOT(0.0,-2.5,-3)
      WRITE(6,102)
      WRITE(6,108)(XZ(I),I=1,KKK)
      CALL LINE(X,XZ,KKK,1,IUNIT,3)
      CALL PLOT(0.0,-2.5,-3)
      WRITE(6,103)
      WRITE(6,108)(XR(I),I=1,KKK)
      CALL LINE(X,XR,KKK,1,IUNIT,3)
      WRITE(6,104)
      WRITE(6,108)(XT(I),I=1,KKK)
      CALL PLOT(0.0,-2.5,-3)
      CALL LINE(X,XT,KKK,1,IUNIT,3)
      CALL PLOT(0.0,0.0,999)
      WRITE(6,112)
      WRITE(6,112)
      STOP
      END
      SUBROUTINE STACK(NBLKS,LWIN,INC,XZ,XT,XR,FZ,FT,FR)
C  STACKS DATA FOR PURPOSES OF PLOTTING
      DIMENSION XZ(10),XT(10),XR(10)
      DIMENSION FZ(1024),FT(1024),FR(1024)
      COMMON/BLK/IBLK
```

```
      NPTS=NBLKS*IBLK
      WINC=FLOAT(LWIN)/FLOAT(INC)
      DO 1 I=1,NPTS
      XZ(I)=0.0
      XT(I)=0.0
      XR(I)=0.0
    1 CONTINUE
      NNPTS=NPTS-LWIN+1
      DO 2 I=1,NNPTS,INC
      READ(1) FZ
      READ(2) FT
      READ(3) FR
      INDEX=I-1
      DO 3 J=1,LWIN
      INDEX=INDEX+1
      XZ(INDEX)=FZ(J)+XZ(INDEX)
      XT(INDEX)=FT(J)+XT(INDEX)
      XR(INDEX)=FR(J)+XR(INDEX)
    3 CONTINUE
    2 CONTINUE
C   TAKE AVERAGES
      DO 4 J=1,NNPTS
      XZ(J)=XZ(J)/WINC
      XT(J)=XT(J)/WINC
      XR(J)=XR(J)/WINC
    4 CONTINUE
      REWIND 1
      REWIND 2
      REWIND 3
      RETURN
      END
      SUBROUTINE SLAVE(LWIN,LOG2N,FZ,FR,FT,AZ,AR,AT,PHIZ,PHIR,PHIT)
C   PERFORMS SURFACE WAVE DISCRIMINATION PROCESS AS PER SIMONS
C   APRIL 1968 BULL.SEIS.SOC.AM.
C   FR,FT,FZ...VECTORS CONTAINING FOURIER TRANSFORMS
C   AZ AR AT...COMPUTED AMPLITUDES OF FT'S
C   PHIZ,PHIR,PHIT...PHASE ANGLES
      COMMON/EXPNT/IM,IK,IN
      COMMON/DV/DR
      COMMON/PIC/PI,TWOPI
      DIMENSION FZ(10),FR(10),FT(10)
      DIMENSION AZ(10),AR(10),AT(10)
      DIMENSION PHIZ(10),PHIR(10),PHIT(10)
      WIN=FLOAT(LWIN)
      NUPON2=LWIN/2
      NPLUS=NUPON2+1
C   CALCULATE AMPLITUDE AND PHASE TERMS
C   FILM GAIN FACTORS AND MODIFY COEFFICIENTS
C   FOR J=2,N UPON 2
      DO 1 J=2,NUPON2
```

```
      K=LMIN+2-J
      JM1=J-1
      AZ(J)=SQRT(FZ(J)**2+FZ(K)**2)
      AR(J)=SQRT(FR(J)**2+FR(K)**2)
      AT(J)=SQRT(FT(J)**2+FT(K)**2)
C     CHECK FOR ATAN2(0.0,0.0)
C     AND FORM PHASE ANGLES...ATAN2 IS A LIBRARY SUBFUNCTION
      IF((FZ(K).EQ.0.0).AND.(FZ(J).EQ.0.0))FZ(J)=1.0
      IF((FR(K).EQ.0.0).AND.(FR(J).EQ.0.0))FR(J)=1.0
      IF((FT(K).EQ.0.0).AND.(FT(J).EQ.0.0))FT(J)=1.0
      PHIZ(JM1)=ATAN2(FZ(K),FZ(J))
      IF(PHIZ(JM1).LT.0.0)PHIZ(JM1)=PHIZ(JM1)+TWOPI
      PHIR(JM1)=ATAN2(FR(K),FR(J))
      IF(PHIR(JM1).LT.0.0)PHIR(JM1)=PHIR(JM1)+TWOPI
      PHIT(JM1)=ATAN2(FT(K),FT(J))
      IF(PHIT(JM1).LT.0.0)PHIT(JM1)=PHIT(JM1)+TWOPI
C     MODIFY AMPLITUDE COEFFICIENTS
      BETA=ATAN2(AT(J),AR(J))
      A=SQRT(AR(J)**2+AT(J)**2)
      PSI=ATAN2(A,AZ(J))
      ALFA=PHIR(JM1)-PHIZ(JM1)
      IF((ALFA.GE.PI).AND.(ALFA.LE.TWOPI))GO TO 10
      AZ(J)=AZ(J)*((COS(BETA))**IM)*((COS(PSI-DR))**IK)*
     .((SIN(ALFA))**IN)
      AR(J)=AR(J)*((COS(BETA))**IM)*((COS(PSI-DR))**IK)*
     .((SIN(ALFA))**IN)
      AT(J)=AT(J)*((SIN(BETA))**IM)*((SIN(PSI))**IK)
      GO TO 15
   10 CONTINUE
      AZ(J)=0.0
      AR(J)=0.0
      AT(J)=AT(J)*((SIN(BETA))**IM)*((SIN(PSI))**IK)
   15 CONTINUE
    1 CONTINUE
C     RELOAD MODIFIED AMPLITUDE COEFFICIENTS AND
C     PHASE ANGLES INTO FZ,FR,FT, TO TAKE INVERSE FT
C     TO DO THIS FORM REAL PART A*COS(PHI) AND IMAGINARY
C     PART A*SIN(PHI) AND STORE IN COMPACT HERMITIAN FORM
C     AS DESCRIBED IN SUBROUTINE TWO FFT. ASIN(PHI) IS COMPLEX CONJUGATED.
      DO 4 J=2,NUPON2
      K=LMIN+2-J
      JM1=J-1
      FZ(J)=AZ(J)*COS(PHIZ(JM1))
      FZ(K)=-AZ(J)*SIN(PHIZ(JM1))
      FR(J)=AR(J)*COS(PHIR(JM1))
      FR(K)=-AR(J)*SIN(PHIR(JM1))
      FT(J)=AT(J)*COS(PHIT(JM1))
      FT(K)=-AT(J)*SIN(PHIT(JM1))
    4 CONTINUE
C     TAKE INVERSE TRANSFORMS
```

```
      CALL CNECFT(LOG2N,FZ)
      CALL CNECFT(LOG2N,FR)
      CALL CNECFT(LOG2N,FT)
C  NORMALIZE
      DO 3 J=1,LWIN
      FZ(J)=FZ(J)/WIN
      FR(J)=FR(J)/WIN
      FT(J)=FT(J)/WIN
    3 CONTINUE
      RETURN
      END
      SUBROUTINE FILL(NBLKS,XZ,XT,XR)
C  FILLS VECTORS XZ,XT,XR WITH ROTATED
C  DATA TRACES.  CHAN1...Z,CHAN2...NORTH,CHAN3...EAST
      DIMENSION XZ(10),XT(10),XR(10)
      COMMON/DISKS/CHAN1(2048),CHAN2(2048),CHAN3(2048)
      COMMON/BLK/IBLK
      COMMON/ANGLE/THETA
      S=SIN(THETA)
      C=COS(THETA)
      DO 1 J=1,NBLKS
      READ(1) CHAN1
      READ(2) CHAN2
      READ(3) CHAN3
      INDEX=IBLK*(J-1)
      DO 2 IK=1,IBLK
      INDEX=INDEX+1
      XZ(INDEX)=CHAN1(IK)
      XT(INDEX)=CHAN2(IK)*S-CHAN3(IK)*C
      XR(INDEX)=CHAN3(IK)*S+CHAN2(IK)*C
    2 CONTINUE
    1 CONTINUE
      REWIND 1
      REWIND 2
      REWIND 3
      RETURN
      END
      SUBROUTINE WINDOW(ISTART,LWIN,XZ,XT,XR,FZ,FT,FR)
C  FILLS VECTORS FZ,FT, FR WITH POINTS OVER
C  WINDOW FROM XZ,XT,XR RESPECTIVELY
      DIMENSION XZ(10),XT(10),XR(10)
      DIMENSION FZ(10),FT(10),FR(10)
      INDEX=ISTART-1
      DO 1 J=1,LWIN
      INDEX=INDEX+1
      FZ(J)=XZ(INDEX)
      FT(J)=XT(INDEX)
      FR(J)=XR(INDEX)
    1 CONTINUE
      RETURN
```

```
      END
      SUBROUTINE TAPER(NPTS,NFPTS,X,Y,Z)
C  TAPERS FIRST(1/NFPTS) AND LAST (1/FPTS) OF A
C  SERIES OF NPTS WITH A COSINE BELL OF THE FORM
C  C.5+C.5COS(NFPTS*PI*T/NPTS)...
      DIMENSION X(10),Y(10),Z(10)
      NTAP=NPTS/NFPTS
      PI=3.1415926536
      ARG=FLOAT(NFPTS)*PI/FLOAT(NPTS)
      DO 10 JA=1,NTAP
      JAA=NPTS-JA+1
      FJA=FLOAT(JA-1)
      W=0.5+0.5*COS(ARG*FJA+PI)
      X(JA)=W*X(JA)
      Y(JA)=W*Y(JA)
      Z(JA)=W*Z(JA)
      X(JAA)=W*X(JAA)
      Y(JAA)=W*Y(JAA)
      Z(JAA)=W*Z(JAA)
   10 CONTINUE
      RETURN
      END
      SUBROUTINE TWO R FT (LOG2N,X,Y)
C.....
C      TWO REAL FOURIER TRANSFORMS
C
C  TWO RFT COMPUTES THE FFT OF TWO REAL TIME SERIES
C  X AND Y.  THE OUTPUT IS STORED IN COMPACT HERMITIAN FORM.
C  THAT IS, FOR N POINTS IN EACH REAL TIME SERIES
C  WE HAVE N/2+1 REAL COEFFICIENTS AND N/2-1
C  IMAGINARY COEFFICIENTS.  FOR EXAMPLE, THE FT OF THE TIME SERIES
C  X AS OUTPUT FROM TWO RFT WILL BE STORED AS FOLLOWS:
C  X(1)=DC COEFFICIENT (PURELY REAL)
C  X(N/2+1)=NYQUIST COEFFICIENT (PURELY REAL)
C  AND FOR J=2,N/2; K=N+2-J WE HAVE
C  X(J)=REAL COEFFICIENT OF THE FT
C  X(K)=CORRESPONDING IMAGINARY COEFFICIENT OF THE FT.
      INTEGER LOG2N
      REAL X (10), Y (10)
C
      INTEGER J,K,N,N OVER 2
      REAL XI,XR,YI,YR
C
      CALL MR 10 FT (LOG2N,X,Y)
      N=2**LOG2N
      N OVER 2=N/2+1
      DO 100 J=2,N OVER 2
      K=N+2-J
      XR=Y(J)+X(K)
      XI=Y(J)-Y(K)
```

```
      YR=Y(J)+Y(K)
      YI=X(K)-X(J)
      X(K)=XI*.5
      X(J)=XR*.5
      Y(K)=YI*.5
      Y(J)=YR*.5
  100 CONTINUE
      RETURN
      END
      SUBROUTINE MR 10 FT (LOG2N,X,Y)
C.....................................................................
C     MIXED RADIX ONE DIMENSIONAL FOURIER TRANSFORM
C
      INTEGER LOG2N
      REAL X (10), Y (10)
C
      INTEGER JJ,JC,J1,J2,J3,N,M4
      REAL ARG,C1,C2,C3,I0,I1,I2,I3,R0,R1,R2,R3,S1,S2,S3,T
C
      INTEGER A,B,C,D,E,F,G,H,I,J,K,L,M,BS,CS,DS,ES,FS,GS,HS,IS,JS,KS,
     .LS,MS,AL,BL,CL,DL,EL,FL,GL,HL,IL,JL,KL,LL,ML, S (13), J (13)
      EQUIVALENCE (BS,S(2)),(CS,S(3)),(DS,S(4)),(ES,S(5)),(FS,S(6)),
     .(GS,S(7)),(HS,S(8)),(IS,S(9)),(JS,S(10)),(KS,S(11)),(LS,S(12)),
     .(MS,S(13)),(AL,J(1)),(BL,J(2)),(CL,J(3)),(DL,J(4)),(EL,J(5)),
     .(FL,J(6)),(GL,J(7)),(HL,J(8)),(IL,J(9)),(JL,J(10)),(KL,J(11)),
     .(LL,J(12)),(ML,J(13))
C
      N=2**LOG2N
      IF (LOG2N.EQ.1) GO TO 500
      DO 400 K=2,LOG2N,2
      M=2**(LOG2N-K)
      M4=4*M
      DO 300 J=1,M
      ARG=6.283185307*FLOAT(J-1)/FLOAT(M4)
      C1=COS(ARG)
      S1=SIN(ARG)
      C2=C1*C1-S1*S1
      S2=C1*S1+C1*S1
      C3=C2*C1-S2*S1
      S3=C2*S1+S2*C1
      DO 200 I=M4,N,M4
      J0=I+J-M4
      J1=J0+M
      J2=J1+M
      J3=J2+M
      R0=X(J0)+X(J2)
      R1=X(J0)-X(J2)
      I0=Y(J0)+Y(J2)
      I1=Y(J0)-Y(J2)
      R2=X(J1)+X(J3)
```

```
      R3=X(J1)-X(J3)
      I2=Y(J1)+Y(J3)
      I3=Y(J1)-Y(J3)
      X(J2)=R0+R2
      Y(J2)=I0+I2
      IF (ARG.EQ.0.0) GO TO 100
      X(J0)=(R1+I3)*C1+(I1-R3)*S1
      Y(J2)=(I1-R3)*C1-(R1+I3)*S1
      X(J1)=(R0-R2)*C2+(I0-I2)*S2
      Y(J1)=(I0-I2)*C2-(R0-R2)*S2
      X(J3)=(R1-I3)*C3+(I1+R3)*S3
      Y(J3)=(I1+R3)*C3-(R1-I3)*S3
      GO TO 200
  100 CONTINUE
      X(J2)=R1+I3
      Y(J2)=I1-R3
      X(J1)=R0-R2
      Y(J1)=I0-I2
      X(J3)=R1-I3
      Y(J3)=I1+R3
  200 CONTINUE
  300 CONTINUE
  400 CONTINUE
  500 CONTINUE
      IF (LOG2N.EQ.LOG2N/2*2) GO TO 700
      DO 600 I=1,N,2
      R0=X(I)+X(I+1)
      R1=X(I)-X(I+1)
      I0=Y(I)+Y(I+1)
      I1=Y(I)-Y(I+1)
      X(I)=R0
      Y(I)=I0
      X(I+1)=R1
      Y(I+1)=I1
  600 CONTINUE
  700 CONTINUE
      BS=N/2
      BL=N
      DO 800 K=2,12
      J=14-K
      S(J)=1
      U(J)=S(J+1)
      IF (S(J+1).GT.1) S(J)=S(J+1)/2
  800 CONTINUE
      AL=BS
      JJ=0
      DO 900 A=1,AL
      DO 900 B=A,BL,BS
      DO 900 C=B,CL,CS
      DO 900 D=C,DL,DS
```

```
      DO 900 E=D,EL,ES
      DO 900 F=E,FL,FS
      DO 900 G=F,GL,GS
      DO 900 H=G,HL,HS
      DO 900 I=H,IL,IS
      DO 900 J=I,JL,JS
      DO 900 K=J,KL,KS
      DO 900 L=K,LL,LS
      DO 900 M=L,ML,MS
      JJ=JJ+1
      IF (JJ.LE.M) GO TO 900
      T=X(JJ)
      X(JJ)=X(M)
      X(M)=T
      T=Y(JJ)
      Y(JJ)=Y(M)
      Y(M)=T
  900 CONTINUE
      RETURN
      END
      SUBROUTINE ONE C FT (LOG2N,X)
C.....
C     ONE COMPLEX FOURIER TRANSFORM
C
      INTEGER LOG2N
      REAL X (10)
C
      INTEGER J,JN,K,KN,N,N OVER 2
      REAL AI,AR,ARG,BI,BR,C,PI,S,T
C
      N=2**(LOG2N-1)
      PI=3.141592654
      N OVER 2=N/2+1
      DO 100 J=2,N OVER 2
      K=N+2-J
      JN=J+N
      KN=K+N
      AR=X(J)+X(K)
      AI=X(KN)-X(JN)
      BR=X(J)-X(K)
      BI=X(JN)+X(KN)
      ARG=PI*FLOAT(J-1)/FLOAT(N)
      C=COS(ARG)
      S=SIN(ARG)
      T=BR*C+BI*S
      BI=BI*C-BR*S
      BR=T
      X(J)=AR-BI
      X(K)=AR+BI
      X(JN)=BI+AI
```

```
      X(KH)=BR-AI
  100 CONTINUE
      AR=X(1)+X(N+1)
      BR=X(1)-X(N+1)
      X(1)=AR
      X(N+1)=BR
      CALL RK 10 FT (LOG2N-1,X(1),X(N+1))
      CALL F SUB B C (LOG2N-1,X(1))
      CALL R SUB B D (LOG2N-1,X(N+1))
      CALL R SUB B C (LOG2N,X)
      RETURN
      END
      SUBROUTINE R SUB B D (LOG2N,X)
C.....................................................................
C     REVERSE SUBSCRIPT BIT ORDER
C
      INTEGER LOG2N
      REAL X (10)
C
      INTEGER JJ
      REAL T
C
      INTEGER A,B,C,D,E,F,G,H,I,J,K,L,M,N,BS,CS,DS,ES,FS,GS,HS,IS,JS,KS,
     .LS,MS,NS,AL,BL,CL,DL,EL,FL,GL,HL,IL,JL,KL,LL,ML,NL, S (14), U (14)
      EQUIVALENCE (BS,S(2)),(CS,S(3)),(DS,S(4)),(ES,S(5)),(FS,S(6)),
     .(GS,S(7)),(HS,S(8)),(IS,S(9)),(JS,S(10)),(KS,S(11)),(LS,S(12)),
     .(MS,S(13)),(NS,S(14)),(AL,U(1)),(BL,U(2)),(CL,U(3)),(DL,U(4)),
     .(EL,U(5)),(FL,U(6)),(GL,U(7)),(HL,U(8)),(IL,U(9)),(JL,U(10)),
     .(KL,U(11)),(LL,U(12)),(ML,U(13)),(NL,U(14))
C
      NS=2**(LOG2N-1)
      NL=2*NS
      DO 100 K=2,13
      J=15-K
      U(J)=S(J+1)
      S(J)=1
      IF(S(J+1).GT.1) S(J)=S(J+1)/2
  100 CONTINUE
      AL=BS
      JJ=0
      DO 200 A=1,AL
      DO 200 B=A,BL,BS
      DO 200 C=B,CL,CS
      DO 200 D=C,DL,DS
      DO 200 E=D,EL,ES
      DO 200 F=E,FL,FS
      DO 200 G=F,GL,GS
      DO 200 H=G,HL,HS
      DO 200 I=H,IL,IS
      DO 200 J=I,JL,JS
```

```
      DO 200 K=J,KL,KS
      DO 200 L=K,LL,LS
      DO 200 M=L,ML,MS
      DO 200 N=M,NL,NS
      JJ=JJ+1
      IF (JJ.LE.N) GO TO 200
      T=X(JJ)
      X(JJ)=X(N)
      X(N)=T
  200 CONTINUE
      RETURN
      END
```